A TALE OF TWO C-TAILS

By

Michael A. Bemben

A dissertation submitted to The Johns Hopkins University in conformity with the requirements for the degree of Doctor of Philosophy

Baltimore, Maryland

December, 2015

ABSTRACT

The processing and integration of information in the brain depends on cell-to-cell communication. Synapses, the sites of communication, are specialized asymmetrical connections between neurons that allow for the efficient transfer of information. Synaptic formation, structure, maturation, and maintenance are sustained by a multifarious network of bidirectional cellular adhesion molecules that span the synaptic cleft, aligning the presynaptic active zone and postsynaptic density. Arguably, the best-characterized synaptic cell adhesion molecules are the presynaptic neurexins and postsynaptic neuroligins. The transsynaptic heterophilic interaction between the extracellular domains of neuroligins and neurexins can induce synapse formation and maturation. Although intensely studied, the signaling pathways that regulate neuroligins ability to generate, maintain, and strengthen functional synapses in the developing and mature brain are largely unknown.

The genesis of new synapses by neuroligin has been shown to be dependent on Ca^{2+}/CaM Kinase II, but the mechanism behind this regulation is unknown. Here, we report that Ca^{2+}/CaM Kinase II robustly phosphorylates the intracellular domain of neuroligin-1 on T739 in response to sensory experience in the brain. Blocking phosphorylation drastically decreases neuroligin-1 surface expression, thereby reducing its ability to induce synaptogenesis. Therefore we report that neuroligin is indeed changed by ongoing activity and a direct link between synaptogenesis and calcium in the cell.

In humans, alterations that perturb neuroligins are implicated in cognitive disorders, highlighting their critical roles at the synapse. However, the mechanisms by

which the majority of these mutations may contribute to the disease are unknown. Here we show that endogenous neuroligin-4X is robustly phosphorylated by protein kinase C at T707. Furthermore, R704C, a well-described autism mutation, completely eliminates T707 phosphorylation. A phospho-mimetic mutation at T707 has a profound effect on neuroligin-4X-mediated excitatory potentiation. Our results now establish an important interplay between a genetic mutation, a key posttranslational modification, and robust synaptic changes, which can provide insights into the synaptic dysfunction of autism spectrum disorders.

The extracellular domain of neuroligin-3 promotes glioma growth. Neuroligin-3 expression inversely correlates with survival in human glioblastoma providing a link between neuroligins and cancer. How neuroligin-3 is processed to produce solely its extracellular domain remains an enigma. Here, we report that protein kinase C signaling induces the proteolytic cleavage of full-length neuroligin-3 to produce the extracellular domain. We show that this regulation is isoform and kinase specific. Therefore we report a functional interplay between protein kinase C signaling and neuroligin-3, which may play a role in the etiology of brain cancer.

Taken together, these studies described in this thesis contribute to and expand the understanding of the mechanisms governing synaptogenesis. Historically, neuroligins have been viewed as static building blocks of synapses. Our research identifies pathways by which neuroligins are transiently modified and acutely enhance synapses in an activity-dependent manner. The aberrant regulation of neuroligins contributes to disorders ranging from autism spectrum disorders to cancer underlying their importance for continued study.

Readers

Katherine W. Roche
Senior Investigator, National Institute of Neurological Disorders and Stroke
National Institutes of Health

Haiqing Zhao
Professor, Biology Department
The Johns Hopkins University

Paul F. Worley
Professor, Neuroscience Department
The Johns Hopkins School of Medicine

Thesis Committee

Katherine W. Roche
Senior Investigator, National Institute of Neurological Disorders and Stroke
National Institutes of Health

Jeffrey S. Diamond
Senior Investigator, National Institute of Neurological Disorders and Stroke
National Institutes of Health

Wei Lu
Investigator, National Institute of Neurological Disorders and Stroke
National Institutes of Health

Haiqing Zhao
Professor, Biology Department
The Johns Hopkins University

Richard L. Huganir
Professor, Neuroscience Department
The Johns Hopkins School of Medicine

Paul F. Worley
Professor, Neuroscience Department
The Johns Hopkins School of Medicine

ACKNOWLEDGMENTS

As I reflect back on graduate school at Johns Hopkins University and the National Institutes of Health, the most valuable lesson I have learned was not at the lab bench or in the microscope room but that substantial achievements and scientific breakthroughs are not accomplished by an individual but through collaboration. The extraordinary scientists I have worked with over the last five years not only provided data and insightful discussions on projects, but also instilled in me confidence, optimism, and made graduate school more enjoyable. I thank them for their support, and I look forward to watching their scientific careers continue to flourish.

Words cannot express how grateful I am to my thesis advisor, Katherine Roche, for allowing me to become a member of her lab and trusting me to conduct the research that is presented in this dissertation. I joined Katherine's lab not just because her lab was involved in cutting-edge research, but I believed her scientific vision, confidence, and compassion would allow me to develop into a successful scientist. Through her example, I learned how to critically analyze data, design and conduct controlled experiments, and write scientific manuscripts. Thanks to her I have met and collaborated with extraordinary scientists and presented this dissertation research around the world. Although this dissertation marks the end of my graduate school career, these rewarding experiences will last a lifetime.

The faculty members at Johns Hopkins University and the National Institutes of Health that have contributed to this dissertation are Drs. Haiqing Zhao, Richard Huganir, Paul Worley, Jeffrey Diamond, and Wei Lu. I am grateful to have these world-renowned scientists on my thesis committee and for their support.

I would also like to thank members of the Roche Laboratory for their friendship, mentorship, and contributions to this dissertation. In particular, John Badger II and Drs. Takaaki Hirai, Antonio Sanz-Clemente, and Marc Lussier who have patiently trained me in all the biochemical techniques described in this dissertation. We have been fortunate to collaborate with Dr. Roger Nicoll's Laboratory at the University of California at San Francisco on the projects described in this dissertation. Specifically, I would like to thank Quynh-Anh Nguyen and Drs. Seth L. Shipman and Bruce E. Herring for providing data and insightful discussions described in the dissertation.

Lastly, I would like to express my deepest gratitude to my family and friends for their love and support along the way. Specifically, my wife, Nina M. Bemben (Cimino) for celebrating each scientific victory, mourning each bump and bruise, and always encouraging me with a smile (and a beer).

TABLE OF CONTENTS

LIST OF FIGURES

Chapter 1

An Overview of Neuroligin Subtype Conservation, Subcellular Localization, and Dimerization

Chapter 1 entitled **An Overview of Neuroligin Subtype Conservation and Subcellular Localization** was published (Bemben et al., 2015b).

Conservation Among Subtypes

A fundamental physical interaction exists across the synapse. It is mediated by synaptic adhesion molecules, and is among the earliest and most indispensable of molecular events occurring during synaptogenesis. The regulation of adhesion molecules and their interactions with other synaptic proteins (receptors, scaffolds, and linkers) likely impacts not only synapse formation, but also ongoing synaptic function (**Figure 1-1**). One major family of postsynaptic adhesion molecules is neuroligins, which bind to their presynaptic partner neurexin across the synaptic cleft.

Neuroligins are a class of adhesion molecules found at postsynaptic sites in neurons (Nguyen and Sudhof, 1997). The four major members of the class are neuroligins (NLGNs) 1, 2, 3, and 4, which each share gross structural similarity and substantial conservation in amino acid sequence (**Figure 1-2A**). Each neuroligin has a single transmembrane region separating an acetylcholinesterase-like domain in the extracellular space from a short cytoplasmic tail (Bemben et al., 2015b; Choi et al., 2011a; Nguyen and Sudhof, 1997; Sudhof, 2008). The extracellular domains of NLGNs1-3 contain two notable alternative splice sites that can affect the specificity of trans-synaptic adhesive interactions with repercussions for cellular function (Chih et al., 2006; Koehnke et al., 2010; Lee et al., 2010; Shipman and Nicoll, 2012b). However, the extracellular domain is otherwise more conserved than the intracellular domain (**Figure 1-2B**). There is an additional fifth gene in humans – NLGN4Y (occasionally referred to as NLGN5) – found on the Y chromosome that is greater than 97% identical in protein sequence to NLGN4X, on the X chromosome (**Figure 1-2C**). Due to the high level of molecular similarity, we will discuss NLGN4X and NLGN4Y together as NLGN4.

Neuroligins are situated within a larger superfamily of post-synaptic adhesion molecules, including, but not limited to: cadherins, SynCAMs, LRRTMs, GluD2, CL1, NGLs, and teneurins (Arikkath and Reichardt, 2008; Biederer et al., 2002; Boucard et al., 2012; de Wit et al., 2009; Ko et al., 2009a; Linhoff et al., 2009; Mosca et al., 2012; Uemura et al., 2010; Woo et al., 2009). On the presynaptic side, the primary adhesion partner of neuroligins is the neurexin family, which is itself composed of many subtypes and a vast number of splice variants (Treutlein et al., 2014; Ullrich et al., 1995). This diversity of synaptic adhesion molecules suggests the possibility that a trans-synaptic molecular code could participate in the formation or ongoing function of the diverse synapses found in the brain (**Figure 1-2D**).

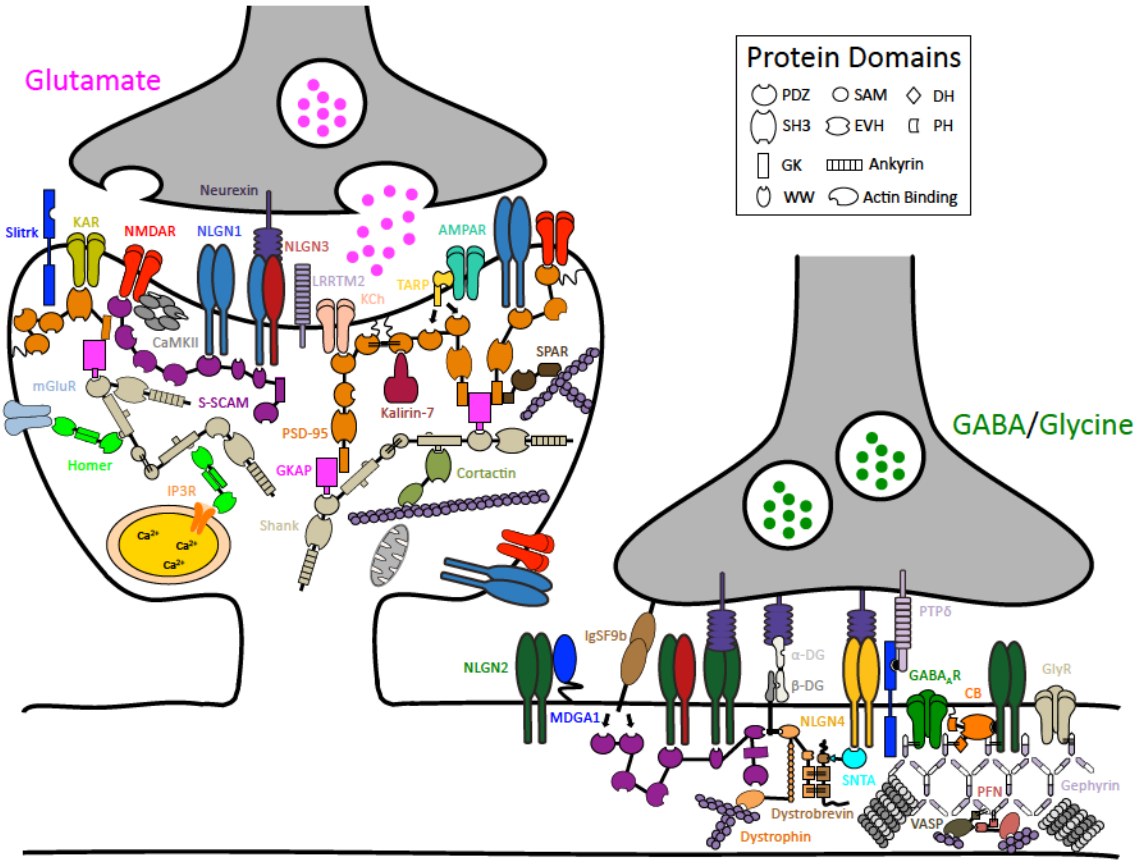

Figure 1-1. Schematic Diagram of a Subset of Protein Constituents at Excitatory and Inhibitory Synapses. Neuroligins bind a diverse set of proteins at glutamatergic and GABAergic/glycinergic synapses. (protein abbreviations are: alpha-dystroglycan (α-DG); α-amino-3-hydroxy-5-methyl-4-isoxazole propionic acid receptor (AMPAR); beta-dystroglycan (β-DG); $Ca2^{+}$/calmodulin-dependent protein kinase II (CaMKII); collybistin (CB); cortical actin binding protein (Cortactin); gamma-aminobutyric $acid_a$ receptor ($GABA_aR$); guanylate kinase-associated protein (GKAP); glycine receptor (GlyR); immunoglobin superfamily member 9b (IgSF9b); inositol trisphosphate 3 receptor (IP3R); kainate receptor (KAR); potassium channel (KCh); leucine-rich transmembrane protein 2 (LRRTM2); MAM domain-containing glycosylphosphatidylinositol anchor 1 (MDGA1); metabotropic glutamate receptor (mGluR); N-methyl-D-aspartate receptor

(NMDAR); profilin (PFN); postsynaptic density protein 95 (PSD-95); protein tyrosine phosphatase rho (PTPσ); synaptic scaffolding molecule (S-SCAM); SH3 and ankyrin repeat-containing protein (Shank); Slit- and NTRK-like family (Slitrk); syntrophin (SNTA); spine-associated RapGAP (SPAR); TCR gamma alternate reading from protein (TARP); vasodilator-stimulated phosphoprotein (VASP); protein domain abbreviations are: Dbl homology domain (DH); enabled/VASP homology domain (EVH); guanylate kinase-like domain (GK); PSD-95/Discs large/ZO-1 (PDZ); pleckstrin homology domain (PH); sterile alpha motif (SAM); Src homology domain (SH3))

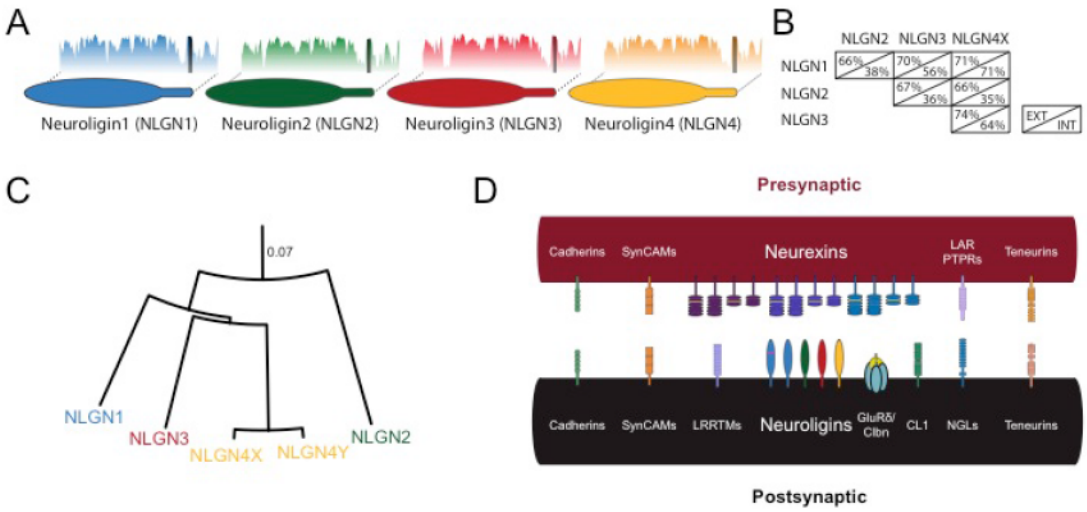

Figure 1-2. Neuroligin Subtypes. **A.** Subtypes of neuroligin with shared identity. Plots behind each molecule show percent identity to a group containing NLGNs 1-4 (blasp, sliding average 10 amino acids). Dark bar in the identity plot indicates the transmembrane domain. **B.** Matrix depicting the approximate percentage identity of the different human neuroligin protein sequences, excluding extracellular splice sites, separated by domain (EXT: extracellular; INT: intracellular). **C.** Distance model of neuroligin subtypes (Jukes-Cantor Model). Scale is given as residue substitutions per site. **D.** Schematic of synaptic adhesion superfamily (abbreviations: leukocyte common antigen-related receptor protein tyrosine phosphatase (LAR PTPR); leucine-rich repeat transmembrane protein (LRRTM); cerebellin (Clbn); CIRL1/latrophilin-1 (CL1); netrin-G ligand (NGL)).

Subcellular Localization

All neuroligins have a conserved domain structure and are postsynaptic molecules. However, the different subtypes of neuroligin each display unique subcellular localizations. Classically, NLGN1 is localized to excitatory (glutamatergic) synapses; NLGN2 is localized to inhibitory (GABAergic) synapses; and NLGN3 is localized to both excitatory and inhibitory synapses (**Figure 1-3A**). This pattern was initially discovered via immunostaining and biochemical analysis (Budreck and Scheiffele, 2007; Graf et al., 2004; Song et al., 1999; Varoqueaux et al., 2004), and has been subsequently supported by functional experiments (Chubykin et al., 2007; Shipman et al., 2011). The odd member of the family, NLGN4, unlike NLGNs1-3, is poorly conserved from humans to mice (~58%), despite strong conservation in other species such as chicken (>93%) and opossum (>95%) among others, and the mouse NLGN4-like gene is not even fully conserved among strains (Bolliger et al., 2008). Nonetheless, a NLGN4-like protein in mice has been shown to localize both to GABAergic synapses in the CNS as well as glycinergic synapses in the retina (Hoon et al., 2011).

Outside the nervous system, NLGN2 has been found on the surface of pancreatic β cells, where it stimulates the secretion of insulin through a trans-cellular, clustering-dependent, but neurexin-independent mechanism (Suckow et al., 2012). Perhaps further study of this related, but clearly unique, system could yield insight into the most conserved core process by which neuroligin induces trans-cellular sites of release.

Dimerization

The canonical interactions between neuroligin molecules follow a pattern that aligns with their subcellular localization. The primary species of neuroligin in the cell is a dimer, if not a higher-order oligomer. The neuroligin dimer was initially inferred from similarity to the protein sequence of acetylcholinesterase (Comoletti et al., 2003), and the presence of a dimer has been supported both biochemically as well as functionally: mutations in the extracellular domain based on the acetylcholinesterase structure abolish both the biochemical dimer and the overexpression phenotype of the molecule (Dean et al., 2003). When the crystal structure of the neuroligin extracellular domain was later determined, it confirmed dimerization highly reminiscent of cholinesterases (Arac et al., 2007; Comoletti et al., 2007; Fabrichny et al., 2007; Koehnke et al., 2008). With structure in hand, function was revisited: a series of mutations that abolish dimerization were found to induce a corresponding reduction in function (Ko et al., 2009b). There is some evidence that dimerization is a necessary step in the trafficking of neuroligin (Poulopoulos et al., 2012), although this is not undisputed (Shipman and Nicoll, 2012a). Finally, using variants of neuroligin in which dimerization of neuroligin can be controlled via a small molecule, it was shown that dimerization is, indeed, necessary for neuroligin's synaptogenic effect (Shipman and Nicoll, 2012a).

Most of the structural and functional work has focused on neuroligin homodimerization. However, biochemical studies have given us insight into the rules that govern inter-type, or heterodimerization. Using co-immunoprecipitation, NLGNs 1-3 were each shown to homodimerize, but; whereas, NLGN3 was able to heterodimerize with both NLGN1 and NLGN2, there was no apparent dimerization between NLGN1 and

NLGN2 (Budreck and Scheiffele, 2007). The heterodimerization between NLGN1 and NLGN3 has been multiply confirmed (Poulopoulos et al., 2012; Shipman et al., 2011), whereas a separate investigation of endogenous neuroligin found traces of a NLGN1/2 dimer and the absence of a NLGN2/3 dimer (Poulopoulos et al., 2012). Moreover, homo- or hetero-dimerization of NLGN4 is completely untested (**Figure 1-3B)**. Rigorous determination of the most prevalent complexes as well as whether there may be cell-type specific complexes is an area that deserves further experimentation.

Finally, it is not clear whether individual dimers of neuroligin or in fact higher-order oligomers are the primary species present at a synaptic site (**Figure 1-3C,D**). There is evidence that a multimer of neuroligin must cluster at least four neurexin molecules to achieve synaptogenic effects (Dean et al., 2003). Moreover, the NLGN1/neurexin1β extracellular domains can form a higher-order lattice sheet when crystalized, whereas the NLGN1/neurexin1α domains cannot (Tanaka et al., 2012). Although yet to be tested functionally, perhaps this is another mechanism by which adhesion molecules may contribute to synaptic diversity.

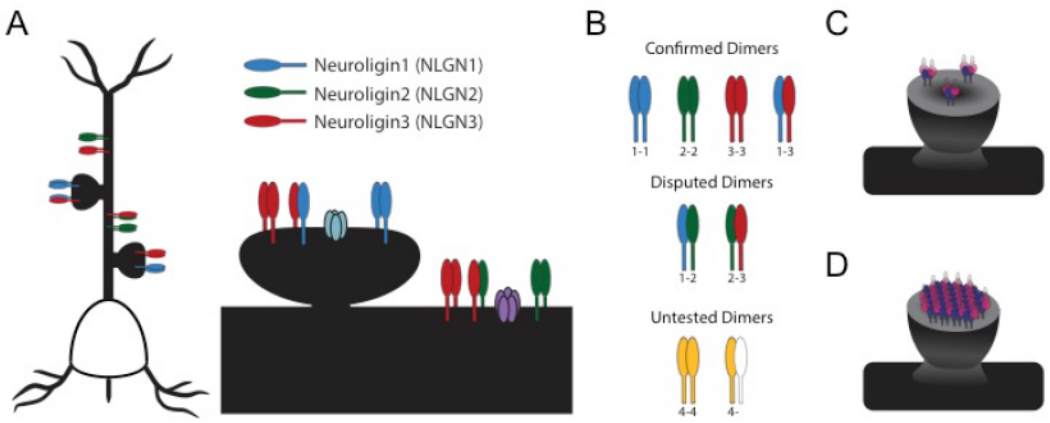

Figure 1-3. Localization and Dimerization. A. Localization of neuroligins: NLGN1 and NLGN3 at excitatory synapses; NLGN2 and NLGN3 at inhibitory synapses. Shown also in the synapse are an AMPA receptor (in light blue) and GABA receptor (in purple). **B.** Confirmed, disputed, and untested dimers of neuroligin subtypes. **C.** Model of a synapse with only neuroligin dimers. **D.** Model of a synapse with higher-order neuroligin oligomers.

Chapter 2

Neuroligin: Binding Partners and Post-Translational Modifications

Chapter 2 entitled **Neuroligin: Binding Partners and Post-Translational Modifications** was published (Bemben et al., 2015b).

Binding Partners

After neuroligin isoforms were found to induce the genesis of distinct synaptic subtypes, researchers looked for the critical domains and protein interactions that are required. The first identified postsynaptic binding partner with the cytoplasmic tail (c-tail) of neuroligins was postsynaptic density protein 95 (PSD-95), a canonical constituent of glutamatergic synapses (Irie et al., 1997). The PDZ ligand is conserved among all neuroligin isoforms (**Figure 2-1**) and interacts with the third PDZ domain within PSD-95. In addition to PSD-95, neuroligins bind to other members of the membrane-associated guanylate kinase (MAGUK) family (Meyer et al., 2004), although the functional significance of these interactions remains to be determined. Interestingly, NLGN1 successfully traffics to the synapse (Dresbach et al., 2004) and NLGN3 is able to robustly potentiate synapses independent of their PDZ ligands (Shipman et al., 2011). Due to complete conservation throughout the family, it seems unlikely the PDZ ligand is the dominant factor that dictates the differential localization of neuroligin subtypes.

Similar to PSD-95, Synaptic Scaffolding Molecule (S-SCAM) was shown to bind to NLGN1 and NLGN2 via a yeast-two hybrid screen (Hirao et al., 1998; Meyer et al., 2004). NLGN1 and NLGN2 bind to two different regions within S-SCAM: a PDZ- and a WW-domain (Iida et al., 2004; Sumita et al., 2007). Researchers only tested S-SCAM binding to NLGN1 and NLGN2, but both the PDZ ligand and WW-binding domain are conserved among all neuroligin subtypes (**Figure 2-1).** Therefore, it is conceivable that all neuroligins bind to S-SCAM, similar to PSD-95 and, indeed, S-SCAM is present at both excitatory and inhibitory synapses. To rigorously test the importance of this

interaction, both the PDZ- and WW-interacting sites would need to be simultaneously mutated in NLGN1 or NLGN2.

At GABAergic synapses, NLGN2 was shown to co-localize with and recruit gephyrin (an inhibitory scaffolding molecule) to nascent postsynaptic specializations (Graf et al., 2004; Varoqueaux et al., 2004) and an unbiased screen further identified gephyrin as a direct NLGN2 interactor. However, like PSD-95 and S-SCAM, the gephyrin-binding domain in NLGN2 is conserved and binds equally well to NLGN1, NLGN2, and NLGN3 (Poulopoulos et al., 2009) (**Figure 2-1**). Therefore NLGN2's specificity to inhibitory synapses cannot solely be attributed to the gephyrin-binding sequence. Recent studies suggest phosphorylation of NLGN1 and NLGN2 may, at least in part, dictate the affinity of gephyrin to a particular neuroligin isoform (Giannone et al., 2013) (discussed further below), providing a possible explanation for synapse specificity.

Research into collybistin may provide another clue to the localization and function of NLGN2. Collybistin is a key inhibitory synapse molecule that binds gephyrin and recruits it to the plasma membrane, where gephyrin can self-assemble and cluster critical inhibitory receptors, a prevailing model for inhibitory postsynaptic differentiation (Harvey et al., 2004; Kins et al., 2000). Remarkably, only inhibitory neuroligins (NLGN2 and mouse NLGN4) bind to collybistin's SH3 domain, promote an open/active confirmation, and traffic gephyrin and collybistin to plasma membrane phosphoinositides (Hoon et al., 2011; Poulopoulos et al., 2009; Soykan et al., 2014). The collybistin-binding domain is unknown but has been predicted to involve the poly-proline region near the terminal end of the NLGN2 c-tail (**Figure 2-1**). This region is not conserved in NLGN1, NLGN3 (Papadopoulos and Soykan, 2011), or NLGN4 (mouse), suggestive of an

independent binding site in NLGN4. A direct test of this two-step, two-domain, three-protein interaction is an area worthy of future research.

All of the early identified postsynaptic interactions with neuroligins (discussed above) involved their c-tails; however, recent studies show that their extracellular domains are also involved in cis interactions in the postsynaptic cell. For example, the ectodomains of NLGN1 and GluN1 interact, and NLGN1 binding acts as a shuttle to deliver NMDA receptors to the synapse (Budreck et al., 2013). This binding is noteworthy because a phenotype of the $NLGN1^{-/-}$ is reduced NMDA currents (Blundell et al., 2010), suggesting a model where NLGN1 can directly interact with a glutamate receptor and affect synaptic strength, in contrast to the canonical model in which scaffolding molecules (such as PSD-95, S-SCAM, and gephyrin) link neuroligins to the receptors at the synapse. A different ectodomain association between NLGN2 and MDGA1 (MAM domain-containing GPI anchor protein) breaks the intercellular interaction between NLGN2 and neurexin, inhibiting NLGN2-mediated presynaptic differentiation (Lee et al., 2013; Pettem et al., 2013). The binding sites within the extracellular domains of NLGN1 and NLGN2 that are required for these interactions remain an enigma, but these studies provide evidence that neuroligin ectodomains' responsibility is not only for dimerization and to trans-synaptically interact with neurexins.

It is likely that the library of neuroligin interacting proteins will continue to expand. Two independent screens identified many proteins that interact with NLGN2 and NLGN3 c-tails, and these interactions have yet to be characterized (Poulopoulos et al., 2009; Shen et al., 2015). Moreover, a critical region was identified in the c-tails of

NLGN1 and NLGN3 that is required for these molecules to potentiate excitatory synaptic transmission (Shipman et al., 2011) without a known direct binding partner (**Figure 2-1**). Additionally, a motif in the c-tail of NLGN1 required for dendritic sorting has been uncovered (**Figure 2-1**), but the molecular basis of this trafficking pathway is unknown and likely requires unidentified interacting proteins (Rosales et al., 2005). A subset of the known molecular constituents of an excitatory and an inhibitory synapse are modeled in **Figure 1-1**, with a focus on the proteins that interact with neuroligins, providing context for the molecular discussion of neuroligin.

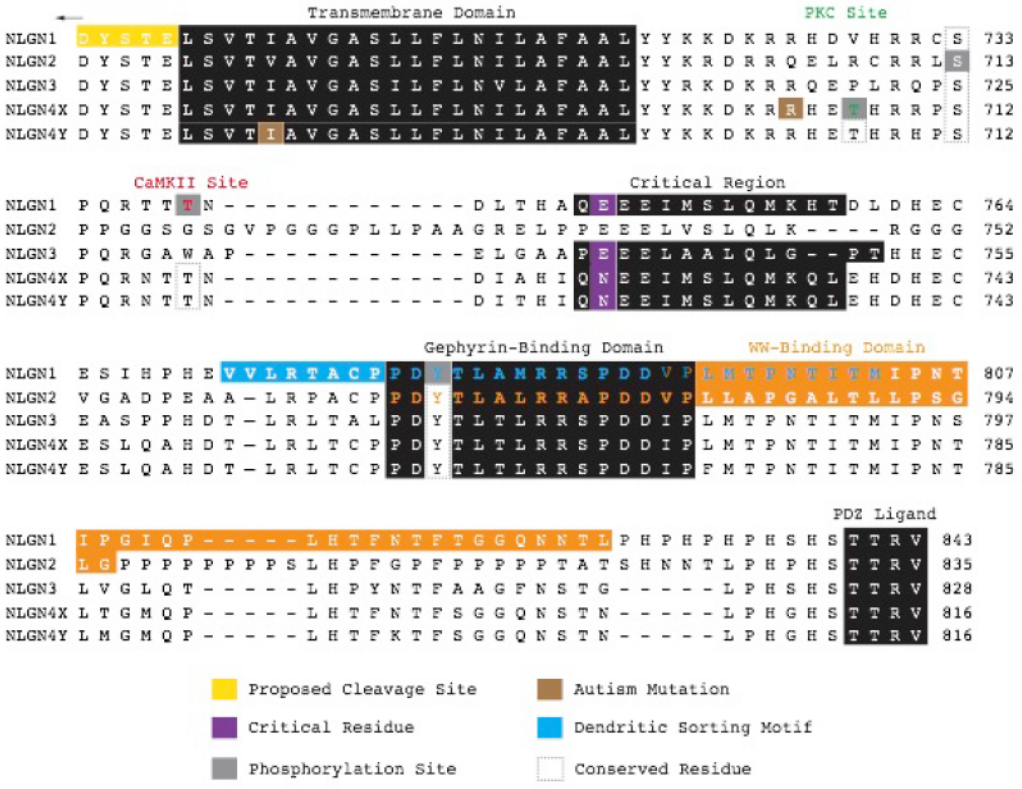

Figure 2-1. Neuroligin Cytoplasmic Domain Comparison. Alignment of the transmembrane and cytoplasmic domains of human neuroligins. Residues identified in rodent neuroligins are depicted on the analogous residues on the human isoforms for comparison purposes. Mapped residues and motifs are boxed. The autism mutation in NLGN4X is arginine (R) 704 mutated to a cysteine and in NLGN4Y isoleucine (I) 679 mutated to a valine. The critical region is necessary for neuroligin-mediated excitatory synaptic potentiation. (abbreviations: $Ca2^{+}$/calmodulin-dependent protein kinase II (CaMKII); PSD-95/Discs large/ZO-1 (PDZ); protein kinase C (PKC))

Post-translational Modifications

Phosphorylation

When comparing protein-interacting domains in the cytoplasmic-domain of neuroligin, it is remarkable that reductionist-binding assays show little to no differences in binding affinities between neuroligin subtypes. How do distinct neuroligin isoforms recruit different postsynaptic machinery? Although the answer still largely remains a mystery, recent research suggests that phosphorylation may, at least in part, underlie isoform-specific regulation.

NLGN1-mediated enhancement of excitatory synapses, for instance, has been shown to depend on synaptic activity, and more specifically, phosphorylation by CaMKII (Bemben et al., 2014; Chubykin et al., 2007). NLGN1 is dynamically and transiently phosphorylated by CaMKII at residue T739 following synaptic activity or sensory experience in the brain (**Figure 2-1**). Blocking phosphorylation of this site drastically decreases the surface expression of NLGN1, thereby reducing its ability to stimulate synaptogenesis **(Figure 2-2A**). Interestingly, CaMKII has also been shown to promote the cleavage of NLGN1(Peixoto et al., 2012; Suzuki et al., 2012). However, an alternate reading is that synaptic activity may promote the cleavage of NLGN1 indirectly by promoting surface expression (through phosphorylation by CaMKII), which increases access to the protease. The phosphorylated residue, T739, is not conserved in NLGNs 2 and 3. However, the CaMKII site is conserved in human NLGN4 and can be phosphorylated *in vitro* (**Figure 2-1**). This phosphorylation provides a transient and isoform-specific mechanism by which NLGN1 can induce synapse formation or

modification in response to synaptic activity and discussed in detail in **Chapter 3** (Bemben et al., 2014).

Not only does phosphorylation modulate NLGN1 surface expression but it also regulates key protein interactions. NLGN1 has a second phosphorylation site within the gephyrin-binding domain at Y782 (**Figure 2-1**), which, when phosphorylated by an unknown kinase, blocks the NLGN1-gephyrin interaction (Giannone et al., 2013). It has been proposed that neurexin1β binding to NLGN1 stimulates phosphorylation at Y782, thereby shifting NLGN1 assembly with excitatory (e.g. PSD-95) from inhibitory scaffolding molecules (**Figure 2-2B**). These findings hint at how NLGN1 can specifically recruit excitatory postsynaptic machinery even though it contains a conserved gephyrin-binding domain. Proline-directed phosphorylation on NLGN2 S714-P (S713 in the human alignment, **Figure 2-1**) also negatively regulates its ability to bind gephyrin (Antonelli et al., 2014). Although this residue is not within the gephyrin-binding domain, like Y782 in NLGN1, phosphorylation at S714 recruits the enzyme Pin1 (peptidyl-proly cis-trans isomerase), which isomerizes NLGN2 and breaks its association with gephyrin (**Figure 2-2C**). Blocking phosphorylation leads to increased NLGN2-gephyrin binding, which results in more synaptic GABA receptors. In both studies, phosphorylation was only tested on NLGN1 Y782 or NLGN2 S714, but the analogous tyrosine and serine residues are conserved among all neuroligins (**Figure 2-1**). To conclude whether these are neuroligin isoform-specific mechanisms, it will be necessary to look at the phosphorylation profile of these analogous residues in tandem and assess gephyrin binding.

Although most of the previously discussed phosphorylation studies have focused on NLGN1 and NLGN2, it is NLGN3 and NLGN4 that have been most closely associated with disease. Might disease-associated mutations in neuroligin impact phosphorylation? Point mutations in NLGN3 and NLGN4 have been discovered in patients with autism spectrum disorders (Jamain et al., 2003; Laumonnier et al., 2004; Lawson-Yuen et al., 2008). However, only a single mutation has been identified thus far in the c-tail, NLGN4X R704C, whereas the other mutations reside in the extracellular and transmembrane domains (Yan et al., 2008; Yan et al., 2005) (**Figure 2-1**). Due to the lack of conservation of rodent and human NLGN4, some researchers have attempted to study this mutation in NLGN3, where the analogous arginine is conserved, but a knock-in mutation resulted in only minor synaptic effects (Etherton et al., 2011).

Human NLGN4X is phosphorylated at T707 by PKC (Bemben et al., 2015a) (**Figure 2-1**). Intriguingly, T707 resides only a few amino acids away from the disease-associated mutation, R704C, which, when present, completely abolishes T707 phosphorylation, thus identifying R704 as a critical residue in a PKC consensus motif in NLGN4X (**Figure 2-1**). A phospho-mimetic mutation at T707 enhanced synaptogenesis. The mechanism behind this enhancement is unknown, but was not a result of changes in NLGN4X surface expression. It is discussed in detail in **Chapter 4**. It may be a result of a novel protein interaction on phosphorylated NLGN4X that induces the recruitment of glutamatergic receptors or increases recruitment of presynaptic terminals (**Figure 2-2D**). Notably, the analogous threonine in NLGN4X is not conserved in NLGN3, possibly explaining why the NLGN3 knock-in mutation had minor synaptic effects (Etherton et al., 2011) (**Figure 2-1**). Furthermore, the R704C mutation has different effects in NLGN3

and NLGN4X underscoring the importance of studying a disease mutation in its correct isoform (Chanda et al., 2015). As with all these sites, a better understanding of when the phosphorylation occurs, by which kinases, and in which brain regions will shed light on neuroligin signaling pathways.

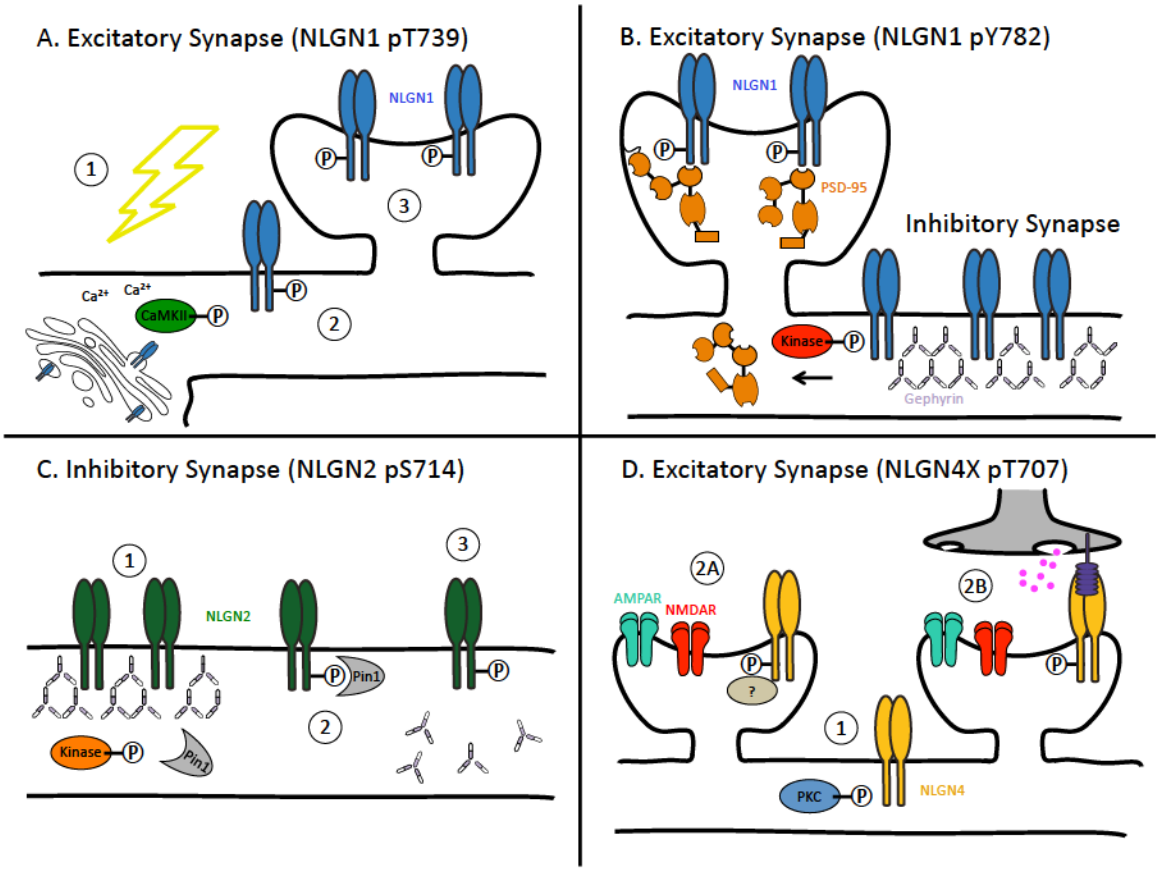

Figure 2-2. Regulation of Neuroligins by Phosphorylation. A. NLGN1 pT739. (1) Synaptic activity drives calcium influx thereby activating CaMKII. (2) CaMKII phosphorylates NLGN1, which leads to increased surface expression. (3) Increased NLGN1 surface expression promotes the creation of new synapses. **B**. NLGN1 pY782. Phosphorylation by an unknown kinase in the gephyrin-binding domain (Y782) drives NLGN1 to release from gephyrin and localize at excitatory synapses as opposed to inhibitory synapses. **C.** NLGN2 pS714. (1) An unknown kinase phosphorylates NLGN2 at S714. (2) Phosphorylation leads to recruitment and binding of Pin1. (3) Pin1 isomerizes NLGN2, which negatively affects the NLGN2-gephyrin interaction. **D.** NLGN4X pT707. (1) Activation of PKC phosphorylates NLGN4X at T707. Phosphorylation of NLGN4X promotes the genesis of excitatory synapses possibly

through an unknown protein interaction (2A) or by increasing the recruitment of presynaptic terminals (2B). (abbreviations: α-amino-3-hydroxy-5-methyl-4-isoxazole propionic acid receptor (AMPAR); $Ca2^{+}$/calmodulin-dependent protein kinase II (CaMKII); N-methyl-D-aspartate receptor (NMDAR); phosphorylation (P); protein kinase C (PKC); peptidyl-proly cis-trans isomerase (Pin1); postsynaptic density protein 95 (PSD-95))

Glycosylation

In addition to phosphorylation of the cytoplasmic domain, differential glycosylation may also play a role in modulating neuroligin activity. In the same screen that identified NLGN1 as a binding partner of neurexin1β, extensive glycosylation was also evident. The predicted molecular weight of NLGN1 is 95 kDa, but it was found to migrate at approximately 116 kDa (Ichtchenko et al., 1995). Bands at both apparent molecular weights are observed when NLGN1 is expressed in heterologous cells and analyzed in the brain (Song et al., 1999). Researchers used glycosidases to show the difference in predicted and expected size was predominantly a result of glycosylation (Comoletti et al., 2003; Ichtchenko et al., 1995). Structural characterization of the extracellular domain of NLGN1 by mass spectrometry identified five N-glycosylated and two O-glycosylated sites; however, insufficient coverage was seen in the highly glycosylated stalk region, which may lead to an underestimate of O-glycosylated sites (Hoffman et al., 2004). N-glycosylation at any of these five sites decreases binding to neurexinβ, yet individual mutants are still able to induce synaptogenesis. Interestingly, one of the N-glycosylation sites occurs in the β insertion of NLGN1 (N303), which is the alternatively spliced insert that dictates its neurexin binding preferences and its ability to potentiate excitatory synapses. Blocking glycosylation at this site (N303A) allows NLGN1 to morphologically enhance inhibitory synapses,(Chih et al., 2006) revealing the critical importance of glycosylation in isoform specificity. No disease-related mutations have yet been identified in neuroligins that directly affect a glycosylation site. However, two autism mutations (NLGN4X: R87W & NLGN3: R451C) have differential glycosylation patterns when compared to WT protein resulting in decreased surface

expression (Tabuchi et al., 2007; Zhang et al., 2009). This differential glycosylation is likely a result of protein misfolding, so rather than implicating glycosylation in disease, they suggest that neuroligin glycosylation may be used as a marker for surface expression. It is likely neuroligins have isoform-specific glycosylation as only one of the five identified N-glycosylated sites on NLGN1 are conserved among all isoforms (N547) but the functional consequences of this distinction await future investigation.

Chapter 3

CaMKII Phosphorylation of Neuroligin-1 Regulates Excitatory Synapses

Chapter 3 entitled **CaMKII Phosphorylation of Neuroligin-1 Regulates Excitatory Synapses** was published (Bemben et al., 2014).

ABSTRACT

Neuroligins are postsynaptic cell adhesion molecules that are important for synaptic function through their transsynaptic interaction with neurexins. The localization and synaptic effects of neuroligin-1 (NLGN1) are specific to excitatory synapses with the capacity to enhance excitatory synapses dependent on synaptic activity or Ca^{2+}/CaM Kinase II (CaMKII). Here, we report that CaMKII robustly phosphorylates the intracellular domain of NLGN1. We show that T739 is the dominant CaMKII site on neuroligin-1 and is phosphorylated in response to synaptic activity in neurons and sensory experience *in vivo*. Furthermore, a phospho-deficient mutant (NLGN1 T739A) reduces the basal and activity-driven surface expression of NLGN1, leading to a reduction in neuroligin-mediated excitatory synaptic potentiation. Therefore we report the first direct functional interplay between CaMKII and NLGN1, two primary components of excitatory synapses.

INTRODUCTION

The processing and integration of information in the brain depends on cell-to-cell communication. Synapses, the sites of communication, are specialized asymmetrical connections between neurons that allow for the efficient transfer of information. Synaptic formation, structure, maturation, and maintenance are sustained by a multifarious network of bidirectional cellular adhesion molecules that span the synaptic cleft, aligning the presynaptic active zone and postsynaptic density. In humans, alterations that perturb these cellular organizers are implicated in cognitive disorders, highlighting their critical roles at the synapse. Arguably, the best-characterized synaptic cell adhesion molecules are the presynaptic neurexins (NRXNs) and postsynaptic NLGNs (Bemben et al., 2015b; Craig and Kang, 2007; Dalva et al., 2007; Dean and Dresbach, 2006; Sudhof, 2008; Yamagata et al., 2003). The transsynaptic heterophilic interaction between the extracellular domains of NLGNs and NRXNs can induce synapse formation and maturation (Bemben et al., 2015b; Chih et al., 2005; Dean et al., 2003; Graf et al., 2004; Levinson et al., 2005; Nam and Chen, 2005; Wittenmayer et al., 2009).

NLGNs are postsynaptic proteins that contain a single transmembrane domain, a large extracellular acetylcholinesterase-like domain, and a short cytoplasmic tail (c-tail) that includes many protein-protein interaction domains (Ichtchenko et al., 1995; Iida et al., 2004; Irie et al., 1997; Poulopoulos et al., 2009; Sudhof, 2008). Rodents express four NLGNs (NLGN1 to NLGN4). Despite high sequence conservation among isoforms, subcellular localization and expression patterns vary between NLGNs (Ichtchenko et al., 1996). NLGN1 is predominantly localized to excitatory synapses, whereas NLGN2 is primarily confined to inhibitory synapses (Chih et al., 2005; Graf et al., 2004; Levinson et

al., 2005; Song et al., 1999; Varoqueaux et al., 2004). In contrast, NLGN3 is expressed at both types of synapses. NLGN4 is enriched at glycinergic synapses with initial studies focusing on the retina (Budreck and Scheiffele, 2007; Hoon et al., 2011).

Consistent with the localization of NLGN1 at excitatory synapses, overexpression of NLGN1 increases evoked excitatory postsynaptic currents (EPSCs) and synaptogenesis (Chih et al., 2005; Chubykin et al., 2007; Ko et al., 2009b; Kwon et al., 2012; Shipman et al., 2011). Moreover, NLGN1 has been shown to be involved in diverse forms of synaptic plasticity across species (Blundell et al., 2010; Choi et al., 2011b; Dahlhaus and El-Husseini, 2010; Jung et al., 2010; Kim et al., 2008; Shipman and Nicoll, 2012b). NLGN1-mediated synaptic potentiation is diminished after chronic blockade of NMDA receptors (NMDARs) or Ca^{2+}/CaM Kinase II (CaMKII), suggesting that NLGN1 function is influenced by NMDAR signaling (Chubykin et al., 2007). While the regulatory mechanisms of NLGN1-mediated, activity-dependent, synaptic enhancement are poorly understood, previous reports have implicated the c-tail in the proper trafficking of NLGN1 to the synapse, although its terminal PDZ ligand is not essential (Dean et al., 2003; Dresbach et al., 2004). Moreover, induction of synaptic plasticity upregulates the surface expression of NLGN1 (Schapitz et al., 2010). Finally, high frequency stimulation increases the mobilization and number of NLGN1 clusters in cultured hippocampal neurons (Gutierrez et al., 2009). Taken together, these results strongly suggest that NLGN1 trafficking and subcellular localization are governed by synaptic activity, but the underlying mechanisms have remained elusive.

Protein phosphorylation is a principal and swift regulatory mechanism in the organization and functional modulation of receptors at the synapse (Kim and Huganir,

1999). CaMKII is a major component of the excitatory postsynaptic density and a critical mediator of synaptic plasticity. CaMKII-mediated phosphorylation acutely regulates the function and trafficking of postsynaptic substrates in response to synaptic activity (Lisman et al., 2002). Although NLGN1-mediated synaptic potentiation depends on CaMKII activity, the direct phosphorylation of NLGN1 by CaMKII has not been reported.

Here, we show that NLGN1 is a direct substrate of CaMKII and identify a phosphorylation site, T739, in the intracellular c-tail of NLGN1 that is not conserved in other rodent NLGN isoforms. We demonstrate that NLGN1 T739 is specifically phosphorylated by CaMKII but not other known activity-dependent kinases in the postsynaptic density. Additionally, T739 phosphorylation is upregulated by synaptic activity. A non-phosphorylatable mutant, T739A, dramatically reduces the basal and activity-induced surface expression of NLGN1 and consequently the postsynaptic actions of NLGN1. Importantly, this study establishes a direct functional and isoform-specific relationship between CaMKII and NLGN1, two critical constituents of the excitatory synapse.

RESULTS

NLGN1 is Phosphorylated on T739 by CaMKII *in vitro*.

NLGN1-mediated potentiation of synaptic transmission depends on CaMKII (Chubykin et al., 2007). Might NLGN1 be a substrate for CaMKII? The intracellular domain of NLGN1 contains several serine (S) and threonine (T) residues that could potentially be phosphorylated by CaMKII (**Figure 3-1A**). An *in vitro* kinase assay with CaMKII, [γ-^{32}P]ATP, and engineered GST-fusion proteins containing the c-tail of NLGN1 (amino acids 718-843) or GluA1 (positive control), revealed that NLGN1 was robustly phosphorylated by CaMKII as assessed by radiography (**Figure 3-1A,B**). CaMKII phosphorylation of NLGN1 and GluA1 displayed similar reaction kinetics and were run to saturation (**Supplementary Figure 3-1A,B**). We also evaluated CaMKII phosphorylation on the c-tails of NLGN2, NLGN3, and NLGN4 and found NLGN2 and NLGN3 not to be phosphorylated, whereas CaMKII phosphorylated human NLGN4, albeit at a much lower level than NLGN1 (**Figure 3-1C**), thus indicating that NLGN1 is the best NLGN substrate for CaMKII.

To identify the individual phosphorylated site(s), we generated point mutations of S/T residues on NLGN1 that are not conserved in NLGN2 and NLGN3, and discovered that mutating T739 to alanine (A) dramatically reduced CaMKII phosphorylation (**Figure 3-D**), whereas similar mutations of neighboring T residues had little to no effect.

Neither cAMP-dependent Protein Kinase (PKA) nor Protein Kinase C (PKC) phosphorylated NLGN1 *in vitro* as robustly as CaMKII (**Figure 3-1B**). Furthermore, to detect if PKA or PKC are able to phosphorylate NLGN1 T739, we analyzed GST-NLGN1 following *in vitro* kinase reactions using liquid chromatography coupled to

tandem mass spectrometry (LC/MS/MS) and found that only CaMKII phosphorylates T739 (**Figure 3-1E-G**). Additionally, using LC/MS/MS method, we found that CaMKII phosphorylates the analogous threonine in human NLGN4 (T718) as in rodent NLGN1 T739 (data not shown), which is not surprising considering the conservation of the CaMKII consensus sequence in human NLGN4 and mouse NLGN1 (**Figure 3-1A**; see sequence alignment). Taken together, these results indicate that NLGN1 T739 is the dominant and CaMKII-specific phosphorylation site in the intracellular tail of NLGN1 and is not conserved in other excitatory synapse-specific NLGNs.

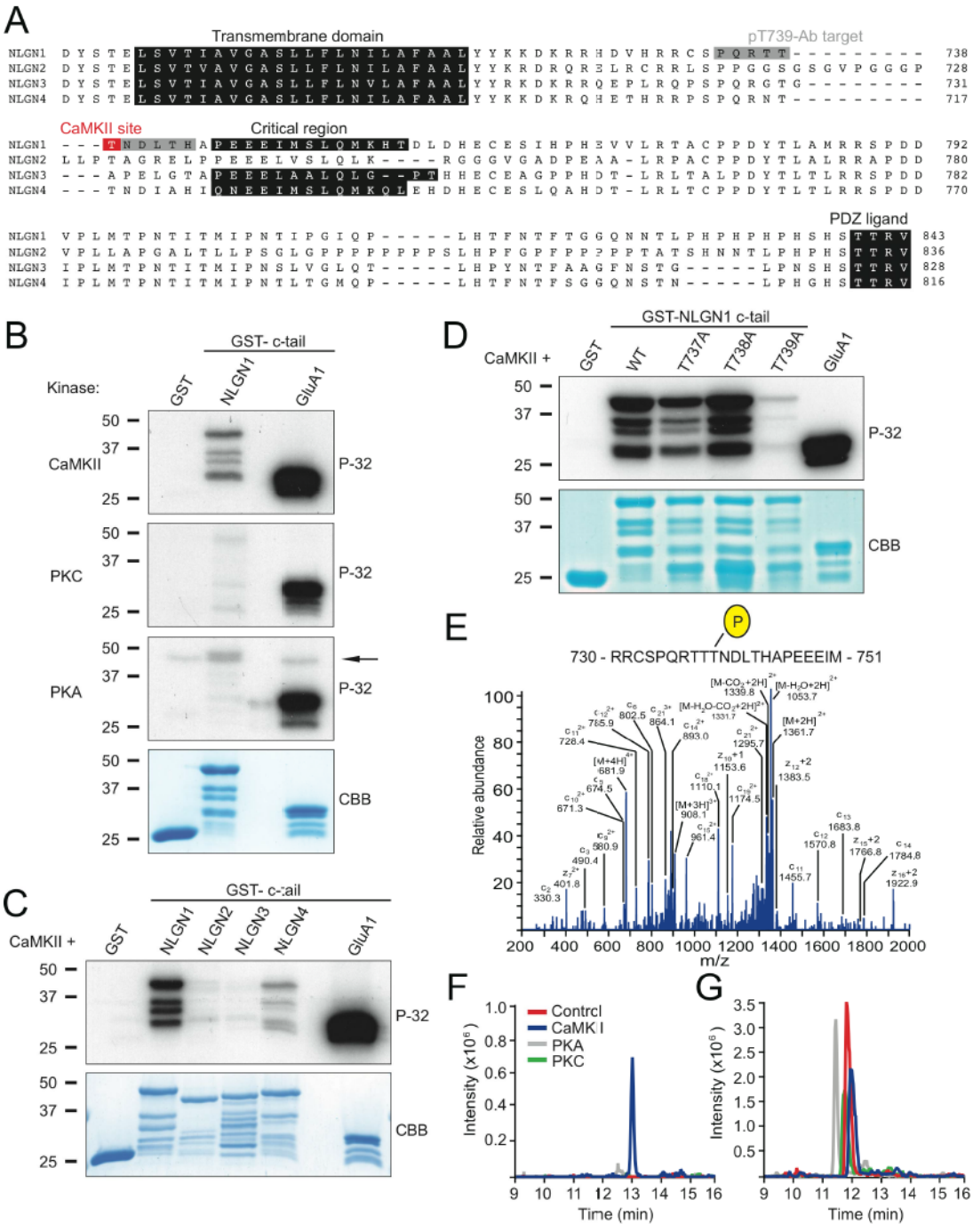

Figure 3-1. **NLGN1 T739 is Phosphorylated by CaMKII *in vitro*. A**. Alignment of the transmembrane domains and c-tails of NLGN1 (mouse), NLGN2 (rat), NLGN3 (human), and NLGN4 (human). CaMKII phosphorylation site boxed in red and pT739-Ab epitope boxed in gray. **B-D**. GST-fusion proteins were incubated with purified CaMKII, PKA, or

PKC and [γ-P^{32}]ATP and analyzed by autoradiography. Arrow denotes autophosphorylated PKA. Total protein was visualized by CBB protein staining, and GST and GST-GluA1 c-tail served as negative and positive phosphorylation controls, respectively, in **B-D**. **E**. ETD MS/MS spectrum of phosphorylated NLGN1 peptide 730 - RRCSPQRTTpTNDLTHAPEEEIM - 751 found only in GST-NLGN1 fusion proteins incubated with ATP and purified CaMKII and not PKA or PKC. Samples were digested with chymotrypsin, and then analyzed using LC/MS/MS method. **F.** Extracted ion chromatogram of quadruply charged ion at m/z 681.30, which corresponds to phosphorylated NL-1 peptide 730 - 751, as shown in **E**, for GST-NLGN1 - enzyme (red), + PKA (grey), + PKC (green), and + CaMKII (blue). **G.** Extracted ion chromatogram of quadruply charged ion at m/z 661.31, which corresponds to non-phosphorylated peptide 730 - 751 in GST-NLGN1 - enzyme (red), + PKA (grey), + PKC (green), and + CaMKII (blue).

T739 Phosphorylation is Regulated by CaMKII in Mammalian Cells

To monitor the phosphorylation of NLGN1 T739 *in vitro* and potentially *in vivo*, we generated a phosphorylation state-specific antibody (Ab), pT739-Ab, against residues 735-744 (**Figure 3-1A**). The specificity of pT739-Ab was tested with an *in vitro* kinase assay in which GST-NLGN1 (wild-type or T739A), 2, 3, and 4 c-tail fusion proteins were incubated with ATP and CaMKII. The proteins were resolved by SDS-PAGE, and immunoblotting revealed that the phosphorylation state-specific Ab specifically recognized only the NLGN1 c-tail that is phosphorylated on T739 (**Figure 3-2A**). Importantly, the non-phosphorylatable mutant (T739A), as well as any of the other NLGN isoforms subjected to the same *in vitro* kinase assay, showed no immunoreactivity with pT739-Ab, highlighting the specificity of pT739-Ab for phosphorylated NLGN1 T739. It is noteworthy that phosphorylated human NLGN4 was not efficiently detected by pT739-Ab, which reveals that either NLGN4 T718 is not robustly phosphorylated by CaMKII or pT739-Ab is, indeed, specific for phosphorylated NLGN1 T739. Regardless, the CaMKII consensus sequence (RXXT) in NLGN1 and human NLGN4 is completely divergent in rodent NLGN4, and therefore would not be detected in rodent lysate preparations and not a concern in this study (Bolliger et al., 2008). We chose human NLGN4, as it is exclusively used in the literature due to its implications in cognitive disorders (Sudhof, 2008).

To test whether the full-length NLGN1 protein is phosphorylated in intact cells and modulated by CaMKII activity, we transfected NLGN1 wild-type (WT) or T739A in COS-7 cells. Immunoblots of cell lysates probed with pT739-Ab indicated that NLGN1 was phosphorylated on T739 under basal conditions and that no signal was observed with

the phospho-deficient mutant (**Figure 3-2B**). However, after cotransfection with a constitutively active form of CaMKII (T286D) or following incubation with KN93 (a CaMKII inhibitor), the basal level phosphorylation of NLGN1 T739 robustly increased or decreased, respectively (**Figure 3-2B**). Analogous regulation was observed in HEK293T cells, another non-neuronal mammalian cell line (**Figure 3-2C**).

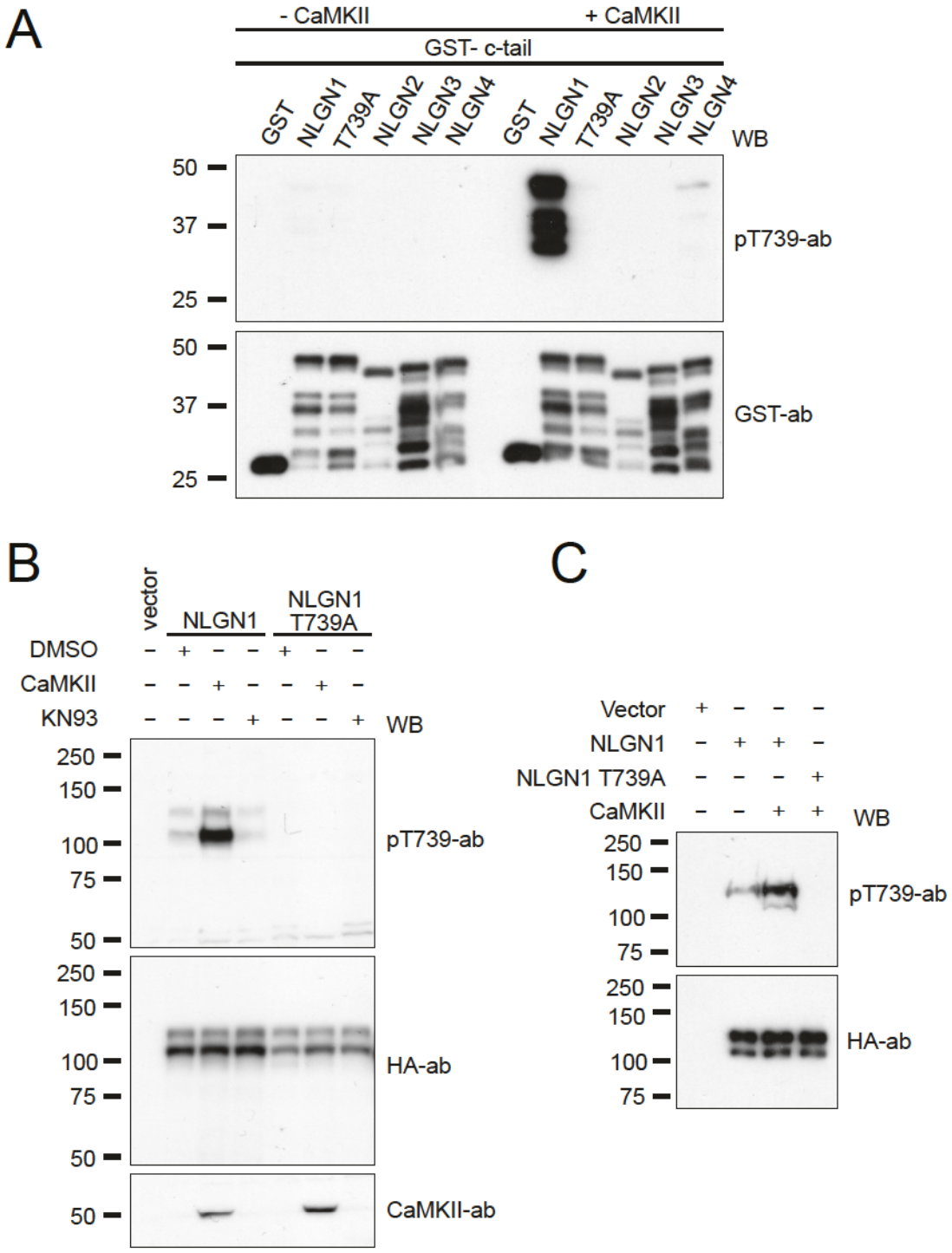

Figure 3-2. NLGN1 T739 is Phosphorylated by CaMKII *in vitro* as Detected by Phosphorylation State-Specific Ab and in Heterologous Cells. A. GST, GST-NLGN1

(WT or T739A), NLGN2, NLGN3, and NLGN4 were phosphorylated *in vitro* with purified catalytic subunits of CaMKII and analyzed by immunoblotting with pT739-Ab. Equal loading of protein was confirmed by immunoblotting with GST-Ab. **B.** NLGN1 (WT or T739A) was transfected in COS cells and treated with a CaMKII inhibitor, KN93, or co-transfected with a constitutively active CaMKII (T286D). **C.** Co-transfection of NLGN1 (WT or T739A) with CaMKII (T286D) in HEK293T cells. Immunoblots were probed with indicated antibodies in **B**,**C**.

T739 Phosphorylation is Regulated by Synaptic Activity and CaMKII in Neurons

The *in vitro* and *in situ* results described thus far demonstrate that CaMKII can phosphorylate NLGN1 T739. To test whether this phosphorylation occurs in neurons, we measured NLGN1 T739 phosphorylation in cultured cortical neurons after 21 days *in vitro* (DIV) and found a specific band at approximately 120 kDa, the estimated molecular weight of full-length, mature NLGN1 (**Figure 3-3A**) indicating basal phosphorylation of this site in neurons. The band was dramatically reduced when cultures were pre-infected with a lentiviral shRNA against NLGN1, demonstrating the specificity of the Ab in neurons. Importantly, total NLGN3 protein levels were not reduced, underscoring the specificity of the NLGN1 knockdown.

To examine if T739 phosphorylation is modulated by synaptic activity, we enhanced synaptic activity by treating cortical cultures with bicuculline (BCC), a $GABA_AR$ antagonist, for 2 hours (hr), which induced a 7-fold increase in NLGN1 T739 phosphorylation relative to a DMSO control (**Figure 3-3B,C**). The induction of phosphorylation with BCC was efficiently blocked with an hour pre-treatment of AP5 and NBQX, NMDA and AMPA receptor antagonists, respectively (**Figure 3-3B,C**), thus indicating NLGN1 T739 phosphorylation is dynamically regulated by changes in neuronal activity. Interestingly, BCC treatment also caused a reduction in total NLGN1 protein that was prevented with AP5/NBQX pretreatment (**Figure 3-3D**), a likely result of NLGN1 N-terminal shedding, as previously observed (Peixoto et al., 2012; Suzuki et al., 2012).

Next, we explored if CaMKII phosphorylates NLGN1 T739 in neurons. To examine this possibility, we used a KD approach in cultured cortical neurons and found

that a 75% reduction in CaMKII levels resulted in a 60% reduction in pT739 levels without effecting total NLGN1 levels (**Figure 3-3E-G**). Taken together with our *in vitro* and *in situ* results, this indicates that CaMKII is the dominant kinase that phosphorylates NLGN1 T739 in neurons.

Finally, to investigate if T739 phosphorylation occurs *in vivo*, we immunoprecipitated (IP) phosphorylated NLGN1 from WT and NLGN1 KO brains and detected a 120 kDa band only in the WT brain (**Figure 3-3H**). This band indicates that a subset of endogenous NLGN1 is phosphorylated at T739 in an intact mouse brain. Collectively, these data highlight that NLGN1 T739 is phosphorylated in live animals and dynamically regulated by synaptic activity in neurons.

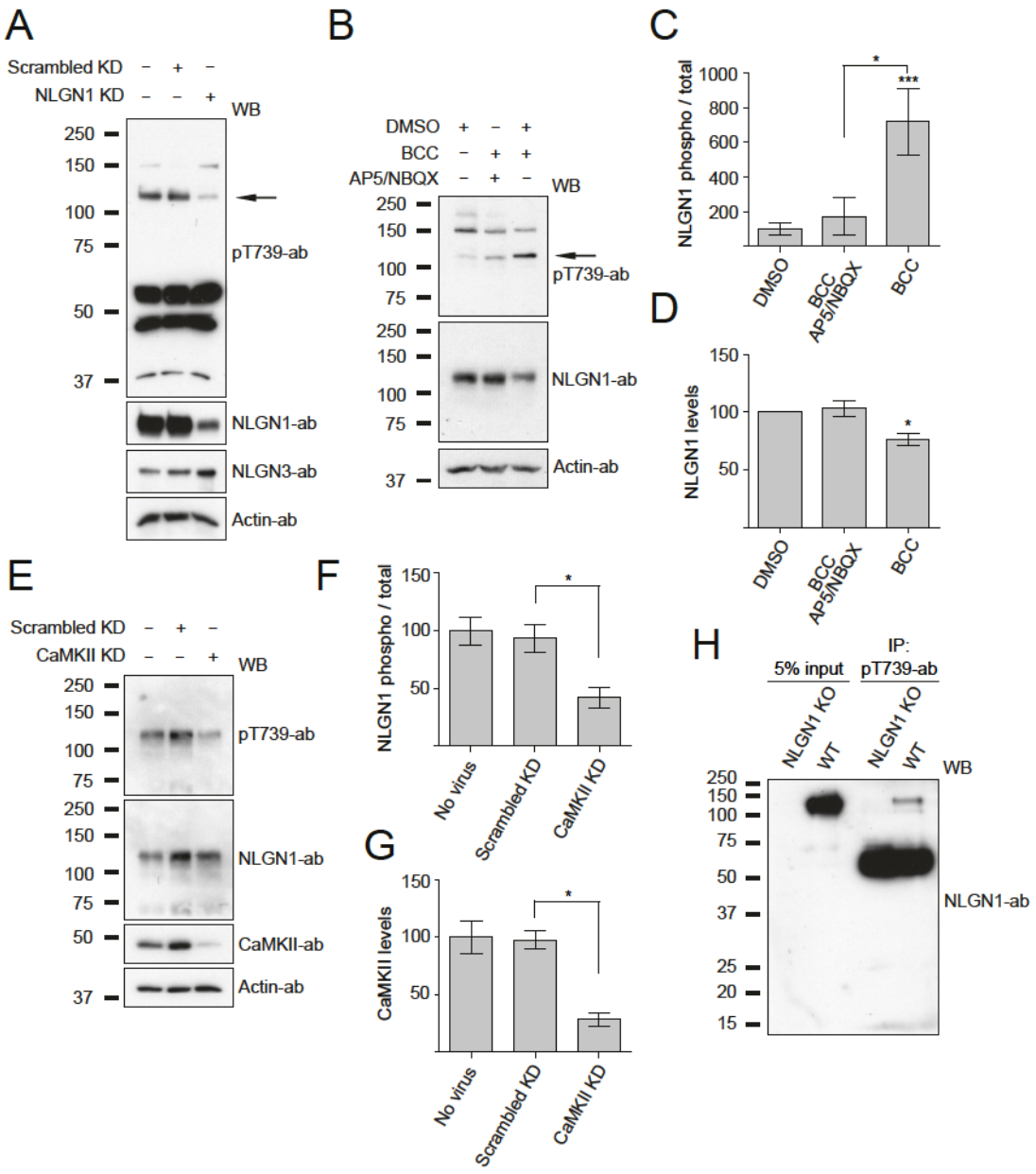

Figure 3-3. **Phosphorylation of NLGN1 T739 in Neurons**. **A.** Detection of NLGN1 T739 phosphorylation in DIV 21 cortical neurons with or without expression of a lentiviral shRNA, scrambled or targeting NLGN1. **B.** Regulation of NLGN1 T739 phosphorylation under control conditions (DMSO) or in the presence of bicuculline (BCC) -/+ pretreatment of AP5/NBQX in DIV 21 cortical neurons. Immunoblots were probed with indicated antibodies. **C.** Means ± SEM of phosphorylated to total NLGN1

normalized to DMSO control (n = 7) with AP-5/NBQX pretreatment + BCC ($P > 0.05$, n = 4), or BCC treatment ($P < 0.0006$, n = 7). **D.** Means ± SEM of total NLGN1 normalized to actin control (n = 7) with AP5/NBQX pretreatment + BCC ($P > 0.05$, n = 4), or BCC treatment ($P = 0.0156$, n = 7). **E.** Detection of NLGN1 T739 phosphorylation in DIV 21 cortical neurons with or without expression of a lentiviral shRNA, scrambled or targeting CaMKII. **F.** Means ± SEM of phosphorylated to total NLGN1 normalized to no virus treatment (n = 4) with scrambled KD ($P > 0.05$, n = 4), or CaMKII KD ($P = 0.0286$, n = 4). **G.** Means ± SEM of total CaMKII normalized to actin control (n = 4) with scrambled KD ($P > 0.05$, n = 4), or CaMKII KD ($P = 0.029$, n = 4). **H.** Detection of NLGN1 T739 phosphorylation in adult WT or NLGN1 KO brains. Arrows denote NLGN1 specific band. $^{*}P < 0.05$, $^{***}P < 0.001$.

Mutation of T739 to A Negatively Regulates the Trafficking of NLGN1

Does T739 function in the trafficking of NLGN1 to the cell surface? We examined the surface expression of NLGN1 (WT or T739A) expressed in cultured hippocampal neurons with immunofluorescence confocal microscopy. As previously described, we performed these experiments on a triple knockdown background to reduce endogenous NLGNs using exogenous chained microRNAs against NLGN1, NLGN2, and NLGN3 (NLmiRs), to prevent the potential masking of NLGN mutation phenotypes by dimerization with WT protein (Shipman et al., 2011). Surface and intracellular receptors were labeled with an anti-hemagglutinin (HA) tag that was inserted downstream of the signal peptide on NLGN1. Remarkably, T739A greatly reduced the surface expression of NLGN1 (**Figure 3-4A,B**) suggesting that phosphorylation regulates NLGN1's forward trafficking or stabilization at the plasma membrane.

NLGN1 T739A reduces functional synapses

Does T739 phosphorylation function in NLGN1-mediated synaptogenesis, by regulating NLGN1 surface expression? To examine this possibility, we used immunofluorescence confocal microscopy and coexpressed NLGN1 (WT or T739A) or GFP with NLmiRs in cultured hippocampal neurons, and assayed endogenous VGLUT1 and PSD-95, presynaptic and postsynaptic markers, respectively. Knockdown of endogenous NLGNs nearly eliminated VGLUT1 and PSD-95 staining, which resulted in a profound decrease in colocalization of these synaptic markers, an anatomical measure of synapse number (**Figure 3-4C-F**). Given the time course of knockdown in a developing neuronal culture, these results are consistent with a role of NLGNs in synapse

assembly or maintenance. T739A expression only partially rescued VGLUT1 and PSD-95 recruitment and colocalization, but to a consistently lesser extent than NLGN1 (**Figure 3-4C-E**).

Moreover, when we compared miniature postsynaptic currents (mEPSCs) in cultured hippocampal neurons transfected with NLmiRs + NLGN1 (WT or T739A), T739A did not enhance mEPSC frequency, as was seen with expression of NLGN1 (**Figure 3-4G,I**). In agreement with previous results, knockdown of endogenous NLGNs (NLmiRs) resulted in a reduction in mEPSC frequency (Shipman et al., 2011) (**Figure 3-4G,I**). Furthermore, no difference in mEPSC amplitudes was observed between NLGN1 and NLGN1 T739A or between GFP and NLmiRs transfected cells (**Figure 3-4G-I**). Interestingly, NLGN overexpression induced a reduction in mEPSC amplitude (**Figure 3-4C,D**), a likely outcome of exogenous NLGN expression increasing cell size. Together, these results implicate a role for T739 phosphorylation in NLGN1-mediated synaptogenesis, a likely consequence of reduced surface expression.

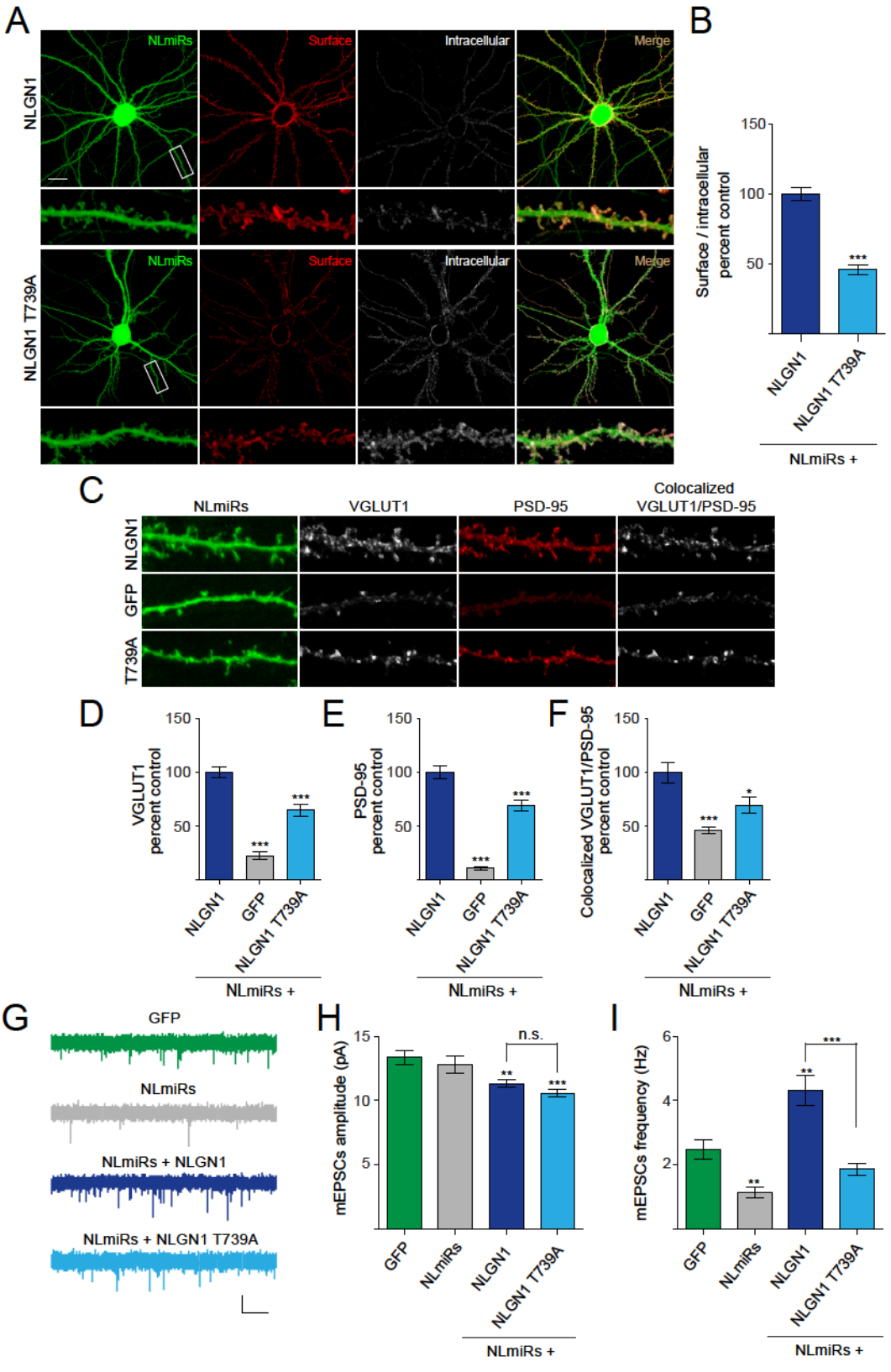
A
NLGN1
NLGN1 T739A
NLmiRs
Surface
Intracellular
Merge
B
Surface / intracellular percent control
150
100
50
***
NLGN1
NLGN1 T739A
NLmiRs +
C
NLmiRs
VGLUT1
PSD-95
Colocalized VGLUT1/PSD-95
NLGN1
GFP
T739A
D
VGLUT1 percent control
E
PSD-95 percent control
F
Colocalized VGLUT1/PSD-95 percent control
*
NLGN1
GFP
NLGN1 T739A
NLmiRs +
G
GFP
NLmiRs
NLmiRs + NLGN1
NLmiRs + NLGN1 T739A
H
mEPSCs amplitude (pA)
15
10
5
n.s.
**
***
GFP
NLmiRs
NLGN1
NLGN1 T739A
NLmiRs +
I
mEPSCs frequency (Hz)
6
4
2
**
***
GFP
NLmiRs
NLGN1
NLGN1 T739A
NLmiRs +

Figure 3-4. **T739A Reduces the Surface Expression and Synaptic Enhancement of NLGN1. A.** Hippocampal neurons co-expressing NLmiRs and NLGN1 (WT or T739A). Surface receptors were labeled with anti-HA Ab and Alexa 555 (red) conjugated secondary Ab. After fixation and permeabilization, internal receptors were visualized with anti-HA and Alexa 647 (pseudo-colored white) conjugated secondary Ab (scale bar = 50 μm). **B.** Means ± SEM normalized to NLGN1 (n = 34) for NLGN1 T739A (P = 0.0001, n = 36). **C.** Neurons transfected as in **a**. VGLUT1 was labeled with anti-VGLUT1 Ab and Alexa 647 (pseudo-colored white) conjugated secondary Ab, and PSD-95 was visualized with anti-PSD-95 and Alexa 555 (red) conjugated secondary Ab. **D.** Means ± SEM of VGLUT1 normalized to NLGN1 (n = 24) for NLmiRs (P = 0.0001, n = 23) and NLGN1 T739A (P = 0.0001, n = 24). **E.** Means ± SEM of PSD-95 normalized to NLGN1 (n = 24) for NLmiRs (P = 0.0001, n = 23) and NLGN1 T739A (P = 0.0001, n = 24). **F.** Means ± SEM of colocalized VGLUT1/PSD-95 puncta normalized to NLGN1 (n = 24) for NLmiRs (P = 0.0001, n = 23) and NLGN1 T739A (P = 0.0182, n = 24). **G.** Representative mEPSC traces of GFP, NLmiRs, and NLmiRs + NLGN1 (WT or T739A) expressing hippocampal neurons (scale bar: 15 pA/500 ms). **H.** Spontaneous mEPSC mean amplitudes ± SEM of cells transfected with GFP (n = 9), NLmiRs (P > 0.05, n = 9), NLmiRs + NLGN1 (P = 0.0028, n = 9), and NLmiRs + NLGN1 T739A (P = 0.0003, n = 9) as compared to GFP transfected cells. NLGN1 T739A has no change in mEPSC amplitude when compared to NLGN1 (P > 0.05, n = 9). **I.** Spontaneous mEPSCs mean frequencies ± SEM of cells transfected with GFP (n = 9), NLmiRs (P = 0.0031, n = 9), NLmiRs + NLGN1 (P = 0.0012, n = 9), and NLmiRs + NLGN1 T739A (P > 0.05, n = 9)

as compared to GFP transfected cells. NLGN1 T739A reduces mEPSC frequency when compared to NL-1 ($P = 0.0001$, $n = 9$). $^{*}P < 0.05$ $^{**}P < 0.01$, $^{***}P < 0.001$.

T739A mitigates activity-induced increases in NLGN1 surface expression

NLGN1 mobilization and surface expression can be dynamically modulated by high frequency stimulation and synaptic plasticity (Gutierrez et al., 2009; Schapitz et al., 2010). Does T739 phosphorylation function in activity-induced increases in NLGN1 surface expression? To investigate this possibility, we used immunofluorescence confocal microscopy to compare the surface expression of NLGN1 (WT and T739A) -/+ 2 hr BCC treatment (the same duration used to induce T739 phosphorylation, **Figure 3-3B,C**) when expressed in cultured hippocampal neurons (analogous setup as in **Figure 3-4**). BCC induced a modest increase in NLGN1 surface expression (**Figure 3-5A,B**). Importantly, the activity-driven increase in NLGN1 surface expression was eliminated in the T739A mutant (**Figure 3-5A,B**).

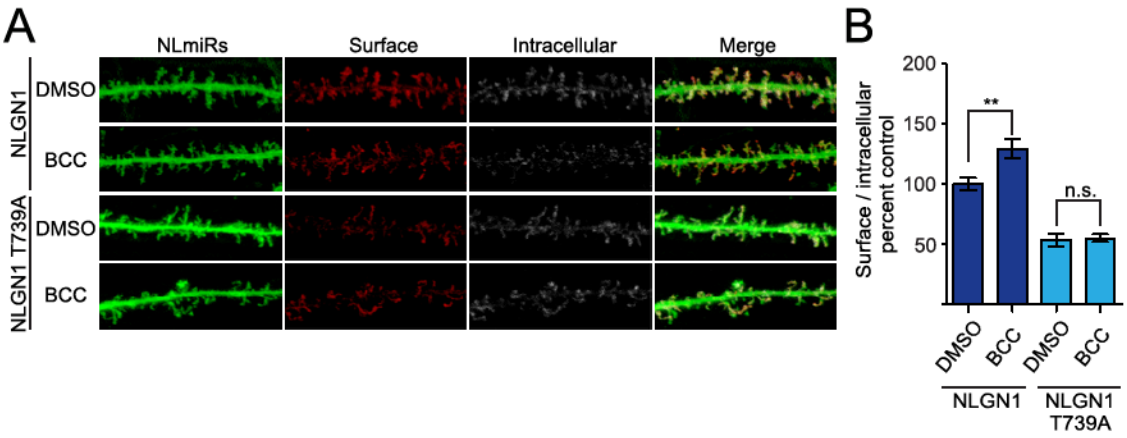

Figure 3-5. Activity-Dependent Increase in NLGN1 Surface Expression is Diminished in NLGN1 T739A. A. Hippocampal neurons co-expressing NLmiRs and NLGN1 (WT or T739A), as in **Figure 3-4A**, were treated for 2 hr with DMSO or BCC. **B.** Means ± SEM normalized to NLGN1 + DMSO (n = 36) for NLGN1 + BCC (P = 0.0027, n = 34) or NLGN1 T739A + DMSO (n = 28) for NLGN1 T739A + BCC (P > 0.05, n = 28). $^{**}P < 0.01$.

NLGN1 Induced Enhancement of Synaptic Currents is Diminished by T739A

Postsynaptic expression of NLGN1 results in a robust enhancement of excitatory postsynaptic currents (Chubykin et al., 2007; Futai et al., 2007; Shipman and Nicoll, 2012a; Shipman et al., 2011). Might T739 function in NLGN1 induced synaptic potentiation? To test this, we expressed NLGN1 (WT or T739A) in organotypic hippocampal slice cultures using sparse biolistic transfection, which allows for the simultaneous recording of evoked excitatory currents in both transfected and neighboring control cells. The magnitude of the evoked current in the transfected cell compared to the non-transfected control cell functions as a readout of the experimental manipulation on synaptic strength. Previously, we saw no significant effect of activity block or the T739A mutant compared to WT upon high levels of NLGN1 expression (data not shown) (Shipman et al., 2011). We wondered if the high levels might have obscured any effect of activity and decided to reduce the expression level by placing the NLGN1 gene after the internal ribosomal entry site (IRES). Under reduced expression levels, NLGN1 was still able to robustly potentiate both AMPAR and NMDAR currents, but interestingly, at these reduced levels, NLGN1 T739A did not potentiate AMPAR (**Figure 3-6A,B**) or NMDAR (**Figure 3-6C,D**) currents beyond those in neighboring control cells. Notably, the differences in synaptic strength between NLGN1 and NLGN1 T739A are not the result of changes in glutamate release, as paired-pulse ratios of AMPAR currents, a measure of presynaptic release probability, were unchanged in the transfected cells as compared to untransfected cells (**Supplementary Figure 3-2A-C**)

A previous report has highlighted that NLGN1-mediated postsynaptic enhancement is dependent on synaptic activity, and specifically on CaMKII activation

(Chubykin et al., 2007). Remarkably, with the reduced expression level we now found that activity blockade with AP5 and NBQX mirrored the diminished postsynaptic enhancement seen with expression of NLGN1 T739A (**Figure 3-6A-D**). Cells expressing NLGN1 T739A with the same drug treatment did not display a further decrease in synaptic strength (**Figure 3-6A-D**).

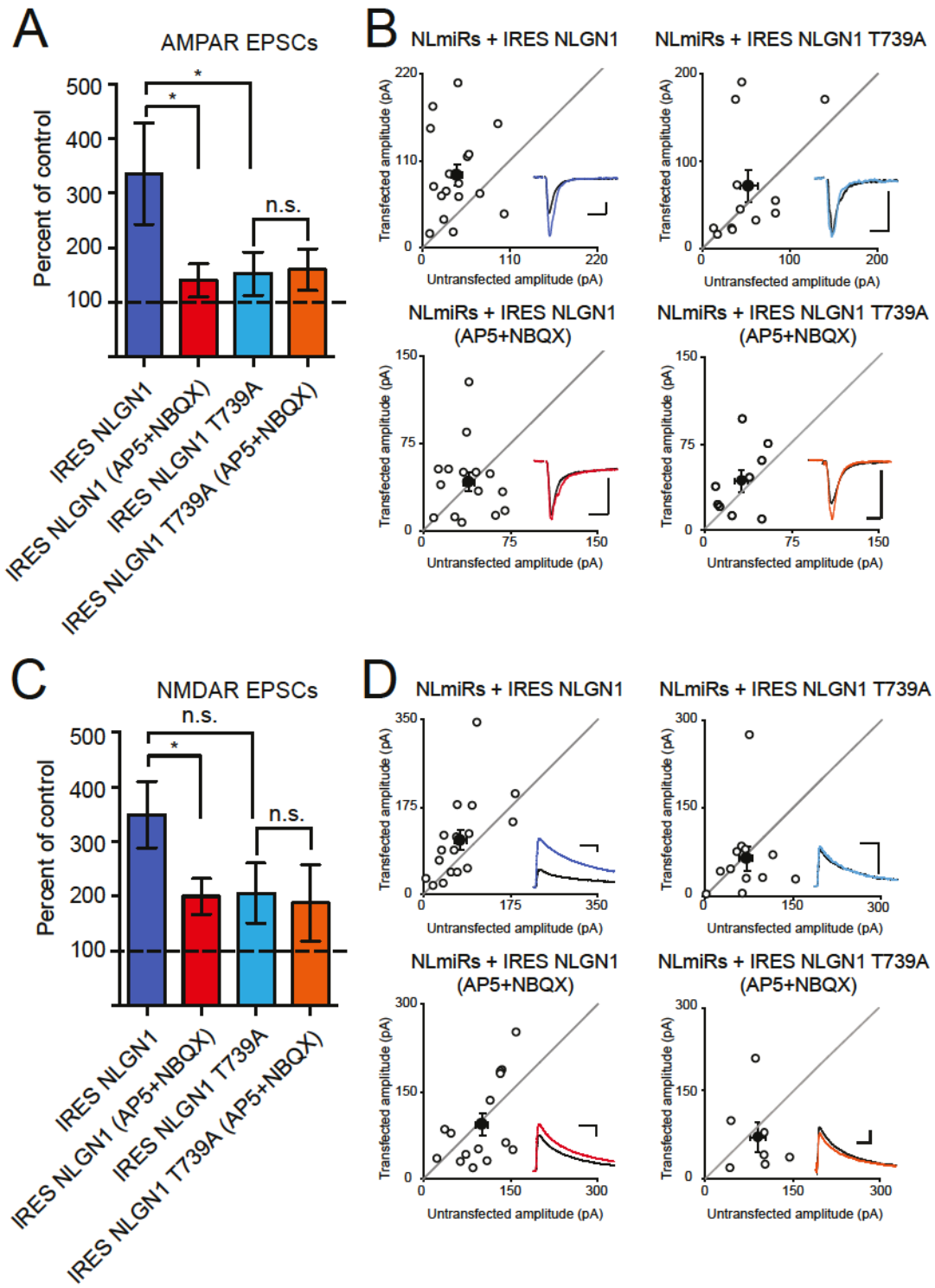
A
AMPAR EPSCs
Percent of control
500
400
300
200
100
*
*
n.s.
IRES NLGN1
IRES NLGN1 (AP5+NBQX)
IRES NLGN1 T739A
IRES NLGN1 T739A (AP5+NBQX)
B
NLmiRs + IRES NLGN1
NLmiRs + IRES NLGN1 T739A
NLmiRs + IRES NLGN1 (AP5+NBQX)
NLmiRs + IRES NLGN1 T739A (AP5+NBQX)
Transfected amplitude (pA)
Untransfected amplitude (pA)
C
NMDAR EPSCs
n.s.
*
n.s.
D

Figure 3-6. Synaptic Enhancement by NLGN1 is Reduced by Either Glutamate Receptor Blockade or the T739A Mutation. A. Low level postsynaptic expression of NLGN1 (n = 17) results in an enhancement of AMPAR-mediated currents to a greater extent than the expression of NLGN1 in the presence of AP5 and NBQX (P = 0.0439, n = 15) or the expression of NLGN1 T739A (P = 0.0470, n = 12). Expression of NLGN1 T739A in presence of AP5/NBQX did not further reduce AMPAR currents (P > 0.05, n = 9). Plotted as percent of control (mean ± SEM), comparing transfected cells to simultaneously recorded, neighboring untransfected cells. All expression is on the background of the NLmiRs. **B.** Scatter plots showing individual conditions summarized in **A**. Open circles represent individual paired recordings, while filled circles represent means ± SEM. Traces show representative currents for each condition, with the transfected cell in color and the control cell in black (scale bar: 30 pA/20 ms). **C.** A similar result is shown for NMDAR-mediated currents, with a greater enhancement by low level postsynaptic expression of NLGN1 (n = 17) than NLGN1 expression in the presence of AP5/NBQX (P = 0.0363, n = 15) or the expression of NLGN1 T739A (P = 0.0599, n = 12). Expression of NLGN1 T739A in the presence of AP5/NBQX did not further reduce NMDAR currents (P > 0.05, n = 7). Bar graph as in **A**. **D.** Scatter plots showing individual conditions summarized in **B**. Open circles represent individual paired recordings, while filled circles represent means ± SEM. Traces show representative currents for each condition, with the transfected cell in color and the control cell in black (scale bar: 60 pA/100 ms). $^{*}P < 0.05$.

Sensory-Experience Induces NLGN1 T739 Phosphorylation

Finally, we examined if NLGN1 T739 phosphorylation is modulated by synaptic activity *in vivo*. Initially, we discovered that T739 is robustly phosphorylated in the visual cortex, an area of sensory-evoked synaptic refinement (Philpot et al., 2001) (**Figure 3-7A**). To accurately identify changes in phosphorylation levels between varying conditions and brain samples, we used protein lysate concentrations that did not saturate the amount of Ab we used to IP (**Supplementary Figure 3-3A,B**). To test if T739 phosphorylation is regulated by synaptic activity *in vivo*, we used a well-established dark-rearing (DR) paradigm that involves light depriving mice for 5 days (P21-26) and re-exposing them to light for 2 hr (DR + LR). This procedure induces anatomical, functional, and synaptic reassembly and refinement of cortical circuits in the developing visual cortex (Philpot et al., 2001; Tropea et al., 2010). DR mice had a reduction in T739 phosphorylation (**Figure 3-7B,C**) compared to their light-reared (LR) littermates. Furthermore, DR mice that were subjected to a 2 hr LR (DR + LR) had an increase in NLGN1 T739 phosphorylation when compared to LR or DR littermates (**Figure 3-7B,C**). These results show that increases or decreases in neuronal activity can modulate NLGN1 T739 phosphorylation *in vivo*.

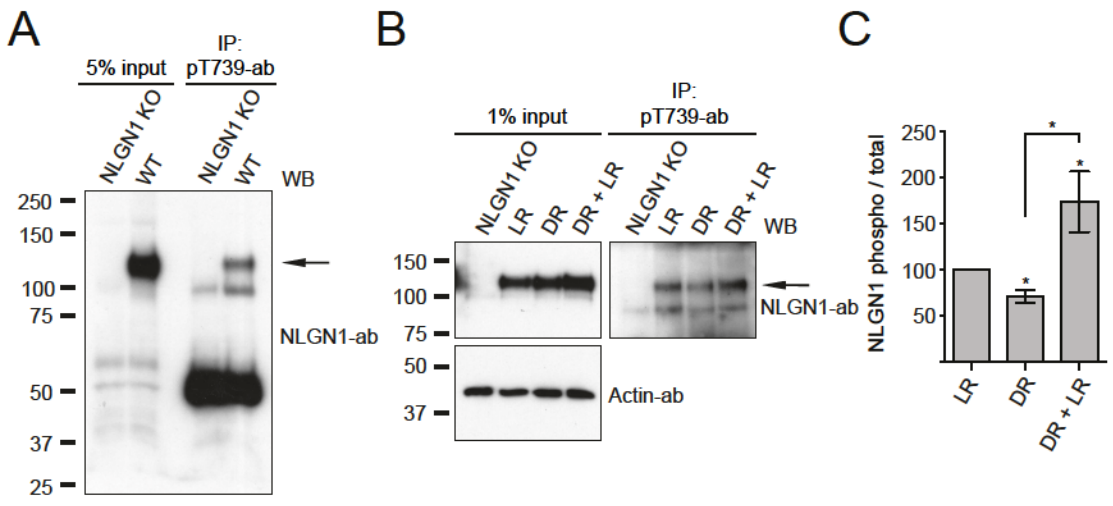

Figure 3-7. Synaptic Activity Dynamically Regulates T739 Phosphorylation *in vivo*.

A. Detection of NLGN1 T739 phosphorylation in adult WT or NLGN1 KO visual cortex. **B.** WT mice were either light-reared for 26 days (LR), LR to P21 then subjected to 5 days dark-rearing from P21-26 (DR), or LR then subjected to a 5 day dark-rearing (P21-26) and finally exposed to a 2 hr light stimulus at P26 (DR + LR). When animals were LR they were maintained on a normal day/night cycle, whereas DR animals were in complete darkness for 5 days. **C.** Regulation of NLGN1 T739 phosphorylation in DR, LR, or DR + LR P26 visual cortices. Adult NLGN1 KO visual cortices served as negative controls and actin served as a total protein control. Non-saturating protein concentrations (0.25 mg) were used as described in **Supplementary Figure 3-3A**,**B**. **D.** Means ± SEM of phosphorylated (IP) to total NL-1 (input) normalized to LR control (n = 7) for DR ($P = 0.0156$, n = 7) and DR + LR ($P = 0.0469$, n = 7). All comparisons between conditions were using littermates. $^{*}P < 0.05$.

DISCUSSION

Our findings indicate a direct and novel functional interplay between NLGN1 and CaMKII, two hallmarks of excitatory synapses, which results in the activity-dependent phosphorylation of NLGN1 at residue T739. Furthermore, using a combination of techniques we found that a non-phosphorylatable mutant, T739A, displayed diminished basal and activity-induced NL-1-mediated synaptic potentiation.

Interestingly, NLGN3, the other NLGN isoform known to localize to excitatory synapses, which can also dimerize with NLGN1, does not undergo the same protein modification. This is also the case for NLGN2, although its endogenous localization is restricted to inhibitory synapses (**Figure 3-1C**). When aligning the c-tail sequences of NLGN1, NLGN2, and NLGN3, the analogous residue in NLGN3 is an alanine and not a threonine and contains a glycine insertion within the RXXT CaMKII consensus motif of NLGN1. Comparably, NLGN2 contains a 12 amino acid insertion in the corresponding region that is not contained in NLGN1, NLGN3, or NLGN4. Therefore, the sequences of NLGN2 and NLGN3 are sufficiently divergent from NLGN1 such that the consensus sequence is not conserved and is unsuitable for CaMKII phosphorylation. To the best of our knowledge, this represents the first reported biochemical distinction between the c-tails of NLGN1 and NLGN3. Conventional domains on the c-tail such as the PDZ ligand and the gephyrin binding domain are conserved among all NLGN isoforms (**Figure 3-1A**) (Poulopoulos et al., 2009). A newly discovered critical residue, important in regulating NLGN-mediated postsynaptic effects at excitatory synapses, is evolutionarily preserved between NLGN1 and NLGN3 (NLGN1 E747 and NLGN3 E740, see **Figure 3-1A**) (Shipman et al., 2011). Additionally, a recent study found Y782 as a phosphorylation

site on the c-tail of NLGN1 (Giannone et al., 2013). This residue is conserved among all NLGNs (NLGN2 Y770, NLGN3 Y772, and NLGN4 Y760, see **Figure 3-1A**) and may represent an evolutionarily conserved phosphorylation site. The significance of CaMKII phosphorylation of NLGN1, but not NLGN3, in this region may underscore differences in synaptogenic strength, mobility, or subcellular localization between NLGN1 and NLGN3. Alternatively, it is possible that through dimerization with NLGN1, T739 phosphorylation could regulate NLGN3 cellular or surface localization. All of these possibilities certainly deserve attention in future studies.

Our findings show that CaMKII phosphorylates NLGN1 T739 *in vitro,* in heterologous cells, and in neurons. PKA and PKC, two activity-dependent kinases with similar consensus sequences and localizations to CaMKII, are unable to phosphorylate NLGN1 T739 *in vitro* (**Figure 3-1E-G**). Moreover, KD of CaMKII in heterologous cells (**Figure 3-2B**) and neurons (**Figure 3-3E-G**) results in a dramatic decrease in T739 phosphorylation. Likewise, overexpression of a constitutively active CaMKII in heterologous cells results in a dramatic increase in T739 phosphorylation (**Figure 3-2B,C**). Furthermore, the previous finding that NLGN1 synaptic potentiation is diminished with chronic blockade of CaMKII again supports CaMKII-specific regulation of NLGN1 (Chubykin et al., 2007). However, we cannot definitively rule out the possibility other kinases phosphorylate T739.

In addition to the proper trafficking of NLGN1 under basal conditions, there is literature that suggests NLGN1 mobility is upregulated following increases in activity, specifically showing an increase in NLGN1 surface expression (Gutierrez et al., 2009; Schapitz et al., 2010). Indeed, we were able to reproduce these findings as we detected a

significant rise in NLGN1 surface expression following elevated network activity. Notably this activity-triggered increase was absent for NLGN1 T739A suggestive of a model in which activity promotes CaMKII phosphorylation of NLGN1 T739 further stabilizing or inducing the forward trafficking of NLGN1 to the plasma membrane. It is tempting to speculate that this increase in surface expression might lead to activity-dependent synaptogenesis or spine growth. Importantly, previous methods to assess activity-driven NLGN1 mobility have varied in the stimuli or drug treatment protocol, whether plasticity was induced, and techniques to gauge surface expression (Schapitz et al., 2010). It is possible there are different mechanisms of increasing NLGN1 surface expression, which are examined under the varying protocols. Because of these caveats we will refrain from concluding that T739 is the master switch in promoting activity-driven NLGN1 surface expression. Additionally, there may be activity-dependent mechanisms independent of increasing NLGN1 surface expression that contribute to NLGN1's activity-dependent potentiation. These possibilities, taken together with our results, still lead us to conclude that T739A is a prominent modulator of activity-induced NLGN1 surface expression.

The molecular mechanism that regulates NLGN1 surface expression through CaMKII phosphorylation of T739 still remains to be elucidated. The substitution of T739 to an alanine (phospho-deficient mutation) decreased the forward trafficking or stabilization of NLGN1 at the cell surface. Thus suggesting that phosphorylation could promote a protein-protein interaction or break a retention interaction in the secretory pathway thereby promoting or stabilizing NLGN1 at the plasma membrane. The substitution of T739 to an aspartate also reduced surface expression of NLGN1 (data not

shown). This supports a dynamic role for T739 phosphorylation and is consistent with the non-phosphorylated threonine being critical at some stage of the trafficking process. Alternatively, the phospho-mimetic may be unable to sterically mimic the phospho group, as is often seen in the literature (Esteban et al., 2003).

A previous report by our group failed to see an activity-dependent effect on NLGN1 induced potentiation in organotypic slice cultures (Shipman et al., 2011). A key distinction between the prior and current study is that we previously used high expression levels of NLGN1, whereas in the current study we reduced total NLGN1 expression levels and now observed a significant activity-dependent effect of NLGN1, as well as a decrease in postsynaptic currents by T739A both of which were not observed upon high expression levels. These results suggest that relative NLGN levels may be critical when assessing trafficking or phenotype of other NLGN mutations. Furthermore, this may underlie apparent inconsistencies in the literature that varied in promoter strength, method, and efficiency of plasmid entry.

Recent studies have identified an activity-dependent proteolytic cleavage of the extracellular domain of NLGN1 that is regulated by the activation of NMDAR and subsequently CaMKII (Peixoto et al., 2012; Suzuki et al., 2012). How might CaMKII, or synaptic activity more generally, induce increases in NLGN1 surface expression and cleavage? In the present study, NLGN1 cleavage was not directly assessed, but we did observe a reduction in endogenous NLGN1 protein after 2 hr BCC treatment that was blocked in the presence of AP5/NBQX (**Figure 3-3B,D**) with the most conceivable explanation being activity-induced NLGN1 cleavage. As previously discussed, if network activity (a mechanism to activate CaMKII) promotes the surface expression of NLGN1, it

would present matrix metalloprotease 9 (MMP9) more NLGN1 substrate on the plasma membrane to cleave. Although increasingly complex hypotheses of how activity can regulate both NLGN1 surface expression and cleavage are plausible, we deem this explanation to be the most parsimonious based on the literature and our results.

The relationship between NLGNs and the etiology of autism remains unclear. Mutations in the extracellular domains of NLGN3 and NLGN4 have been associated with the disease with a sole mutation found in the cytoplasmic tail of NLGN3 (Etherton et al., 2011; Jamain et al., 2003; Yan et al., 2005). Although we cannot directly relate NLGN1 T739 phosphorylation to the pathogenesis of autism, the principle of posttranslational modifications modulating NLGN function and subcellular localization may indirectly contribute to the pathology. Interestingly, NLGN3 R451C, the most intensely studied NLGN autism mutation, displays secretory trafficking deficits and is retained in the endoplasmic reticulum, thus underlining the importance of the proper targeting of NLGNs and the drastic phenotypes seen by a single point mutant on the localization (Comoletti et al., 2004). We believe our findings elucidate a new avenue of future research, which may focus on how point mutations affect posttranslational modifications that perturb NLGN function.

Our present results further advance the NLGN field and introduce a compelling new acute and local mechanism of NLGN regulation, protein phosphorylation. Although protein phosphorylation has been shown to positively or negatively regulate numerous neuronal proteins, this is the first isoform-specific phosphorylation site described on any NLGN protein. Such a mechanism of regulation may also be observed in other NLGN isoforms or in other recently discovered postsynaptic organizer molecules such as

LRRTMs and may contribute to isoform specificities seen in imaging and electrophysiological experiments (Linhoff et al., 2009). Furthermore, the expanding association of NLGNs with cognitive disorders, particularly implications of improper NLGN trafficking, leads one to speculate that better understanding of NLGN function and regulation may provide therapeutic strategies for synaptic dysfunction in clinical applications.

ACKNOWLEDGEMENTS

We are grateful to Antonio Sanz-Clemente and Annalisa Scimemi for technical assistance, and for discussions on the project and manuscript. We thank the NINDS sequencing facility and light imaging facility for their expertise.

AUTHOR CONTRIBUTIONS

M.A.B. designed experiments, performed all biochemical and imaging experiments, conducted electrophysiology experiments in disassociated hippocampal cultures, executed data analysis. M.A.B. and K.W.R. wrote the manuscript. S.L.S. and B.E.H. designed and conducted all electrophysiology experiments in slice cultures. T.H. designed constructs and aided in biochemistry and imaging experiments. Y.L. performed and analyzed all mass spectrometry data. J.D.B. aided in animal and biochemical experiments. K.W.R., J.S.D., and R.A.N. helped design experiments and supervised the project.

MATERIALS and METHODS

Plasmids, Antibodies, and Neuronal Cultures. Mouse pCAG-HA-NLGN1 (or T739A)-IRES-mCherry, pCAG-eGFP, pCAG-NLmiRs-GFP, and pCMV-CaMKII T286D plasmids were used for biochemical, electrophysiological (dispersed hippocampal cultures), and imaging experiments (Shipman et al., 2011). pCAG-IRES-NLGN1 (or T739A), in which the protein was subcloned under IRES to reduce expression, was used for organotypic slice culture experiments. All NLGN1 constructs were RNAi proof as described previously (Shipman et al., 2011). Point mutations were made using PCR-

based mutagenesis (QuikChange Site-Directed Instruction Manual). The primers used to construct NLGN1 T737A were Forward (FOR) 5'-GTGCAGCCCTCAGCGCGCGACC ACCAACGACCTAAC-3' and Reverse (REV) 5'-GTTAGGTCGTTGGTGGTCG CGCGCTGAGGGCTGCAC-3', NLGN1 T738A were FOR 5'-GCAGCCCTCAGCG CACGGCCACCAACGACCTAACCC-3' and REV 5'-GGGTTAGGTCGTTGT GGCCGTGCGCTGAGGGCTGC-3', and NLGN1 T739A were FOR 5'-CTCAGCGC ACGACCGCCAACGACCTAACC-3' and REV 5-'GGTTAGGTCGTTGGCGGTC GTGCGCTGAG-3'. GST c-tail constructs were amplified with synthetic primers containing EcoR1 and XhoI flanking regions from pCAG-NLGN1 (mouse), NLGN2 (rat), NLGN3 (human), and NLGN4 (human) plasmids and subcloned into the glutathione S-transferase (GST) fusion vector pGEX-6P-1 (GE Healthcare). To generate the phosphorylation state-specific antibody (pT739-Ab), rabbits were immunized with a synthetic phosphopeptide Ac-CQRTT(pT)NDLTH-amide corresponding to amino acids 735-744 of NLGN1 generated by New England Peptide. Sera were collected and affinity-purified with an antigen-phosphopeptide. All immunoblotting using NLGN1 T739-Ab began with an hour blocking in 5% PhosphoBLOCKER (CELL BIOLABS, INC) at room temperature, followed by 1% PhosphoBLOCKER in the primary and secondary Ab incubations. Antibodies used in the study were anti-NLGN1 4C12 (Synaptic Systems, 1:1000), anti-GST (Bethyl Laboratories, 1:50000), anti-HA rat (Roche, 1:1000), anti-HA rabbit (Abcam, 1:1000), anti-NLGN3 (Neuromab, 1:1000), anti-CaM Kinase II (Thermo Scientific, 1:1000), anti-PSD-95 (Neuromab, 1:1000), anti-VGLUT1 (Millipore, 1:5000) and anti-actin (ABM, 1:5000). Primary cultured neurons were isolated from E18 Sprague-Dawley rats. Cortical neurons were used for biochemical experiments as the

cortex provides sufficient material for protein analysis. Hippocampal cultures were used for immunocytochemistry and electrophysiology experiments. The use and care of animals used in this study followed the guidelines of the NIH Animal Research Advisory Committee.

GST-Fusion Protein Production and *In Vitro* Phosphorylation. Using the protocol provided by GE Healthcare, GST-fusion proteins were purified from BL21 bacterial cells transformed with pGEX-NLGN1 NLGN2, NLGN3, NLGN4, or GluA1. 50-ml cultures were grown at 37°C to A_{600}=1.1-1.2 after adding 1 ml of overnight cultures. To induce protein expression, 50 uM IPTG was added to the cultures, and they were grown at 16°C for 10-12 hr. The cells were then lysed with a sonicator in a TBS buffer containing protenase inhibitors (Roche), 100 ug/ml lysozyme, 1 mM DTT, and 0.2 mM EDTA. The sonicated lysate was incubated with a 10:1 ratio with glutathione-Sepharose 4B (GE Healthcare) for 1 hr at 4°C and subsequently washed extensively with TBS buffer. For PKA *in vitro* phosphorylation, GST-fusion proteins were phosphorylated in 10 mM HEPES (pH 7.0), 20 mM $MgCl_2$, 50 µM ATP, 1 pmol of [γ-^{32}P]ATP (3000 Ci/mmol) with 50 ng of purified PKA catalytic subunit (Promega). For PKC phosphorylation, reactions were performed in 20 mM HEPES, pH 7.4, 1.67 mM $CaCl_2$, 1 mM DTT, 10 mM $MgCl_2$, 50 µM ATP, 1 pmol of [γ-^{32}P]ATP (3000 Ci/mmol) with 10 ng of purified PKC (Promega). For CaMKII phosphorylation, reactions were executed in 20 mM Tris-HCl (pH 7.5), 10 mM $MgCl_2$, 0.5 mM DTT, 0.1 mM EDTA, 2.4 µM calmodulin, 2 mM $CaCl_2$, 100 µM ATP, 1 pmol of [γ-^{32}P]ATP (3000 Ci/mmol) with 25 ng of recombinant CaMKIIα (Calbiochem). All *in vitro* kinase assays were performed at 30°C for 30 minutes (min), except when otherwise stated. The reactions were halted with addition of

SDS-PAGE sample buffer and incubation at 65°C for 5 min. The proteins were resolved by SDS-PAGE and visualized by autoradiography. For *in vitro* kinase assays analyzed by immunoreactivity, SDS-PAGE separated proteins were transferred to PVDF membranes and assayed for phosphorylation (or total protein) by immunoblotting with their respective antibodies.

Mass Spectrometry. Samples were alkylated with iodoacetamide, digested with chymotrypsin overnight at 25°C. Peptides were analyzed by a nano-LC/MS/MS system with an Ultimate 3000 HPLC (Thermo-Dionex) connected to an Orbitrap Elite mass spectrometer (Thermo Scientific) via an Easy-Spray ion source (Thermo Scientific). Peptides were separated on ES800 Easy-Spray column (75 μm inner diameter, 15 cm length, 3 μm C18 beads; Thermo Scientific) at a flow rate of 300 nl/min with a 25 min linear gradient of 2–27% mobile phase B (mobile phase A: 2% acetonitrile, 0.1% formic acid; mobile phase B: 98% acetonitrile, 0.1% formic acid). Thermo Scientific Orbitrap Elite mass spectrometer was operated in positive nano-electrospray mode. MS data were acquired in both profile and data dependent modes. The resolution of the survey scan was set at 60k at m/z 400 with a target value of 1×10^6 ions. The m/z range for MS scans was 300–2000. The isolation window for MS/MS fragmentation was set to 1.9 and the top two most abundant ions were selected for product ion analysis. Ion trap enhanced scan rate was used for the MS/MS data acquisition with decision tree procedure activated. Dynamic exclusion was 9 seconds and early expiration was abled. Xcalibur RAW files were converted to peak list files in mgf format using Mascot Distiller (version 2.4.3.3). Database search was performed using Mascot Daemon (2.4.0) against a house-built database containing NCBI human sequences and GST-NLGN1 sequence.

Immunoblotting. HEK293T or COS cells were transfected using Liptofectamine 2000 Reagent (Invitrogen). 1-2 days following transfection, cells were washed in PBS and collected in a TBS buffer containing 150 mM NaCl, 50 mM Tris-HCl, 1 mM EDTA, protease (Roche), and phosphatase (Sigma) inhibitors. After centrifugation, pelleted cells were lysed directly with SDS-PAGE sample buffer and subjected to Western blotting. KN93 (Tocris) or DMSO (Sigma) treatment occurred 2 hr before cell isolation. DIV 21 cortical neurons were isolated and lysed with the same protocol as HEK293T and COS cells. Treatment with 40 μM bicuculline (Tocris) or DMSO began 2 hr before cell isolation or an hour after AP5 (Tocris) and NBQX (Tocris) treatment. For brain IPs, WT or NLGN1 KO brains were homogenized in TEVP buffer (20 mM Tris (pH 7.5), 0.32 M sucrose, 5 mM EDTA, and protease and phosphatase inhibitors). Homogenates were centrifuged at 800*g* for 10 min, then the nuclear pellet was discarded and the supernatant was centrifuged at 9400*g* for 15 min. The P2 membrane fraction was resuspended in TEVP buffer supplemented with 1% SDS and 150 mM NaCl, gently sonicated, and incubated at 37°C for 15 min. The lysate was then neutralized with 10-fold TEVP buffer supplemented with 2% triton x-100 and 150 mM NaCl for a minimum of 15 min at 4°C. The neutralized lysate was incubated with pT739-Ab and protein A-Sepharose beads (GE Healthcare) at 4°C overnight. Samples were immunoblotted with NLGN1 4C12 Ab after 3 washes in TEVP buffer. To knockdown NLGN1 or CaMKII in neurons, we subcloned a short hairpin targeting the rodent NLGN1 sequence GGAAGGTACTGGAAATCTATA (previously characterized) (Chih et al., 2005) or CaMKII sequence TCCTCTGAGAGCA CCAACA under the ubiquitin promoter in a FUGW lentivirus vector. To produce the virus, the hairpin targeting vector, a viral packaging vector, and a VSVG envelope vector

were co-transfected into HEK-293FT cells using FUGENE (Roche). Supernatants were collected 48 h after transfection, centrifuged at 82,000*g* to pellet the lentivirus, and resuspended in phosphate-buffered saline. Cortical neurons (6-well dish) were infected with 3-5 μL of concentrated virus for 7-10 days.

Immunocytochemistry. Cultured hippocampal neurons (DIV 10-12) were grown on glass coverslips precoated with poly-D-Lysine (Sigma) and co-transfected with NLmiRs and HA-NLGN1 (WT or T739A) with Liptofectamine 2000 and analyzed at DIV 14-16. To label surface protein, transfected live cells were labeled with anti-HA (rat) Ab for 10 min at room temperature. Cells were washed in PBS and then fixed in 4% paraformaldehyde/4% sucrose in PBS for 8 min. The cells were incubated with Alexa 555 conjugated (red) anti-rat secondary Ab (Molecular Probes). Following surface staining, cells were extensively washed and permeabilized in 0.25% TX-100, blocked in 10% normal goat serum, and labeled with anti-HA (rabbit, 1:200) Ab. After being washed with PBS, cells were labeled with Alexa 647 conjugated (blue) anti-rabbit secondary Ab (shown in white, 1:500) and mounted with a ProLong Gold Antifade kit (Molecular Probes). Experiments that involved treating cultures with DMSO or 40 μM bicuculline had drug application 2 hr prior to surface staining. For endogenous VGLUT1 and PSD-95 staining, cells were fixed, permeabilized, and blocked as described above. Then labeled with anti-VGLUT1 (guinea pig, 1:5000) and anti-PSD-95 (mouse, 1:100) Ab(s). Following primary Ab incubation, the cells were washed extensively and labeled with Alexa 647 conjugated (blue) anti-guinea pig secondary Ab (shown in white, 1:500) and Alexa 555 conjugated (red, 1:500) anti-mouse secondary Ab and mounted as described above. All primary and secondary Ab incubations were performed in the

BioWave Pro (Pelco). Neurons were imaged with a 63X objective on a Zeiss LSM 510 confocal microscope. For analysis, images from three dendrites per neuron from at least seven neurons per experiment were collected and quantitated by normalizing the fluorescence intensity of the surface expressed NLGN1 (or T739A) with the fluorescence intensity of total NLGN1 (or T739A) in each cell using MetaMorph Version 7 (Universal Imaging). The fluorescence intensities of VGLUT1 and PSD-95 were measured similarly with the number of colocalized puncta obtained from 3-4 regions of 30 μm/cell. Cell selection was not done in the blind and was based on positive transfection but all data analysis was done in the blind. Three independent experiments were performed per experiment, and the number of neurons (n) per condition is located in the corresponding figure legend.

Electrophysiology. Whole-cell voltage clamp recordings of miniature excitatory postsynaptic currents (mEPSC) were performed in cultured hippocampal neurons. The time, duration, and co-transfection protocol are analogous to the procedures used in the immunocytochemistry experiments. Recordings were made at 20-25°C using glass patch electrodes filled with an internal solution consisting of 140 mM $CsMeSO_4$, 5 mM NaCl, 10 mM HEPES, 10 mM EGTA, 4 mM Mg-ATP, and 0.3 mM Na-GTP with a pH of 7.4 and Osm of 290, and an external solution containing 140 mM NaCl, 4 mM KCl, 2 mM $MgCl_2$, 2 mM $CaCl_2$, 10 mM HEPES, 1 μM TTX, and 5 mM glucose. Co-transfected cells with NLmiRs and NLGN1 (WT or T739A) were visualized with fluorescence, mEPSCs were measured at -60 mV, and only cells with capacitances of 60 pF or above were analyzed to reduce variability. mEPSCs were measured offline with customized software (IGOR). Dual whole-cell recordings were made similarly using an internal

solution containing 120 mM $CsMeSO_4$, 20 mM CsCl, 4 mM NaCl, 10 mM HEPES, 4 mM NaCl, 0.4 mM EGTA, 0.3 mM $CaCl_2$, 4 mM Mg-ATP, 0.3 mM Na-GTP, and 5 mM QX-314, and an external solution containing 125 mM NaCl, 2.5 mM KCl, 4 mM $MgCl_2$, 4 mM $CaCl_2$, 1.25 mM NaH_2PO_4, 25 mM $NaHCO_3$, and 11 mM glucose bubbled continuously with 95%O_2/5% CO_2. Recordings were made in the presence of picrotoxin (100 μM) to block inhibitory currents at -70 mV (AMPA) and +40 mV (NMDA). AMPAR-mediated currents were measured at the peak of the current, whereas NMDAR-mediated currents were measured 100 ms after the simulation. Slices pretreated with AP5 and NBQX had drugs washed out prior to recordings. Paired-pulse ratio was determined by providing two pulses separated by 40 ms. The ratio was expressed as the peak current of the second EPSC over the peak current of the first EPSC. Cell selection was not done in the blind and was based on positive transfection but all data analysis was done in the blind. At least three independent experiments were performed per condition, and the number of neurons per mEPSCs or dual whole-cell recordings (n) per condition is located in the corresponding figure legend.

Dark Rearing Experiments. Male and female C57BL/6j littermates were either maintained in a traditional light dark cycle (12 hr light/12 hr dark) from P0 to P26 (LR), relocated to complete darkness at P21 to P26 (DR), or transferred to darkness at P21 to P26 and shifted back to light for 2 hr before euthanization (DR + LR). The primary visual cortex was macrodissected in the dark for the DR condition or in light for the LR and DR + LR conditions. Homogenization of the visual cortex and NLGN1 IPs were performed as described in **immunoblotting**.

Statistical Analysis. Statistical significance of immunoblots, immunocytochemistry, mEPSC, and dual whole-cell recordings were tested using a Mann-Whitney U test. Data distribution was assumed to not be normal. All experiments were done at least three independent times. No statistical methods were used to predetermine sample sizes but our sample sizes are similar to those reported in the literature. All data were collected and processed randomly.

SUPPLEMENTAL DATA

The following section contains supplemental figures describing additional data that was previous published (Bemben et al., 2014) that supports our conclusions from the Results Section. The materials and methods for these experiments are explained in the chapter's Materials and Methods section.

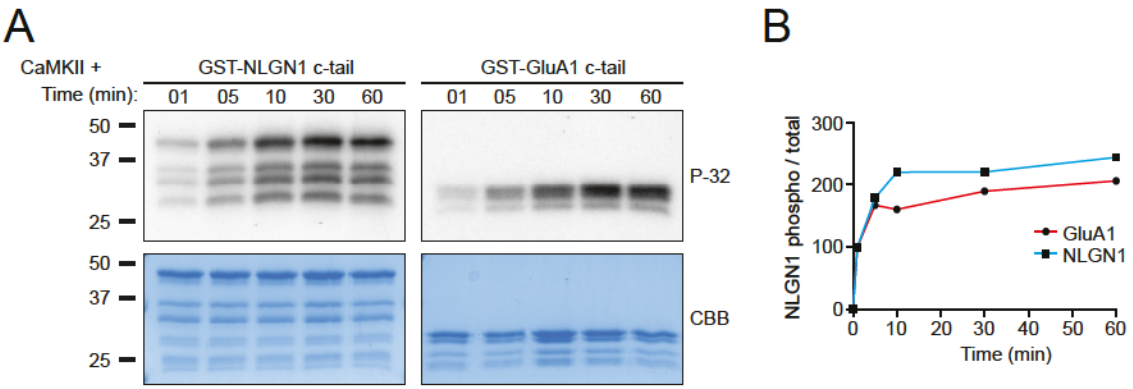

Supplementary Figure 3-1. **NLGN1 and GluA1 c-tails Have Similar Reaction Kinetics**. **A.** GST-NLGN1 or GluA1 were incubated with purified CaMKII and [γ-P^{32}]ATP and analyzed by autoradiography. Reactions were stopped at their marked time. **B.** Protein concentrations are plotted as a ratio of phosphorylated NLGN1 (P-32) to total NLGN1 (CBB) normalized to the 1 min reaction condition. Saturation of phosphorylated NLGN1 and GluA1 occurred at approximately 10 min. Total protein was visualized by CBB protein staining, in **A,B**.

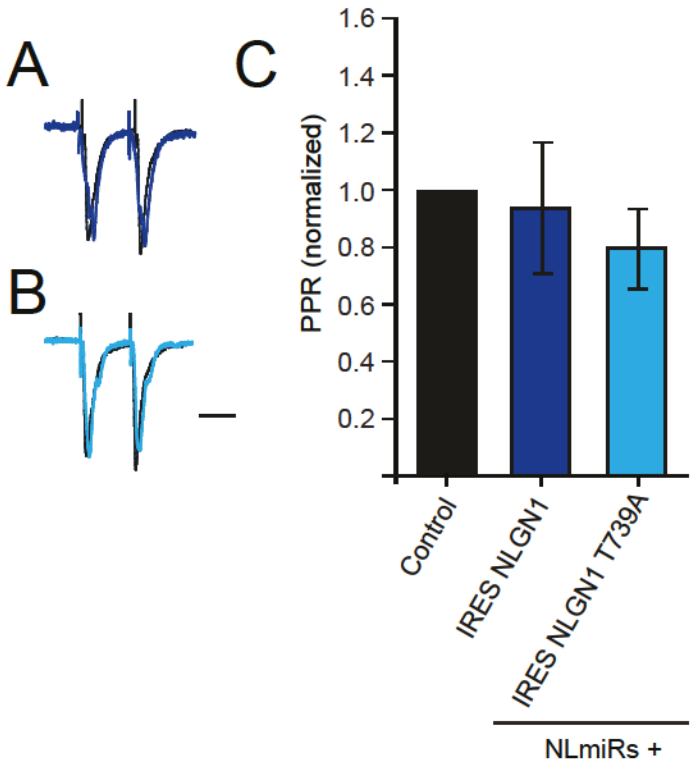

Supplementary Figure 3-2. NLGN1 T739A does not Affect Presynaptic Release Probability. Paired-pulse ratio (PPR), second EPSC over first EPSC for consecutive stimuli separated by 40 ms. Example traces normalized at first EPSC for **A**. NLGN1. **B**. NLGN1 T739A. **C**. Second EPSC over first ± SEM. NLGN1 and NLGN1 T739A had similar PPRs ($P > 0.05$, $n = 5$). Scale bars represent 25 ms.

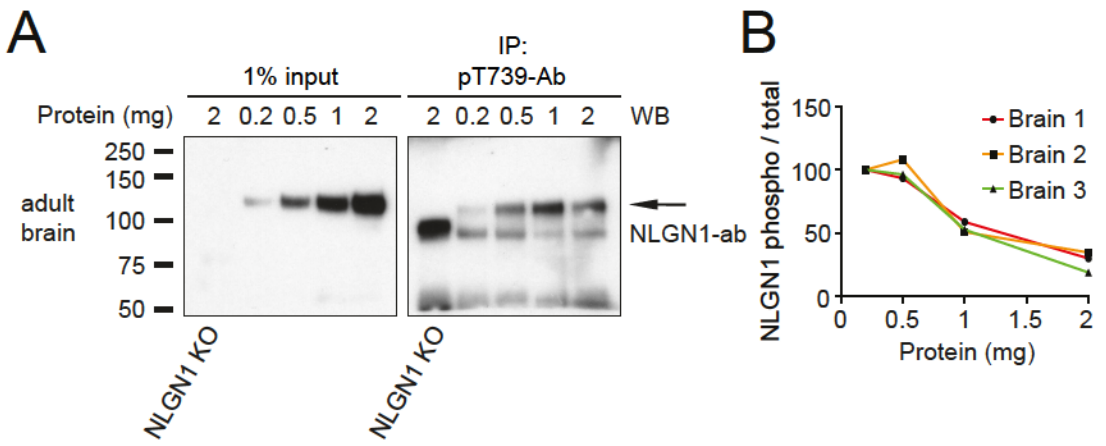

Supplementary Figure 3-3. **Titration of Phosphorylated NLGN1 with pT739-Ab**. **A.** Protein concentrations from adult WT or NLGN1 KO brains were titrated with pT739-Ab. **B.** Protein concentrations are plotted as ratio of phosphorylated (IP) to total NLGN1 (input) normalized to the 0.2 mg protein condition for an individual brain. Saturation of the pT739-Ab occurs between 0.5 and 1 mg of protein.

Chapter 4

Autism-Associated Mutation Inhibits Protein Kinase C-Mediated Neuroligin-4X Enhancement of Excitatory Synapses

Chapter 4 entitled **Autism-associated mutation inhibits protein kinase C-mediated neuroligin-4x enhancement of excitatory Synapses** was published (Bemben et al., 2015a).

ABSTRACT

Autism spectrum disorders (ASDs) comprise a highly heritable, multifarious group of neurodevelopmental disorders, which are characterized by repetitive behaviors and impairments in social interactions. Point mutations have been identified in X-linked *Neuroligin* (NLGN) *3* and *4X* genes in patients with ASDs and all of these reside in their extracellular domains except for a single point mutation in the cytoplasmic domain of NLGN4X in which an arginine is mutated to a cysteine (R704C). Here we show that endogenous NLGN4X is robustly phosphorylated by protein kinase C (PKC) at T707, and R704C completely eliminates T707 phosphorylation. Endogenous NLGN4X is intensely phosphorylated on T707 upon PKC stimulation in human neurons. Furthermore, a phospho-mimetic mutation at T707 has a profound effect on NLGN4X-mediated excitatory potentiation. Our results now establish an important interplay between a genetic mutation, a key posttranslational modification, and robust synaptic changes, which can provide insights into the synaptic dysfunction of ASDs.

INTRODUCTION

In a 2014 report published by the Centers for Disease Control and Prevention (CDC), it was estimated that 1 in 68 children in the United States have an ASD (2014). These neuropsychiatric disorders have a strong genetic component consistent with high recurrence rates between siblings and a higher concordance frequency seen in monozygotic than dizygotic twins. Furthermore, deletions, insertions, and substitutions have been identified within the genome that increase the risk of these disorders (Abrahams and Geschwind, 2008; Zoghbi and Bear, 2012). These cytogenetic and genome sequencing studies have revealed that NLGNs are one of a subset of genes encoding synaptic proteins associated with ASDs (Bemben et al., 2015b; Jamain et al., 2003).

The NLGN gene family consists of five members (*Nlgn1, 2, 3, 4X,* and *4Y*) within the human genome that encode transsynaptic cell adhesion molecules that are critical for synapse assembly, maintenance, and plasticity (Bemben et al., 2015b; Craig and Kang, 2007; Dean and Dresbach, 2006; Sudhof, 2008). Numerous studies have identified a variety of mutations in X-linked NLGN3 and 4X genes that range from copy number variants (Levy et al., 2011; Marshall et al., 2008; Sanders et al., 2011; Thomas et al., 1999) to protein truncations and amino acid substitutions in patients with ASDs (Jamain et al., 2003; Laumonnier et al., 2004; Lawson-Yuen et al., 2008). Interestingly, all of the point mutations in NLGN3 and NLGN4X reside in their extracellular domains except for a single point mutation in the cytoplasmic domain (c-tail) of NLGN4X at arginine (R) 704, which is modified to a cysteine (C) (Yan et al., 2005). How this mutation or other NLGN disease mutations contribute to the pathophysiology is unknown.

Protein phosphorylation is a critical modulator of NLGN function (Bemben et al., 2014; Giannone et al., 2013). Recently, we showed that Ca^{2+}/CaM Kinase II (CaMKII) phosphorylates the c-tail of NLGN1 in an isoform-specific and activity-dependent manner, which regulates its ability to enhance excitatory synapses (Bemben et al., 2014). Next, we wondered if different kinases might regulate the function of other NLGN isoforms?

In the present study, we show *in vitro* and *in vivo* that NLGN4X is robustly phosphorylated by PKC. We identified the dominant phosphorylation site as T707, a residue not conserved in NLGN1, NLGN2, and NLGN3. Intriguingly, PKC phosphorylation is eliminated with the autism-associated mutation R704C. Most dramatically, we found that the phospho-mimetic mutation at T707 profoundly enhances anatomical markers for synapses and potentiates NLGN4X-mediated excitatory synaptic transmission. This study establishes compelling evidence that NLGN4X can act at and regulate excitatory synapses. Furthermore, it demonstrates, strikingly, how a single point mutation in NLGNs can acutely adjust synaptic properties.

RESULTS

PKC Phosphorylates NLGN4X at T707

To test if NLGNs are substrates for kinases other than CaMKII, we conducted an *in vitro* kinase assay with GST-fusion constructs with the c-tails of NLGN1, NLGN2, NLGN3, and NLGN4X (**Figure 4-1A** and **Supplementary Figure 4-1**), and found that NLGN4X was robustly phosphorylated by PKC as evaluated by radiography (**Figure 4-1B**). Weak phosphorylation of NLGN1 and NLGN3 was observed when compared to NLGN4X (**Figure 4-1B**, see longer exposure), indicating NLGN4X to be the best NLGN substrate for PKC. To identify the individual PKC phosphorylation site(s), we subjected NLGN4X to the same *in vitro* kinase assay and evaluated phosphorylation using liquid chromatography coupled to tandem mass spectrometry (LC-MS/MS) and identified the major phosphorylation site as T707 (**Figure 4-1C**), a residue that is not conserved in NLGN1, NLGN2, and NLGN3 (**Figure 4-1A** and **Supplementary Figure 4-1** for complete alignment).

Autism-Associated Mutation Eliminates PKC Phosphorylation of NLGN4X

Interestingly, T707 resides only a few amino acids away from the only known autism-associated mutation (R704C) in the c-tail of any NLGN protein (**Figure 4-1A**). This substitution replaces a positive charge for a polar amino acid, and occupies a critical residue in a potential PKC consensus sequence (RXXS/T, where X denotes any amino acid). Might the autism-related R704C mutation abolish PKC phosphorylation of NLGN4X at T707? To independently verify the mass spectrometry results, we performed the same *in vitro* kinase assay with a non-phosphorylatable point mutation, T707A, and showed that T707 was the dominant NLGN4X PKC phosphorylation site, which resulted

in an approximately 75% reduction in NLGN4X phosphorylation. Likewise, NLGN4X R704C eliminated T707 phosphorylation (**Figure 4-1D,E**). Importantly, CaMKII phosphorylation of NLGN4X T718, the only other known phosphorylation site near T707, was not reduced by the R704C mutation demonstrating that this mutation did not result in a generalized problem rendering the protein unphosphorylated (**Supplementary Figure 4-2A,B**). Taken together, these results indicate that NLGN4X is a robust substrate for PKC, and the only autism-associated NLGN4X c-tail mutation abolishes T707 phosphorylation.

To detect NLGN4X T707 phosphorylation *in vivo*, we produced a phosphorylation state-specific antibody (Ab), pT707-Ab, against residues 703-712 in NLGN4X (**Figure 4-1A**). The pT707-Ab only detected NLGN4X that was phosphorylated on T707 as detected by a PKC *in vitro* kinase assay that was resolved by SDS-PAGE and subsequent immunoblotting (**Figure 4-1F**). Critically, the pT707-Ab did not show any immunoreactivity with the non-phosphorylated NLGN4X, the non-phosphorylatable mutants (R704C or T707A), or any of the other NLGN isoforms that were tested.

The *in vitro* experiments were performed with fusion proteins of NLGN c-tail isoforms. To test whether full-length NLGN4X can be phosphorylated in mammalian cells and modulated by PKC activity, we transfected wild-type (WT) NLGN4X or various NLGN4X mutants (R704C, T707A, or T707D) in COS-7 cells and immunoblotted cell lysates with the pT707-Ab. Under basal conditions, NLGN4X was not phosphorylated at T707, but transient activation of PKC by phorbol 12-myristate 13-acetate (PMA) triggered a robust increase in pT707 phosphorylation (**Figure 4-1G**).

NLGN4X R704C resulted in an approximately 95% reduction in pT707 phosphorylation, whereas NLGN4X T707A or the phospho-mimetic mutation, T707D, were not detected by the pT707-Ab (**Figure 4-1G,H**). Phosphorylation of serine (S) 831 on GluA1 was used as a positive control for PMA activation of PKC (Roche et al., 1996) (**Figure 4-1G,I**). Additionally, the pT707-Ab had astonishing specificity for immunoprecipitating (IP) only NLGN4X phosphorylated on T707 as validated by Western blotting with two independent NLGN4X Abs and a pan NLGN-Ab (**Supplementary Figure 4-3**). Collectively, these data demonstrate that NLGN4X T707 is phosphorylated in heterologous cells, and the pT707-Ab is a dynamic and isoform- specific reagent that faithfully distinguishes the phosphorylated form of NLGN4X on T707.

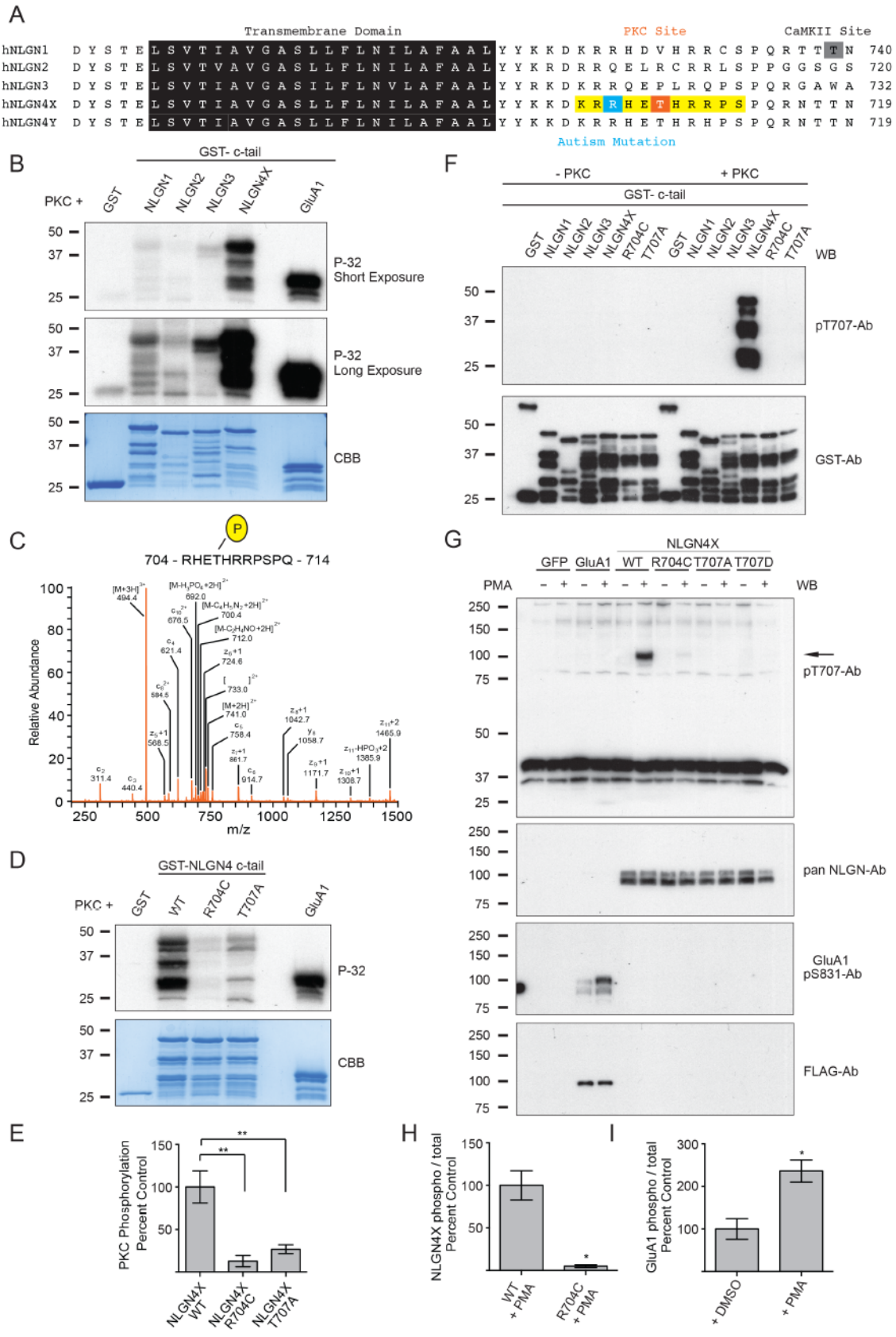
A
Transmembrane Domain
PKC Site
CaMKII Site
Autism Mutation
hNLGN1 D Y S T E L S V T I A V G A S L L F L N I L A F A A L Y Y K K D K R R H D V H R R C S P Q R T T T N 740
hNLGN2 D Y S T E L S V T V A V G A S L L F L N I L A F A A L Y Y K R D R R Q E L R C R R L S P P G G S G S 720
hNLGN3 D Y S T E L S V T I A V G A S I L F L N V L A F A A L Y Y R K D K R R Q E P L R Q P S P Q R G A W A 732
hNLGN4X D Y S T E L S V T I A V G A S L L F L N I L A F A A L Y Y K K D K R R H E T H R R P S P Q R N T T N 719
hNLGN4Y D Y S T E L S V T I A V G A S L L F L N I L A F A A L Y Y K K D K R R H E T H R H P S P Q R N T T N 719
B
GST- c-tail
PKC +
GST
NLGN1
NLGN2
NLGN3
NLGN4X
GluA1
P-32
Short Exposure
P-32
Long Exposure
CBB
C
704 - RHETHRRPSPQ - 714
Relative Abundance
m/z
D
GST-NLGN4 c-tail
PKC +
GST
WT
R704C
T707A
GluA1
P-32
CBB
E
PKC Phosphorylation
Percent Control
NLGN4X WT
NLGN4X R704C
NLGN4X T707A
F
- PKC
+ PKC
GST- c-tail
GST
NLGN1
NLGN2
NLGN3
NLGN4X
R704C
T707A
WB
pT707-Ab
GST-Ab
G
NLGN4X
GFP
GluA1
WT
R704C
T707A
T707D
PMA
WB
pT707-Ab
pan NLGN-Ab
GluA1
pS831-Ab
FLAG-Ab
H
NLGN4X phospho / total
Percent Control
WT
+ PMA
R704C
+ PMA
I
GluA1 phospho / total
Percent Control
+ DMSO
+ PMA

Figure 4-1. **Autism-Associated Mutation Eliminates PKC Phosphorylation of NLGN4X. A.** Alignment of the transmembrane domains and partial c-tails of human NLGN1, NLGN2, NLGN3, NLGN4X, and NLGN4Y. The PKC phosphorylation site, T707, is boxed in orange; autism mutation, R704, boxed in blue; and pT707-Ab epitope boxed in yellow. The CaMKII phosphorylation site on NLGN1 is boxed in gray. **B,D.** Purified PKC and [γ-P-32]ATP were incubated with GST-fusion proteins and analyzed by autoradiography. CBB protein staining was used to visualize total protein, and GST (negative) and GST-GluA1 c-tail (positive) functioned as phosphorylation controls. **C.** ETD MS/MS spectrum of chymotrypsin digested phosphorylated NLGN4X peptide 704 - RHETHRRPSPQ - 714 found in GST-NLGN4X fusion proteins that were incubated with ATP and purified PKC. Samples were analyzed using LC/MS/MS method. **E.** Means ± SEM of phosphorylated NLGN4X by PKC normalized to WT (n = 4) for NLGN4X R704C ($P = 0.0013$, n = 4) and NLGN4X T707A ($P = 0.0030$, n = 4). **F.** GST, GST-NLGN1, NLGN2, NLGN3, and NLGN4X (WT, R704C, and T707A) were incubated with PKC and phosphorylation was evaluated by immunoblotting with pT707-Ab. Total protein was evaluated with a GST-Ab. **G**. GFP, GluA1, or NLGN4X (WT, R704C, T707A, or T707D) were transfected in COS cells and treated with DMSO or PMA, a PKC activator. GluA1 pS831 served as control for PKC activation and the arrow denotes the NLGN4X specific band. **H.** Means ± SEM of phosphorylated NLGN4X pT707 achieved by PMA activation normalized to WT (n = 3) and NLGN4X R704C ($P = 0.0310$, n = 3). **I.** Means ± SEM of phosphorylated GluA1 S831 achieved by PMA activation ($P = 0.0187$, n = 3) normalized to no treatment (n = 3). Immunoblots were probed with indicated antibodies in **F**,**G**. $^{*}P < 0.05$ $^{**}P < 0.01$.

Phosphorylation of NLGN4X at T707 Induces Synaptogenesis

Previously, two autism-associated mutations in NLGN3 (R451C) and NLGN4X (R87W) were shown to disrupt surface expression (Tabuchi et al., 2007; Zhang et al., 2009). Moreover, phosphorylation of the NLGN1 c-tail regulates its forward trafficking (Bemben et al., 2014). Does T707 regulate NLGN4X surface expression? To test this possibility, cultured rat hippocampal neurons were transfected with NLGN4X (WT, R704C, T707A, or T707D) and visualized with immunofluorescence confocal microscopy. To prevent potential heterodimerization, we performed these experiments on a reduced endogenous NLGN background using an exogenous chained microRNA against NLGN1, NLGN2, and NLGN3 (NLmiRs) as previously described (Shipman et al., 2011). Human NLGN4X and NLGN4Y are absent in rats (Bolliger et al., 2008). Consequently, rat neurons were used in all imaging and physiology experiments to ensure a NLGN4 null background to avoid any complications that might occur between dimerization of WT and mutant NLGN4 receptors. Phosphorylation at T707 did not affect the trafficking of NLGN4X to the cell surface (**Figure 4-2A,B**). However, we noticed that expression of a phospho-mimetic mutation of NLGN4X T707 (T707D) resulted in a robust increase in dendritic protrusions when compared to NLGN4X WT and the non-phosphorylatable mutants, R704C and T707A (**Figure 4-2A,C**). To examine if the increase in spines resulted in new excitatory synapses, we co-expressed NLmiRs with NLGN4X (WT, R704C, T707A, or T707D) in rat hippocampal cultures and assayed for anatomical measures of functional synapses, namely increases in presynaptic VGLUT1 and postsynaptic PSD-95. Using immunofluorescence confocal microscopy, we found that the NLGN4X phospho-mimetic (T707D) mutation resulted in an increase

in both VGLUT1 and PSD-95 staining, an enhancement that was absent in non-phosphorylated NLGN4X protein (**Figure 4-2D-F**). These results indicate that T707 phosphorylation promotes NLGN4X-induced synaptogenesis independent of regulating its surface expression.

To test whether these new synapses were functional, we biolistically co-expressed NLmiRs with NLGN4X (WT, R704C, T707A, or T707D) in rat organotypic hippocampal slice cultures and used a dual whole cell recording configuration to simultaneously record evoked excitatory postsynaptic currents in both transfected and neighboring control, untransfected cells. Expression of NLGN4X T707D resulted in a profound increase in both AMPA receptor (AMPAR) and NMDA receptor (NMDAR) mediated currents when compared to a control cell or NLGN4X (WT, R704C, or T707A) (**Figure 4-3A-D**). Previously, we, as well as others, have reported that NLGN4X expression on a WT background decreased postsynaptic excitatory currents (Shipman et al., 2011; Zhang et al., 2009). However, on a reduced NLGN background, which alone reduces AMPAR and NMDAR mediated currents by about 50% (**Supplementary Figure 4- 4**), NLGN4X expression induced a modest, but significant, increase in AMPAR transmission, an enhancement that was absent in R704C and T707A (**Figure 4-3A-D**). Together, these results show that phosphorylation at T707 dynamically regulates NLGN4X's ability to robustly induce the genesis of functional excitatory synapses.

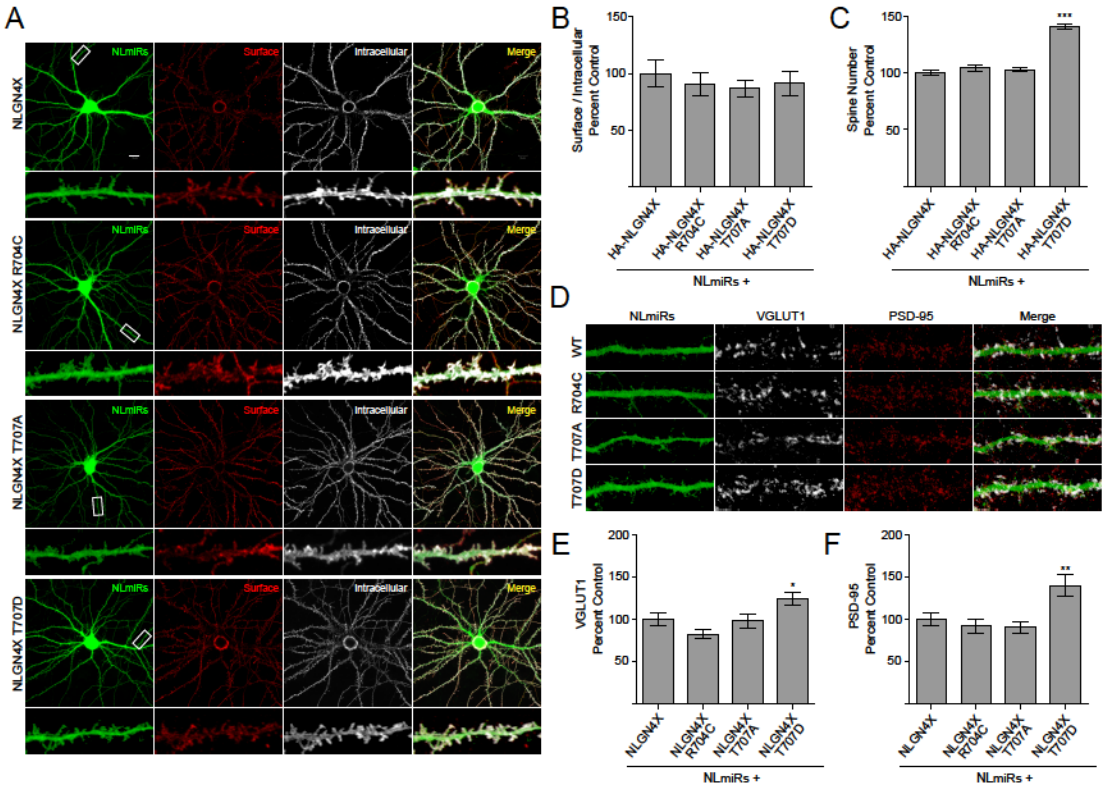

Figure 4-2. NLGN4X Phosphorylation at T707 Induces Synaptogenesis. A. Co-expression of NLmiRs and NLGN4X (WT, R704C, T707A, or T707D) in rat hippocampal neurons. Surface and intracellular receptors were labeled with an anti-hemagglutinin (HA) antibody, which recognized a tag inserted downstream of the signal peptide (scale bar = 20 μm). **B**. Means ± SEM normalized to NLGN4X (n = 27), NLGN4X R704C ($P > 0.05$, n = 29), NLGN4X T707A ($P > 0.05$, n = 30), and NLGN4X T707D ($P > 0.05$, n = 29). **C.** Means of spine number ± SEM normalized to NLGN4X (n = 30), NLGN4X R704C ($P > 0.05$, n = 30), NLGN4X T707A ($P > 0.05$, n = 30), and NLGN4X T707D ($P = 0.001$, n = 30). **D.** Same transfections as in **A.** except NLGN4X constructs did not contain an HA-tag. Endogenous VGLUT1 and PSD-95 were stained and visualized as described in Experimental Procedures. **E**. Means ± SEM of VGLUT1 normalized to NLGN4X (n = 30) for NLGN4X R704C ($P > 0.05$, n = 30), NLGN4X

T707A ($P > 0.05$, $n = 30$) and NLGN4X T707D ($P = 0.0466$, $n = 30$). **F**. Means ± SEM of PSD-95 normalized to NLGN4X ($n = 30$) for NLGN4X R704C ($P > 0.05$, $n = 27$), NLGN4X T707A ($P > 0.05$, $n = 28$), and NLGN4X T707D ($P = 0.0049$, $n = 30$). $^{*}P < 0.05$ $^{**}P < 0.01$, $^{***}P < 0.001$.

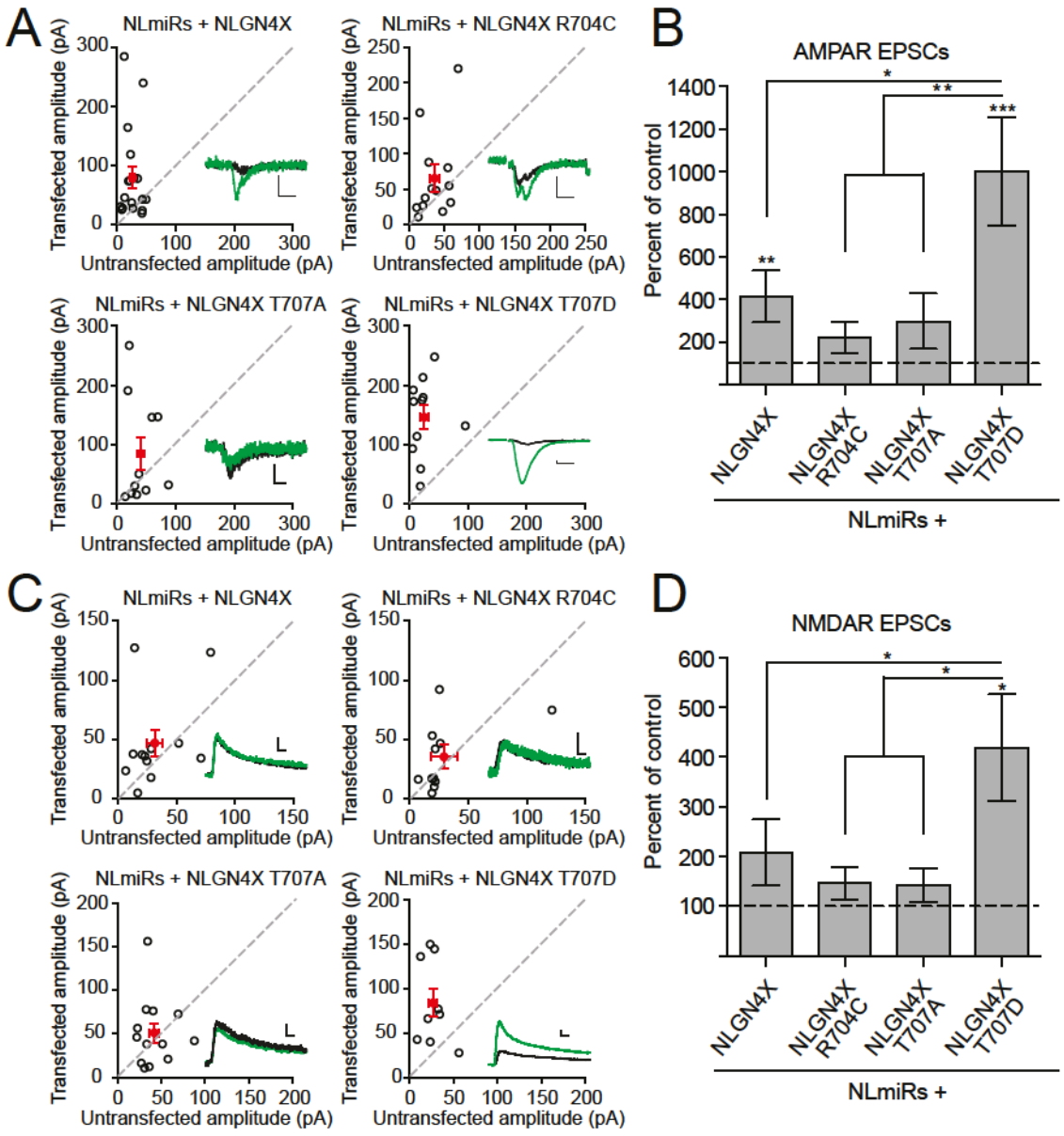

Figure 4-3. NLGN4X T707D Dramatically Enhances Excitatory Postsynaptic Currents. A. AMPAR-mediated EPSC scatter plots. Expression of either NLGN4X or NLGN4X T707D results in a potentiation of AMPAR-mediated currents compared to control, untransfected cells (P = 0.0023, n = 18; P = 0.0010, n = 11). The enhancement was absent in NLGN4X R704C (P > 0.05, n = 13) and NLGN4X T707A (P > 0.05, n = 11) expressing cells. Experiments were performed in rat organotypic slice cultures on a

reduced NLGN background (NLmiRs). Open circles are individual pairs, filled (in red) are mean ± SEM. Black sample traces are control; green are transfected. Scale bars represent 15 pA and 10 ms. **B.** Summary graph of data in **A**. Expression of NLGN4X T707D resulted in a greater enhancement of AMPAR-mediated currents compared to NLGN4X ($P = 0.0143$), NLGN4X R704C ($P = 0.0025$), or NLGN4X T707A ($P = 0.0066$). **C**. NMDAR-mediated EPSC scatter plots. Expression of NLGN4X ($n = 12$) or phosphodeficient mutants, NLGN4X R704C ($n = 11$) or NLGN4X T707A ($n = 13$), did not enhance NMDAR-mediated currents compared to control untransfected cells ($P > 0.05$), whereas expression of NLGN4X T707D significantly potentiated NMDA-mediated currents ($P = 0.0117$, $n = 9$). Open circles are individual pairs, filled (in red) are mean ± SEM. Black sample traces are control; green are transfected. Scale bars represent 30 pA and 20 ms. **D**. Summary graph of data in **C**. Expression of NLGN4X T707D resulted in a enhancement of NMDAR-mediated currents compared to NLGN4X ($P = 0.0409$), NLGN4X R704C ($P = 0.0250$), and NLGN4X T707A ($P = 0.0138$). $^{*}P < 0.05$ $^{**}P < 0.01$, $^{***}P < 0.001$.

Endogenous NLGN4X is Phosphorylated by PKC in Human Neurons

Because our NLGN4X pT707-Ab was so specific, we were able to investigate endogenous NLGN4X T707 phosphorylation in cultured human embryonic neurons. These cultures consisted primarily of MAP2 positive neurons (**Figure 4-4A**) and transient activation of PKC with PMA resulted in approximately an 8-fold increase in NLGN4X pT707 phosphorylation (**Figure 4-4B,C**). Consistent with previous reports, NLGN4X was expressed in human embryonic neurons, as detected with two independent NLGN4X Abs and a pan NLGN-Ab (Marei et al., 2012). Taken together, these results show that endogenous NLGN4X is phosphorylated in human neurons by PKC.

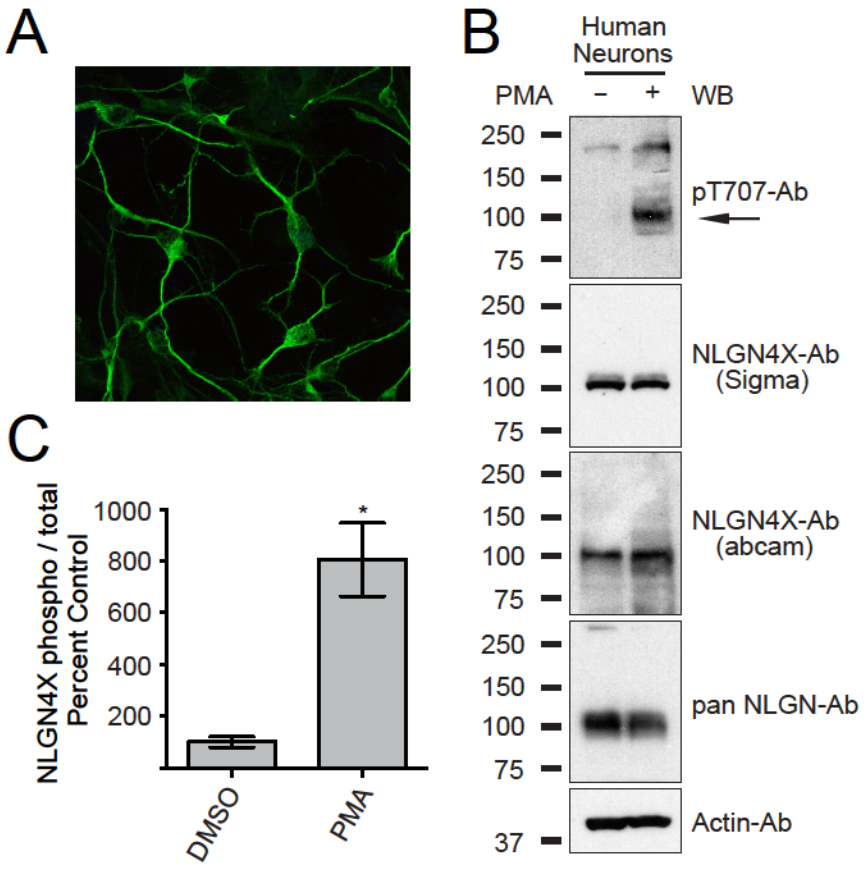

Figure 4-4. PKC phosphorylates Endogenous NLGN4X in Human Neurons. A. Immunofluorescence image of human embryonic neurons stained with the neuronal marker MAP2. **B**. Regulation of NLGN4X phosphorylation at T707 in human embryonic neurons -/+ PMA treatment. Arrow denotes the NLGN4X pT707 specific band. Immunoblots were probed with indicated antibodies. **C**. Means ± SEM of phosphorylated NLGN4X T707 achieved by PMA activation normalized to no treatment (n = 4) and + PMA treatment (P = 0.0148, n = 4).

DISCUSSION

We set out to examine whether other NLGN isoforms, like NLGN1, were regulated by phosphorylation. We identified a PKC phosphorylation site on human NLGN4X at T707, which establishes a novel interplay between two critical constituents of the synapse. It was to our surprise, R704, a residue mutated in a familial case of autism (Yan et al., 2005), resided within the PKC consensus sequence in the c-tail of NLGN4X. However, after identification, it was not unexpected that the autism mutation (R704C) abolished the kinase's ability to chemically modify NLGN4X at T707. Using a diverse combination of techniques, we show that phosphorylated NLGN4X can dynamically enhance excitatory synapses.

Prior to this report, the importance of protein phosphorylation on NLGN1 was established (Bemben et al., 2014; Giannone et al., 2013). CaMKII phosphorylation of T739 regulates NLGN1's ability to potentiate excitatory synaptic transmission by regulating its surface expression. This current study demonstrates that PKC phosphorylation of T707 dramatically enhances NLGN4X's ability to potentiate excitatory currents independent of modulating its surface expression. Therefore phosphorylation is a key regulatory modification modulating both NLGN1 and NLGN4X's function but by different kinases, at different sites, and likely by different molecular mechanisms. Collectively, these studies raise two exciting questions: Might other kinases phosphorylate NLGN2 and NLGN3 and regulate their synaptic functions similarly to NLGN1 and NLGN4X? Secondly, what is the molecular mechanism by which T707 phosphorylation induces the genesis of functional synapses independent of

surface expression? These answers remain to be elucidated but are currently an area of future investigation.

Interestingly, human NLGN4X is not well conserved in rodents, unlike NLGN1, NLGN2, and NLGN3. NLGN4 is absent in *Rattus norvegicus* and highly divergent and on an autosome in *Mus musculus* (Bolliger et al., 2008). This has made the investigation of human autism mutations in NLGN4X challenging and led some researchers to study the R704C point mutation in NLGN3. Although R704 is conserved in all human NLGNs, the residue analogous to NLGN4X T707 is not conserved. A knock-in mutation in NLGN3 resulted in minor synaptic phenotypes (Etherton et al., 2011). Therefore we believe it is imperative to study the R704C mutation in NLGN4X, and more generally for all disease mutations to be studied in their respective isoforms independent of residue(s) conservation.

Canonically, NLGN1 is known as a critical component of the excitatory synapse based on its cellular localization (Chih et al., 2005; Song et al., 1999), regulation by CaMKII (Bemben et al., 2014), and its ability to robustly potentiate AMPAR and NMDAR postsynaptic currents (Chubykin et al., 2007; Shipman et al., 2011). Conversely, mouse NLGN4 is known to localize to and modulate inhibitory transmission (Hoon et al., 2011). However, the human and mouse isoforms are not well conserved. This raises the possibility that these proteins might perform distinct functions in different species. Here, we show that like NLGN1, human NLGN4X can enhance excitatory synapses, suggesting that NLGN4X may associate with excitatory synapses in humans. At a minimum, this underscores the reservations of studying human NLGN4X and rodent NLGN4 interchangeably. However, it is important to note our study does not preclude the

possibility that human NLGN4X may act or be expressed at inhibitory synapses in humans.

Notably, all the NLGN-associated autism point mutations reported thus far reside in their extracellular or transmembrane domains, except for NLGN4X R704C. This may be a result of chance or may highlight the critical importance of T707 phosphorylation in regulating NLGN4X's synaptic properties. It is tempting to speculate whether this phosphorylation occurs at a critical developmental period to shape synaptic properties or whether it is a global switch that happens continually at excitatory synapses. The profound effect the phospho-mimetic mutation (T707D) has on excitatory synapses may suggest the prior.

Mouse models of autism have increasingly revealed underlying imbalances of excitatory/inhibitory transmission, which are believed to play a central role in the etiology of ASDs (Foldy et al., 2013; Rothwell et al., 2014; Tabuchi et al., 2007). Our results are consistent with this hypothesis, which support a pathophysiological model by which NLGN4X R704C decreases excitatory transmission by abolishing PKC-mediated NLGN4X potentiation of excitatory transmission. Furthermore, we believe given the overlap of synaptic proteins found to be candidate genes in ASDs that by understanding the biology of specific mutations such as R704C has implications for clinical research, as well as future therapeutic treatment for ASDs.

ACKNOWLEDGEMENTS

We are grateful to Dr. Antonio Sanz-Clemente and John D. Badger, as well as other members of Roche lab, for technical assistance and for discussions on the project and manuscript. We thank Dr. Avindra Nath for providing human embryonic neuron cultures, and the NINDS sequencing facility and light imaging facility for their expertise.

AUTHOR CONTRIBUTIONS

M.A.B., Q.-A.N., Y.L., R.A.N., and K.W.R. designed research. M.A.B., Q.-A.N., T.W., and Y.L. performed research. T.W. contributed new reagents/analytic tools. M.A.B., Q.-A.N., Y.L., R.A.N., and K.W.R. analyzed data; and M.A.B. and K.W.R. wrote the paper.

MATERIALS and METHODS

Plasmids and Antibodies. Human pCAG-NLGN4X (WT, R704C, T707A, or T707D)-IRES-mCherry, pCAG-eGFP, pCAG-NLmiRs-GFP, and pRK5-FLAG-GluA1 plasmids were used for biochemical, electrophysiological, and imaging (synaptic markers) experiments. Human pCAG-HA-NLGN4X (WT, R704C, T707A, or T707D) were used in surface expression imaging experiments. pGEX-GST-NLGN c-tail constructs were made as previously described (Bemben et al., 2014). Point mutations were introduced using QuikChange Site-Directed mutagenesis. The primers used to construct NLGN4X R704C were Forward (FOR) 5' - ACAAAAAGGACAAGAGGTGCCATGAGACTCA CAGG - 3' and Reverse (REV) 5' - CCTGTGAGTCTCATGGCACCTCTTGTCCTTTT TGT - 3', NLGN4X T707A were FOR 5' - AGGCGCCATGAGGCTCACAGGCGCC -

3' and REV 5' - GGCGCCTGTGAGCCTCATGGCGCCT - 3', and NLGN4X T707D were FOR 5'- GAGGCGCCATGAGGATCACAGGCGCCCC - 3' and REV 5' - GGGGCGCCTGTGACCTCATGGCGCCTC - 3'. The primers used to insert the HA-tag in pCAG-NLGN4X were FOR 5'- TATCCATACGACGTTCCGGACTACGCTCCAGT TGTCAACACAAATTATGGC -3' and REV 5'- AGCGTAGTCCGGAACGTCGTATG GATAATACTGTGCTTGGCTGTCAATGAG -3'. To generate the rabbit NLGN4X pT707-Ab (against residues 703-712 in NLGN4X), animals were immunized with synthetic phosphopeptide Ac-CKRRHE(pT)HRRP-amide (New England Peptide). All Immunoblotting with the NLGN4X T707-Ab began with blocking in 5% PhosphoBLOCKER (CELL BIOLABS, INC) at room temperature, followed by 1% PhosphoBLOCKER in the primary and secondary Ab incubations. Antibodies used in the study were anti-NLGN4X (Sigma), anti-NLGN4X (abcam), anti-pan NLGN 4F9 (Synaptic Systems), anti-GST (Bethyl Laboratories), anti-FLAG (Sigma), anti-HA rat (Roche), anti-HA rabbit (abcam), anti GluA1 pS831 (Covance), anti-PSD-95 (Neuromab), anti-VGLUT1 (Millipore), anti-MAP2 (Cell Signaling), and anti-actin (ABM). All antibodies were used at 1 µg/µL.

GST-Fusion Protein Production, *In Vitro* Phosphorylation, and Mass Spectrometry. Reagents were prepared and assays were performed and analyzed as previous described (Bemben et al., 2014).

Immunoblotting. HEK293T cells were maintained, transfected, and proteins were isolated as previously described (Bemben et al., 2014). Treatment with 200 ng/µL PMA (Tocris) or DMSO (Sigma) began 30-60 minutes before protein isolation. For IPs, cell lysates were incubated with 6 µg of NLGN4X pT707-Ab and protein A-Sepharose beads

(GE Healthcare) at 4°C overnight. The following day the IPs were washed in TBS buffer containing 150 mM NaCl, 50 mM Tris-HCl, 1 mM EDTA, protease (Roche), and phosphatase (Sigma) inhibitors. The antibody conjugated beads were resuspended in SDS-PAGE sample buffer and subjected to Western blotting.

Neuronal Cultures and Immunocytochemistry. Hippocampal neurons were prepared from E18 Sprague-Dawley rats and used for all immunocytochemistry experiments. The use and care of animals used in this study followed the guidelines of the NIH Animal Research Advisory Committee. Neurons were grown on precoated poly-D-Lysine (Sigma) glass coverslips and co-transfected (Liptofectamine 2000) at DIV10 with NLmiRs and HA-NLGN4X constructs for surface expression experiments and without the HA tag for staining with synaptic markers. Cells were fixed at DIV 14. Spine number was counted using the GFP signal from the NLmiRs construct from 3-4 regions of 30 µm/cell. Methods, reagents, and analysis for imaging were done as previously described (Bemben et al., 2014).

Electrophysiology. Hippocampal organotypic slice cultures were prepared from 6–8 day-old rats as described previously (Stoppini et al., 1991). All experiments were performed in accordance with established protocols approved by the University of California San Francisco Institutional Animal Care and Use Committee.

Sparse biolistic transfections of organotypic slice cultures were performed 4 days after culturing as previously described (Schnell et al., 2002). Briefly, 100 µg total of mixed plasmid DNA was coated on 1 µM-diameter gold particles in 0.5 mM spermidine, precipitated with 0.1 mM $CaCl_2$, and washed four times in pure ethanol. The gold particles were coated onto PVC tubing, dried using ultra-pure N_2 gas, and stored at 4°C in

desiccant. DNA-coated gold particles were delivered with a Helios Gene Gun (BioRad). When biolistically expressing two plasmids, gold particles were coated with equal amounts of each plasmid and plasmids always expressed different fluorescent markers. Observed frequency of coexpression was nearly 100%. Slices were maintained at 34 °C with media changes every other day.

Recordings were performed at DIV 7-8 after 3-4 days of expression. Dual whole-cell recordings in area CA1 were done by simultaneously recording responses from a fluorescent transfected neuron and neighboring untransfected control neuron. Synaptic responses were evoked by stimulating with a monopolar glass electrode filled with aCSF in stratum radiatum of CA1. Typically each pair of neurons is from a separate slice, whereas on rare occasions two pairs may come from one slice. For all paired recordings, the number of experiments (*n*) reported in the figure legends refer to the number of pairs. Pyramidal neurons were identified by morphology and location. To ensure stable recording, membrane holding current, input resistance, and pipette series resistance were monitored throughout recording. All recordings were made at 20-25°C using glass patch electrodes filled with an internal solution consisting of 135 mM $CsMeSO_4$, 8 mM NaCl, 10 mM HEPES, 0.3 mM EGTA, 4 mM Mg-ATP, 0.3 mM Na-GTP, 5 mM QX-314, and 0.1 mM spermine and an external solution containing 119 mM NaCl, 2.5 mM KCl, 4 mM $MgSO_4$, 4 mM $CaCl_2$, 1 mM NaH_2PO_4, 26.2 mM $NaHCO_3$ and 11 mM glucose bubbled continuously with 95% O_2 and 5% CO_2. Recordings were made in the presence of picrotoxin (100 μM) to block inhibitory currents and a small (50 nM) amount of NBQX to reduce epileptiform activity at −70 mV (AMPA) and +40 mV (NMDA). AMPAR-

mediated currents were measured at the peak of the current, whereas NMDAR-mediated currents were measured 150 ms after the stimulation.

Human Neuron Cultures. Human fetal neural cells were cultured as previously reported (Wang et al., 2006). Total NLGN4X protein was quantified using the anti-NLGN4X Ab (Sigma).

Statistical Analysis. Statistical significance of immunoblots was tested using a t-test, immunocytochemistry with a one-way ANOVA, paired whole-cell recordings with a Wilcoxon signed-rank test, and comparisons between sets of paired data with a Mann-Whitney U test. All experiments were done at least three independent times.

SUPPLEMENTAL DATA

The following section contains supplemental figures describing additional data that was previous published (Bemben et al., 2015a) that supports our conclusions from the Results Section. The materials and methods for these experiments are explained in the chapter's Materials and Methods section.

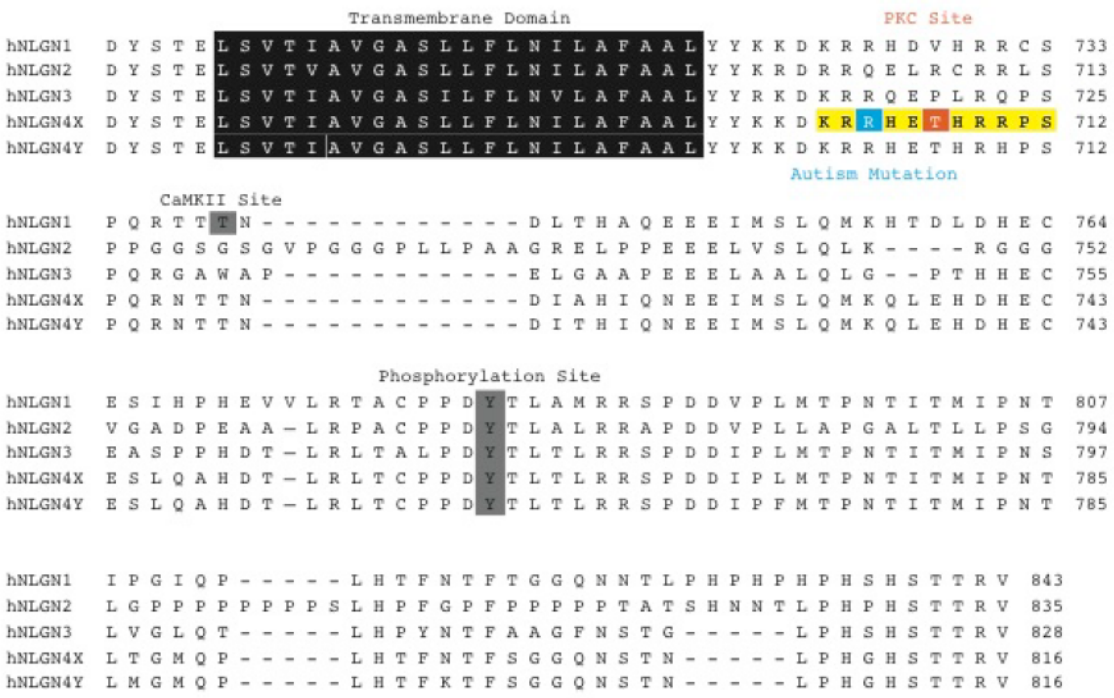

Supplementary Figure 4-1. Alignment of the Transmembrane Domains and Complete c-tails of Human NLGN1, NLGN2, NLGN3, NLGN4X, and NLGN4Y.

The PKC phosphorylation site boxed in orange; key autism residue boxed in blue, and pT707-Ab epitope boxed in yellow. All other known NLGN phosphorylation sites boxed in gray.

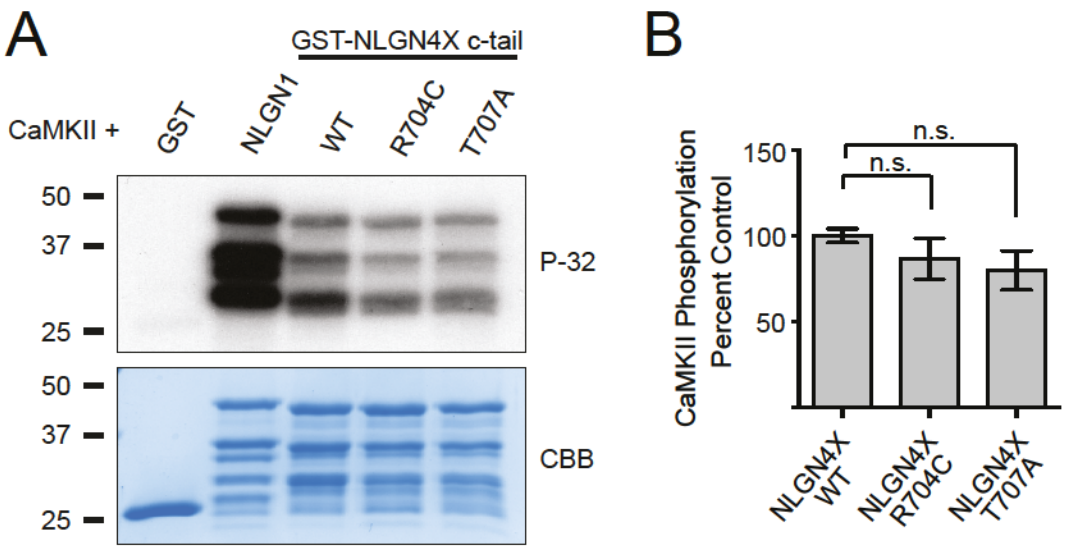

Supplementary Figure 4-2. Autism-Associated Mutation does not Reduce CaMKII Phosphorylation of NLGN4X. A .Purified CaMKII and [γ-P-32]ATP were incubated with GST-fusion proteins and analyzed by autoradiography. CBB protein staining was used to visualize total protein, and GST (negative) and GST-NLGN1 c-tail (positive) functioned as phosphorylation controls. **B**. Means ± SEM of phosphorylated NLGN4X by CaMKII normalized to WT (n = 4) for NLGN4X R704C ($P > 0.05$, n = 4) and NLGN4X T707A ($P > 0.05$, n = 4).

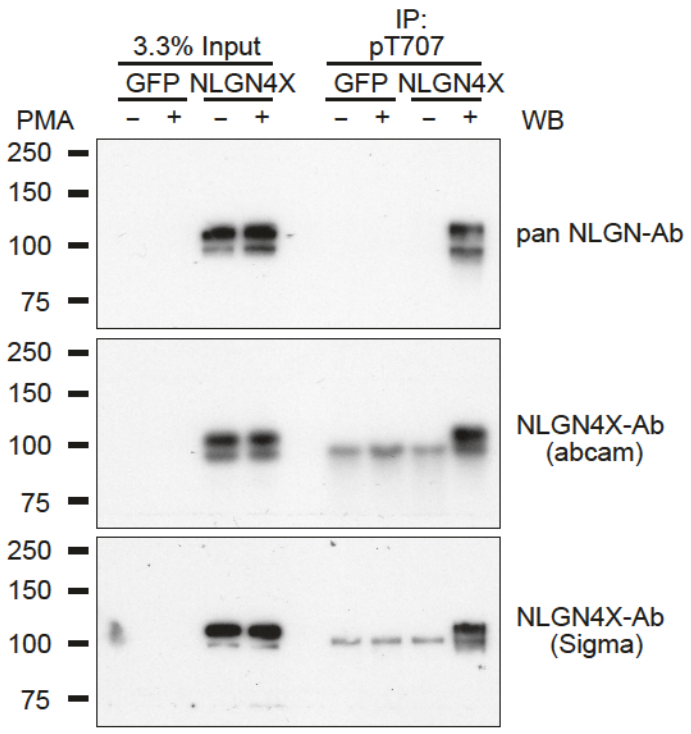

Supplementary Figure 4-3. NLGN4X pT707-Ab Specifically Immunoprecipitates Phosphorylated NLGN4X. GFP or NLGN4X were transfected in COS cells and treated with DMSO (-) or PMA (+) and immunoprecipitated with pT707-Ab. Immunoblots were probed with indicated antibodies.

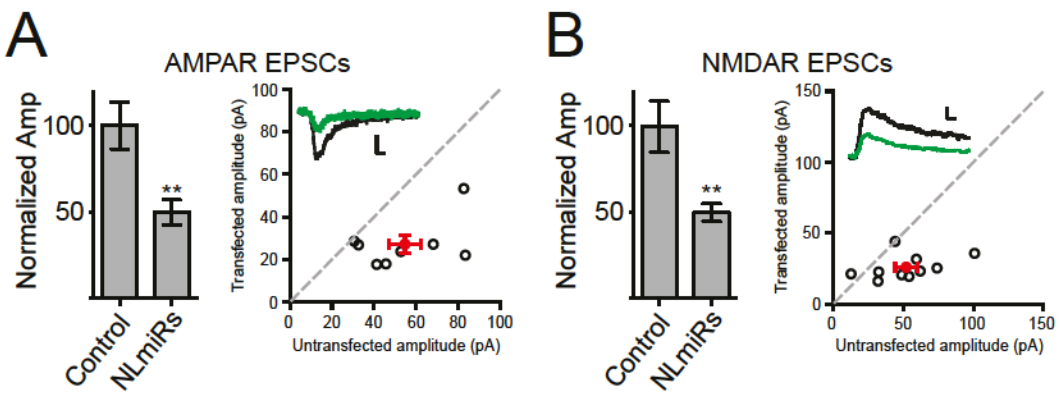

Supplementary Figure 4-4. NLmiRs Reduces AMPA and NMDA currents. A. AMPAR-mediated EPSC scatter plot. Expression of NLmiRs (3-4 days) results in a reduction of AMPAR-mediated currents compared to control, untransfected cells ($P = 0.0078$, $n = 8$). Open circles are individual pairs, filled (in red) are mean ± SEM. Black sample traces are control, green are transfected. Scale bar represents 15 pA and 10 ms. Bar graph of data is transfected amplitude (NLmiRs) normalized to neighboring, non-transfected cell (control). **B**. NMDAR-mediated EPSC scatter plot, showing similar reductions in NMDAR-mediated currents ($P = 0.0098$, $n = 10$) as seen in **A**. Scale bar represents 30 pA and 20 ms. $^{**}P < 0.01$.

Chapter 5

Protein Kinase C-Mediated Neuroligin-3 Ectodomain Shedding

Chapter 5 entitled **Protein Kinase C-Mediated Neuroligin-3 Ectodomain Shedding** has not been published but will be submitted for publication in 2016.

ABSTRACT

Neuroligins (NLGNs) are cell adhesion molecules that form a transsynaptic interaction with neurexins that regulate synaptic function. NLGN3 is localized at excitatory and inhibitory synapses but the mechanisms underlying its trafficking and elimination from the synapse remain unknown. Here, we report that protein kinase C (PKC) activation leads to the robust loss of NLGN3 protein. We show that this regulation is isoform- and kinase-specific and dependent on the NLGN3 extracellular domain. Therefore we report the first direct functional interplay between PKC signaling and NLGN3. Furthermore, we provide evidence that NLGN3, like NLGN1, can undergo extracellular domain shedding.

INTRODUCTION

NLGNs are postsynaptic cell adhesion molecules that are critical mediators of synapse development, maturation, and plasticity. NLGNs are one of the best-known inducers of synaptogenesis, underlying the critical importance of their regulation within the cell (Bemben et al., 2015b). Researchers have identified a mechanism that regulates how NLGN1 is trafficked to the cellular membrane, yet how NLGNs are removed from the synapse remains largely unknown (Bemben et al., 2014).

Synaptic activity induces local proteolytic cleavage and removal of NLGN1 from the synapse, which tunes down glutamatergic transmission (Peixoto et al., 2012; Suzuki et al., 2012). However, it still remains a mystery if other NLGNs, which are expressed at different types of synapses, are subjected to the same type of regulation.

Moreover, an unbiased screen identified a NLGN3 protein product that acts as a mitogen to promote glioma growth. The protein product was identified by mass spectrometry (MS) in the cellular media and contained only the extracellular domain (ECD) and not the intracellular domain (ICD) of NLGN3, suggesting it was a product of NLGN3 proteolytic cleavage. However, the MS coverage was incomplete of the ECD and ectodomain shedding of NLGN3 has not been empirically shown. Critically, this provides a potential link between synapse regulation and brain cancer (Venkatesh et al., 2015).

These studies offer a possible explanation for how NLGN3 may be removed from the synapse, similarly to NLGN1, but does not provide evidence for the functional consequences of removal from the synapse. Interestingly, it also implies that that ECDs and ICDs may not simply be degraded after proteolytic cleavage but may provide

auxiliary functions such as the NLGN3 ECD promoting glioma growth. Might the NLGN3 ECD have a physiological role in the nervous system?

Here, we show that PKC activation leads to the rapid loss of cellular NLGN3, which is dependent on its ECD. This establishes that NLGN3 protein can undergo ectodomain shedding. Moreover, it identifies an isoform specific pathway that can regulate total NLGN3 levels in the cell.

RESULTS

PKC Activation Induces Loss of NLGN3 Protein

Previously, we have shown that PKC phosphorylation of NLGN4X induces excitatory synaptogenesis. Interestingly, NLGN4X was the only neuroligin isoform to be robustly phosphorylated by PKC (Bemben et al., 2015a). Although not directly phosphorylated by PKC, we uncovered that PKC activation leads to the removal of total NLGN3 protein from cellular lysate and subsequent accumulation in the cellular media (**Figure 5-1A-C**). NLGN1, NLGN2, and NLGN4X did not show similar reductions in protein levels or accumulation of the ECD in the media. Moreover, cAMP-dependent protein kinase (PKA) signaling did not result in a decrease of NLGN3 protein levels (**Figure 5-2A-C**). Intriguingly, NLGN1 and NLGN3 were identified in the media, suggestive of a basal mechanism of protein turnover for these isoforms. Taken together, these results indicate an isoform- and kinase-specific signaling pathway regulating NLGN3 protein levels.

To test if NLGN3 ectodomain shedding was dependent on its extracellular (ECD) or intracellular domain (ICD), we engineered chimeras NLGN1 ECD / NLGN3 ICD (NLGN1/3) and NLGN3 ECD / NLGN1 ICD (NLGN3/1) and found NLGN3 protein loss was dependent on the NLGN3 ECD (**Figure 5-3A-C**). This indicates that NLGN3 ectodomain shedding is not dependent on PKC phosphorylation of the intracellular domain of NLGN3 but on protease recognition of the ECD of NLGN3.

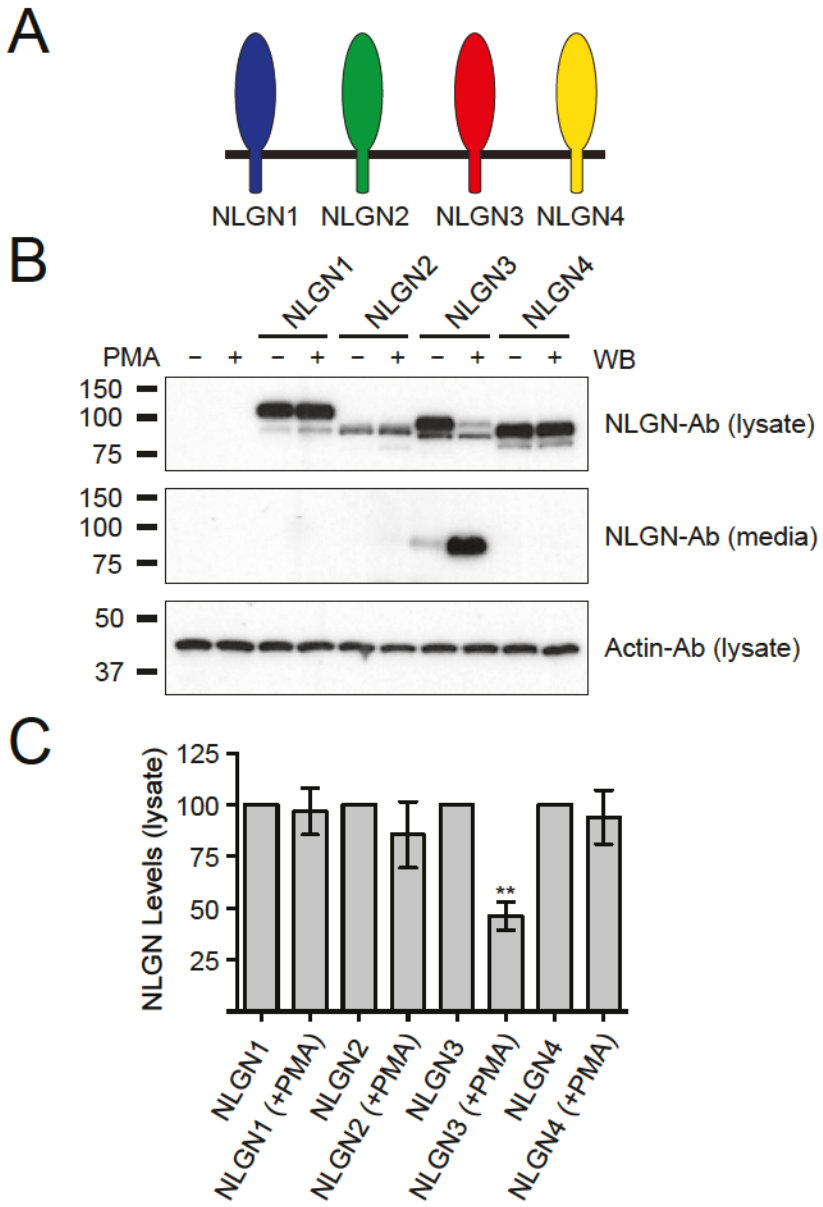

Figure 5-1. **PKC-Mediated NLGN3 Protein Loss in Heterologous Cells**. **A.** Schematic of neuroligin subtypes. **B.** Total neuroligin levels in cells (lysate) and in culture media (media) in HEK293T cells under control conditions (DMSO) or in the presence of phorbol 12-myristate 13-acetate (PMA), a transient activator of PKC. Immunoblots were probed with indicated antibodies. **C.** Means ± SEM of total NLGN1, NLGN2, NLGN3,

or NLGN4 normalized to actin control (n = 5) with NLGN1 + PMA ($P > 0.05$), NLGN2 + PMA ($P > 0.05$), NLGN3 + PMA ($P = 0.0079$), or NLGN4 + PMA ($P > 0.05$). $^{**}P < 0.01$.

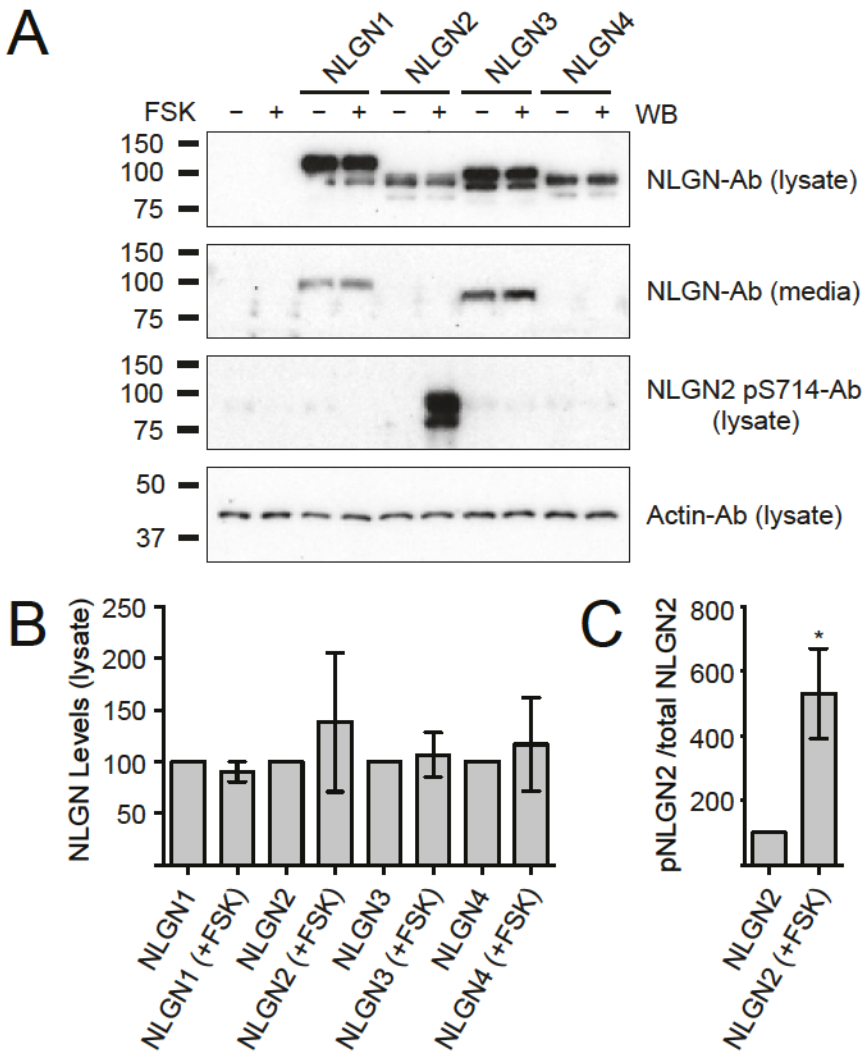

Figure 5-2. **PKA does not Induce Neuroligin Protein Loss**. **A.** Total neuroligin levels in cells (lysate) and in culture media (media) in HEK293T cells under control conditions (DMSO) or in the presence of forskolin (FSK), a transient activator of PKA. Immunoblots were probed with indicated antibodies. NLGN2 phosphorylation served as a positive control for FOR treatment. **B.** Means ± SEM of total NLGN1, NLGN2, NLGN3, or NLGN4 normalized to actin control (n = 3) with NLGN1 + FSK ($P > 0.05$), NLGN2 + FSK ($P > 0.05$), NLGN3 + FSK ($P > 0.05$), or NLGN4 + FSK ($P > 0.05$). **C.**

Means ± SEM of phosphorylated to total NLGN2 normalized to DMSO control (n = 3) with FSK ($P = 0.0365$). $^{*}P < 0.05$.

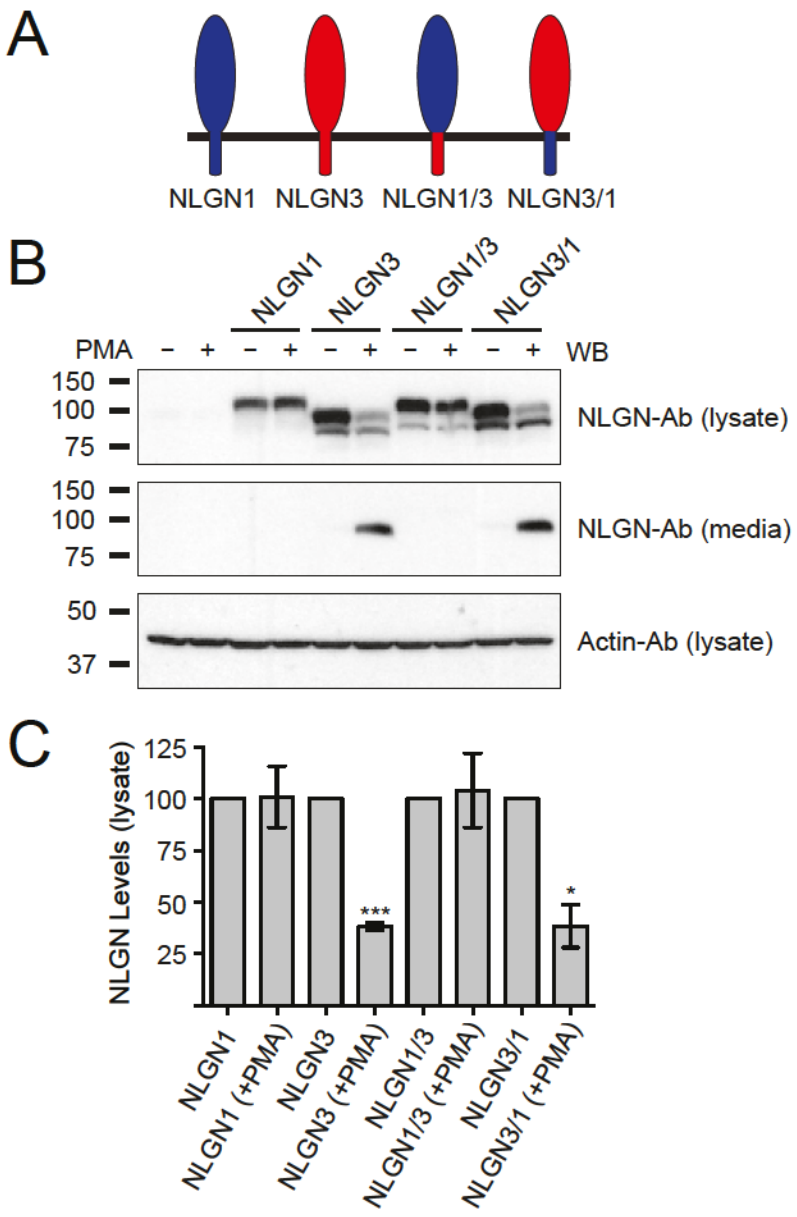

Figure 5-3. **PKC-mediated NLGN3 Protein Loss is Dependent on its Extracellular Domain**. **A.** Schematic of neuroligin subtypes. **B.** Total neuroligin levels in cells (lysate) and in culture media (media) in HEK293T cells under control conditions (DMSO) or in the presence of phorbol 12-myristate 13-acetate (PMA), a transient activator of PKC. Immunoblots were probed with indicated antibodies. **C.** Means ± SEM of total NLGN1, NLGN3, NLGN1/3, or NLGN3/1 normalized to actin control (n = 3) with NLGN1 +

PMA ($P > 0.05$), NLGN3 + PMA ($P = 0.0009$), NLGN1/3 + PMA ($P > 0.05$), or NLGN3/1 + PMA ($P = 0.0271$). $^{*}P < 0.05$, $^{***}P < 0.001$.

DISCUSSION

The importance of the NLGN3 ECD remains unquestioned. The NLGN3 ECD promotes glioma growth and its expression inversely correlates with survival in human glioblastoma (Venkatesh et al., 2015). Identification of the protease(s) that cleaves NLGN3, how it is regulated, and the receptor that NLGN3 ECD binds to in glioma cells to promote proliferation may lead to cancer therapeutics and underlies our biochemical goals for this project.

Secondly, when proteins are cleaved by proteases, they are most often subsequently degraded, removed, and no longer provide a function within or at a nearby cell. However, the fact that the NLGN3 ECD can induce proliferation in glioma cells provides an alternative explanation that the NLGN3 ECD may provide a function after proteolytic cleavage (Venkatesh et al., 2015). The initial finding focused on the NLGN3 ECD function in cancer cells but suggests that maybe the NLGN3 ECD or ICD may serve a role within the nervous system, an area of current focus.

It is difficult to predict the direction of a project in its infancies. However, if we find the NLGN3 ECD to have a function within the nervous system, we will look at the other NLGN isoforms to see if they may have a similar or disparate function. Moreover, it is clear that NLGN1 and NLGN3, the two NLGN isoforms localized at excitatory synapses, undergo proteolytic cleavage. Is this solely a mechanism to regulate excitatory synapses or do inhibitory NLGN isoforms, such as NLGN2, undergo a similar process? Regardless of the answers to these questions, the NLGN3 ECD remains an exciting area of focus for disease biology and basic science research.

ACKNOWLEDGEMENTS

We are grateful to John D. Badger, as well as other members of Roche lab, for technical assistance and for discussions on the project and manuscript.

AUTHOR CONTRIBUTIONS

M.A.B. and K.W.R. designed research. M.A.B. performed research. M.A.B. and K.W.R. analyzed data; and M.A.B. and K.W.R. wrote the paper.

MATERIALS and METHODS

Immunoblotting. HEK293T cells were maintained, transfected, and proteins were isolated as previously described (Bemben et al., 2014). Treatment with 200 ng/μL PMA (Tocris) or DMSO (Sigma) began 60 minutes before protein isolation.

Chapter 6

Concluding Remarks

The discovery of neuroligins twenty years ago unlocked new avenues of research into the molecular dynamics of the synaptic site. The research that has followed has greatly enhanced our understanding of functional synaptogenesis in the developing and mature brain. The involvement of neuroligins in cognitive disorders and more recently cancer underlies the broad interest and critical importance of their investigation. These preliminary investigations have enabled researchers to develop genetic models to study the etiology of these diseases and one day will hopefully lead to therapeutics (Bemben et al., 2015b).

The preliminary studies on neuroligins focused on two key aspects: 1) their ability to induce synaptogenesis, and 2) their ability to eliminate synapses when reduced from an individual cell. These now canonical studies have made neuroligins the gold standard of molecules that dynamically form and modulate synapses. Since their initial identification, neuroligins have garnered broad interest from the scientific community, but many key questions still remain unanswered. For example, if neuroligins are such key mediators of synaptic function, how does the cell transiently regulate or faithfully modify these molecules to prevent aberrant expression, which would be detrimental to the cell? Secondly, how does a single molecule recruit the machinery necessary to form a functional synapse?

My dissertation research attempted to answer these questions and expand on the limited research on the regulation of neuroligin proteins. We reasoned that neurons need to tightly regulate potent synaptic inducers, such as neuroligins, as loss of control would lead to too many or too few synapses on a particular neuron. In **Chapter 3,** we identified an individual phosphorylation site on neuroligin-1 that drastically effects its expression

on the plasma membrane. If neuroligin-1 is unable to achieve surface expression, it cannot induce synaptogenesis, essentially rendering the protein inactive. In short, this posttranslational modification acts as an on/off switch for neuroligin-1 function, which argues against dogma that neuroligins are only static building blocks of a synapse and cannot be transiently activated molecules. Although this chapter focused on a single neuroligin isoform, it is reasonable to hypothesize that other neuroligin isoforms may be modified in a similar fashion and is under current investigation in the Roche Laboratory. Furthermore, it begs the question if other posttranslational modifications regulate neuroligin proteins? Researchers have taken a holistic approach at comparing neuroligin isoforms and found they are highly conserved. However, different neuroligin isoforms are able to induce different types of synapses, which requires recruiting vastly different cellular machinery. Which domains within neuroligins are critical for this isoform specificity remains an enigma, but our research sheds light on the need to dissect these molecules on what may be single amino acid differences, such as a phosphorylation site, to elucidate critical isoform-specific domains.

This approach led us to another key finding in the neuroligin field, which focused on how an individual molecule can recruit the necessary machinery and generate a functional synapse. In **Chapter 4**, we uncovered a phosphorylation site on neuroligin-4X that enables this isoform to robustly generate excitatory synapses. In contrast to phosphorylation of the cytoplasmic tail (c-tail) of neuroligin-1 regulating surface expression and thereby its ability to generate synapses (**Chapter 3**), phosphorylation of neuroligin-4X c-tail did not regulate its expression on the plasma membrane but led to the robust genesis of functional excitatory synapses. Hence, the title of the thesis, *A Tale of*

Two C-Tails, describing how phosphorylation on a different site in neuroligin-1 and neuroligin-4x can lead to the genesis of excitatory synapses but by independent mechanisms. Then how might neurolgin-4X phosphorylation induce the genesis of synapses independent of regulating surface expression?

Unfortunately, we have not uncovered this mechanism of synaptic enhancement but it is under current investigation. We reason this could be achieved in several ways. The most likely of these hypotheses is that phosphorylated neuroligin-4X binds to a linker or scaffolding protein that promotes the recruitment of excitatory synapse machinery such as glutamate receptors. To the best of our knowledge, there are few published reports of proteins that bind to neuroligin-4X, therefore we do not have many candidate molecules to test. An unbiased screen for differential binding partners of non/phosphorylated neuroligin-4X protein could potentially yield interesting results. A second hypothesis is that phosphorylated neuroligin-4X could increase the binding affinity for neurexin, which would result in an increase in synaptogenesis. We deem this scenario to be less likely because it would require an intracellular modification (phosphorylation) to result in a conformational change in the extracellular domain (location of neurexin binding site) on neuroligin-4X. Regardless of the mechanism, elucidating this pathway will deepen our understanding of synaptogenesis in the brain. For detailed analysis on neuroligin-1 and neuroligin-4X phosphorylation, please refer to those individual sections.

Phosphorylation of neuroligin-1 and neuroligin-4X focused on how neuroligins are trafficked to synaptic sites and promote synaptogenesis. However, how are neuroligins removed from the synapse and what are the functional consequences of this

release from the synaptic site? While we were studying protein kinase C phosphorylation of neuroligin-4X, we observed an unusual phenomenon. Whenever we activated protein kinase C within the cell, nearly all neuroligin-3 protein was degraded and the extracellular domain was released into the media. Although interesting, this result piqued our interest when an unbiased screen found the extracellular domain of neuroligin-3 could act as a mitogen to promote glioma growth (Venkatesh et al., 2015). The neuroligin-3 ectodomain acts as a ligand on glioma cells to change gene expression, establishing a new or off-target function for neuroligins. The importance of the neuroligin-3 ectodomain was identified in this study, but it did not provide any information on the production of the truncated form of neuroligin-3. Moreover, given the fact that the neuroligin-3 ectodomain provides a function outside the nervous system, might it also provide one in the nervous system? For example, could it act as a dominant negative by binding to neurexins without its c-tail, and therefore be unable to recruit synaptic receptors, thus suppressing synaptic transmission?

These are questions we will be investigating in the future. However, uncovering the mechanism of proteolytic processing to produce the neuroligin-3 ectodomain will be useful in cancer therapeutics. For example, the protease that cleaves neurolgin-3 in neurons or the receptor that binds the neuroligin-3 ectodomain in glioma cells to promote cell proliferation are potential drug targets.

Despite outstanding advances in the field, many key questions remain unsolved. Furthermore, as investigations continue on neuroligins, new functions continue to be identified. Our results described in this thesis expand our knowledge and identify new mechanisms of acute activation of neuroligin proteins. This shift in focus from

neuroligins as static to transient synaptic molecules may change the direction of future research in the field. The scope of diseases with which neuroligins are associated continues to expand and now range from autism spectrum disorders to cancers. This underscores the importance of their continued dissection.

REFERENCES

(2014). Prevalence of autism spectrum disorder among children aged 8 years - autism and developmental disabilities monitoring network, 11 sites, United States, 2010. MMWR Surveill Summ *63*, 1-21.

Abrahams, B.S., and Geschwind, D.H. (2008). Advances in autism genetics: on the threshold of a new neurobiology. Nature reviews Genetics *9*, 341-355.

Antonelli, R., Pizzarelli, R., Pedroni, A., Fritschy, J.M., Del Sal, G., Cherubini, E., and Zacchi, P. (2014). Pin1-dependent signalling negatively affects GABAergic transmission by modulating neuroligin2/gephyrin interaction. Nature communications *5*, 5066.

Arac, D., Boucard, A.A., Ozkan, E., Strop, P., Newell, E., Sudhof, T.C., and Brunger, A.T. (2007). Structures of neuroligin-1 and the neuroligin-1/neurexin-1 beta complex reveal specific protein-protein and protein-Ca2+ interactions. Neuron *56*, 992-1003.

Arikkath, J., and Reichardt, L.F. (2008). Cadherins and catenins at synapses: roles in synaptogenesis and synaptic plasticity. Trends in neurosciences *31*, 487-494.

Bemben, M.A., Nguyen, Q.A., Wang, T., Li, Y., Nicoll, R.A., and Roche, K.W. (2015a). Autism-associated mutation inhibits protein kinase C-mediated neuroligin-4X enhancement of excitatory synapses. Proceedings of the National Academy of Sciences of the United States of America *112*, 2551-2556.

Bemben, M.A., Shipman, S.L., Hirai, T., Herring, B.E., Li, Y., Badger, J.D., 2nd, Nicoll, R.A., Diamond, J.S., and Roche, K.W. (2014). CaMKII phosphorylation of neuroligin-1 regulates excitatory synapses. Nature neuroscience *17*, 56-64.

Bemben, M.A., Shipman, S.L., Nicoll, R.A., and Roche, K.W. (2015b). The cellular and molecular landscape of neuroligins. Trends in neurosciences *38*, 496-505.

Biederer, T., Sara, Y., Mozhayeva, M., Atasoy, D., Liu, X., Kavalali, E.T., and Sudhof, T.C. (2002). SynCAM, a synaptic adhesion molecule that drives synapse assembly. Science *297*, 1525-1531.

Blundell, J., Blaiss, C.A., Etherton, M.R., Espinosa, F., Tabuchi, K., Walz, C., Bolliger, M.F., Sudhof, T.C., and Powell, C.M. (2010). Neuroligin-1 deletion results in impaired spatial memory and increased repetitive behavior. The Journal of neuroscience : the official journal of the Society for Neuroscience *30*, 2115-2129.

Bolliger, M.F., Pei, J., Maxeiner, S., Boucard, A.A., Grishin, N.V., and Sudhof, T.C. (2008). Unusually rapid evolution of Neuroligin-4 in mice. Proceedings of the National Academy of Sciences of the United States of America *105*, 6421-6426.

Boucard, A.A., Ko, J., and Sudhof, T.C. (2012). High affinity neurexin binding to cell adhesion G-protein-coupled receptor CIRL1/latrophilin-1 produces an intercellular adhesion complex. The Journal of biological chemistry *287*, 9399-9413.

Budreck, E.C., Kwon, O.B., Jung, J.H., Baudouin, S., Thommen, A., Kim, H.S., Fukazawa, Y., Harada, H., Tabuchi, K., Shigemoto, R., *et al.* (2013). Neuroligin-1 controls synaptic abundance of NMDA-type glutamate receptors through extracellular coupling. Proceedings of the National Academy of Sciences of the United States of America *110*, 725-730.

Budreck, E.C., and Scheiffele, P. (2007). Neuroligin-3 is a neuronal adhesion protein at GABAergic and glutamatergic synapses. The European journal of neuroscience *26*, 1738-1748.

Chanda, S., Aoto, J., Lee, S.J., Wernig, M., and Sudhof, T.C. (2015). Pathogenic mechanism of an autism-associated neuroligin mutation involves altered AMPA-receptor trafficking. Molecular psychiatry.

Chih, B., Engelman, H., and Scheiffele, P. (2005). Control of excitatory and inhibitory synapse formation by neuroligins. Science *307*, 1324-1328.

Chih, B., Gollan, L., and Scheiffele, P. (2006). Alternative splicing controls selective trans-synaptic interactions of the neuroligin-neurexin complex. Neuron *51*, 171-178.

Choi, U.B., McCann, J.J., Weninger, K.R., and Bowen, M.E. (2011a). Beyond the random coil: stochastic conformational switching in intrinsically disordered proteins. Structure *19*, 566-576.

Choi, Y.B., Li, H.L., Kassabov, S.R., Jin, I., Puthanveettil, S.V., Karl, K.A., Lu, Y., Kim, J.H., Bailey, C.H., and Kandel, E.R. (2011b). Neurexin-neuroligin transsynaptic interaction mediates learning-related synaptic remodeling and long-term facilitation in aplysia. Neuron *70*, 468-481.

Chubykin, A.A., Atasoy, D., Etherton, M.R., Brose, N., Kavalali, E.T., Gibson, J.R., and Sudhof, T.C. (2007). Activity-dependent validation of excitatory versus inhibitory synapses by neuroligin-1 versus neuroligin-2. Neuron *54*, 919-931.

Comoletti, D., De Jaco, A., Jennings, L.L., Flynn, R.E., Gaietta, G., Tsigelny, I., Ellisman, M.H., and Taylor, P. (2004). The Arg451Cys-neuroligin-3 mutation associated with autism reveals a defect in protein processing. The Journal of neuroscience : the official journal of the Society for Neuroscience *24*, 4889-4893.

Comoletti, D., Flynn, R., Jennings, L.L., Chubykin, A., Matsumura, T., Hasegawa, H., Sudhof, T.C., and Taylor, P. (2003). Characterization of the interaction of a recombinant soluble neuroligin-1 with neurexin-1beta. The Journal of biological chemistry *278*, 50497-50505.

Comoletti, D., Grishaev, A., Whitten, A.E., Tsigelny, I., Taylor, P., and Trewhella, J. (2007). Synaptic arrangement of the neuroligin/beta-neurexin complex revealed by X-ray and neutron scattering. Structure *15*, 693-705.

Craig, A.M., and Kang, Y. (2007). Neurexin-neuroligin signaling in synapse development. Current opinion in neurobiology *17*, 43-52.

Dahlhaus, R., and El-Husseini, A. (2010). Altered neuroligin expression is involved in social deficits in a mouse model of the fragile X syndrome. Behavioural brain research *208*, 96-105.

Dalva, M.B., McClelland, A.C., and Kayser, M.S. (2007). Cell adhesion molecules: signalling functions at the synapse. Nature reviews Neuroscience *8*, 206-220.

de Wit, J., Sylwestrak, E., O'Sullivan, M.L., Otto, S., Tiglio, K., Savas, J.N., Yates, J.R., 3rd, Comoletti, D., Taylor, P., and Ghosh, A. (2009). LRRTM2 interacts with Neurexin1 and regulates excitatory synapse formation. Neuron *64*, 799-806.

Dean, C., and Dresbach, T. (2006). Neuroligins and neurexins: linking cell adhesion, synapse formation and cognitive function. Trends in neurosciences *29*, 21-29.

Dean, C., Scholl, F.G., Choih, J., DeMaria, S., Berger, J., Isacoff, E., and Scheiffele, P. (2003). Neurexin mediates the assembly of presynaptic terminals. Nature neuroscience *6*, 708-716.

Dresbach, T., Neeb, A., Meyer, G., Gundelfinger, E.D., and Brose, N. (2004). Synaptic targeting of neuroligin is independent of neurexin and SAP90/PSD95 binding. Molecular and cellular neurosciences *27*, 227-235.

Esteban, J.A., Shi, S.H., Wilson, C., Nuriya, M., Huganir, R.L., and Malinow, R. (2003). PKA phosphorylation of AMPA receptor subunits controls synaptic trafficking underlying plasticity. Nature neuroscience *6*, 136-143.

Etherton, M.R., Tabuchi, K., Sharma, M., Ko, J., and Sudhof, T.C. (2011). An autism-associated point mutation in the neuroligin cytoplasmic tail selectively impairs AMPA receptor-mediated synaptic transmission in hippocampus. The EMBO journal *30*, 2908-2919.

Fabrichny, I.P., Leone, P., Sulzenbacher, G., Comoletti, D., Miller, M.T., Taylor, P., Bourne, Y., and Marchot, P. (2007). Structural analysis of the synaptic protein neuroligin and its beta-neurexin complex: determinants for folding and cell adhesion. Neuron *56*, 979-991.

Foldy, C., Malenka, R.C., and Sudhof, T.C. (2013). Autism-associated neuroligin-3 mutations commonly disrupt tonic endocannabinoid signaling. Neuron *78*, 498-509.

Futai, K., Kim, M.J., Hashikawa, T., Scheiffele, P., Sheng, M., and Hayashi, Y. (2007). Retrograde modulation of presynaptic release probability through signaling mediated by PSD-95-neuroligin. Nature neuroscience *10*, 186-195.

Giannone, G., Mondin, M., Grillo-Bosch, D., Tessier, B., Saint-Michel, E., Czondor, K., Sainlos, M., Choquet, D., and Thoumine, O. (2013). Neurexin-1beta binding to neuroligin-1 triggers the preferential recruitment of PSD-95 versus gephyrin through tyrosine phosphorylation of neuroligin-1. Cell reports *3*, 1996-2007.

Graf, E.R., Zhang, X., Jin, S.X., Linhoff, M.W., and Craig, A.M. (2004). Neurexins induce differentiation of GABA and glutamate postsynaptic specializations via neuroligins. Cell *119*, 1013-1026.

Gutierrez, R.C., Flynn, R., Hung, J., Kertesz, A.C., Sullivan, A., Zamponi, G.W., El-Husseini, A., and Colicos, M.A. (2009). Activity-driven mobilization of post-synaptic proteins. The European journal of neuroscience *30*, 2042-2052.

Harvey, K., Duguid, I.C., Alldred, M.J., Beatty, S.E., Ward, H., Keep, N.H., Lingenfelter, S.E., Pearce, B.R., Lundgren, J., Owen, M.J., *et al.* (2004). The GDP-GTP exchange factor collybistin: an essential determinant of neuronal gephyrin clustering. The Journal of neuroscience : the official journal of the Society for Neuroscience *24*, 5816-5826.

Hirao, K., Hata, Y., Ide, N., Takeuchi, M., Irie, M., Yao, I., Deguchi, M., Toyoda, A., Sudhof, T.C., and Takai, Y. (1998). A novel multiple PDZ domain-containing molecule interacting with N-methyl-D-aspartate receptors and neuronal cell adhesion proteins. The Journal of biological chemistry *273*, 21105-21110.

Hoffman, R.C., Jennings, L.L., Tsigelny, I., Comoletti, D., Flynn, R.E., Sudhof, T.C., and Taylor, P. (2004). Structural characterization of recombinant soluble rat neuroligin 1: mapping of secondary structure and glycosylation by mass spectrometry. Biochemistry *43*, 1496-1506.

Hoon, M., Soykan, T., Falkenburger, B., Hammer, M., Patrizi, A., Schmidt, K.F., Sassoe-Pognetto, M., Lowel, S., Moser, T., Taschenberger, H., *et al.* (2011). Neuroligin-4 is localized to glycinergic postsynapses and regulates inhibition in the retina. Proceedings of the National Academy of Sciences of the United States of America *108*, 3053-3058.

Ichtchenko, K., Hata, Y., Nguyen, T., Ullrich, B., Missler, M., Moomaw, C., and Sudhof, T.C. (1995). Neuroligin 1: a splice site-specific ligand for beta-neurexins. Cell *81*, 435-443.

Ichtchenko, K., Nguyen, T., and Sudhof, T.C. (1996). Structures, alternative splicing, and neurexin binding of multiple neuroligins. The Journal of biological chemistry *271*, 2676-2682.

Iida, J., Hirabayashi, S., Sato, Y., and Hata, Y. (2004). Synaptic scaffolding molecule is involved in the synaptic clustering of neuroligin. Molecular and cellular neurosciences *27*, 497-508

Irie, M., Hata, Y., Takeuchi, M., Ichtchenko, K., Toyoda, A., Hirao, K., Takai, Y., Rosahl, T.W., and Sudhof, T.C. (1997). Binding of neuroligins to PSD-95. Science *277*, 1511-1515.

Jamain, S., Quach, H., Betancur, C., Rastam, M., Colineaux, C., Gillberg, I.C., Soderstrom, H., Giros, B., Leboyer, M., Gillberg, C., *et al.* (2003). Mutations of the X-linked genes encoding neuroligins NLGN3 and NLGN4 are associated with autism. Nature genetics *34*, 27-29.

Jung, S.Y., Kim, J., Kwon, O.B., Jung, J.H., An, K., Jeong, A.Y., Lee, C.J., Choi, Y.B., Bailey, C.H., Kandel, E.R., *et al.* (2010). Input-specific synaptic plasticity in the amygdala is regulated by neuroligin-1 via postsynaptic NMDA receptors. Proceedings of the National Academy of Sciences of the United States of America *107*, 4710-4715.

Kim, J., Jung, S.Y., Lee, Y.K., Park, S., Choi, J.S., Lee, C.J., Kim, H.S., Choi, Y.B., Scheiffele, P., Bailey, C.H., *et al.* (2008). Neuroligin-1 is required for normal expression of LTP and associative fear memory in the amygdala of adult animals. Proceedings of the National Academy of Sciences of the United States of America *105*, 9087-9092.

Kim, J.H., and Huganir, R.L. (1999). Organization and regulation of proteins at synapses. Current opinion in cell biology *11*, 248-254.

Kins, S., Betz, H., and Kirsch, J. (2000). Collybistin, a newly identified brain-specific GEF, induces submembrane clustering of gephyrin. Nature neuroscience *3*, 22-29.

Ko, J., Fuccillo, M.V., Malenka, R.C., and Sudhof, T.C. (2009a). LRRTM2 functions as a neurexin ligand in promoting excitatory synapse formation. Neuron *64*, 791-798.

Ko, J., Zhang, C., Arac, D., Boucard, A.A., Brunger, A.T., and Sudhof, T.C. (2009b). Neuroligin-1 performs neurexin-dependent and neurexin-independent functions in synapse validation. The EMBO journal *28*, 3244-3255.

Koehnke, J., Jin, X., Budreck, E.C., Posy, S., Scheiffele, P., Honig, B., and Shapiro, L. (2008). Crystal structure of the extracellular cholinesterase-like domain from neuroligin-2. Proc Natl Acad Sci U S A *105*, 1873-1878.

Koehnke, J., Katsamba, P.S., Ahlsen, G., Bahna, F., Vendome, J., Honig, B., Shapiro, L., and Jin, X. (2010). Splice form dependence of beta-neurexin/neuroligin binding interactions. Neuron *67*, 61-74.

Kwon, H.B., Kozorovitskiy, Y., Oh, W.J., Peixoto, R.T., Akhtar, N., Saulnier, J.L., Gu, C., and Sabatini, B.L. (2012). Neuroligin-1-dependent competition regulates cortical synaptogenesis and synapse number. Nature neuroscience *15*, 1667-1674.

Laumonnier, F., Bonnet-Brilhault, F., Gomot, M., Blanc, R., David, A., Moizard, M.P., Raynaud, M., Ronce, N., Lemonnier, E., Calvas, P., *et al.* (2004). X-linked mental retardation and autism are associated with a mutation in the NLGN4 gene, a member of the neuroligin family. American journal of human genetics *74*, 552-557.

Lawson-Yuen, A., Saldivar, J.S., Sommer, S., and Picker, J. (2008). Familial deletion within NLGN4 associated with autism and Tourette syndrome. European journal of human genetics : EJHG *16*, 614-618.

Lee, H., Dean, C., and Isacoff, E. (2010). Alternative splicing of neuroligin regulates the rate of presynaptic differentiation. The Journal of neuroscience : the official journal of the Society for Neuroscience *30*, 11435-11446.

Lee, K., Kim, Y., Lee, S.J., Qiang, Y., Lee, D., Lee, H.W., Kim, H., Je, H.S., Sudhof, T.C., and Ko, J. (2013). MDGAs interact selectively with neuroligin-2 but not other neuroligins to regulate inhibitory synapse development. Proceedings of the National Academy of Sciences of the United States of America *110*, 336-341.

Levinson, J.N., Chery, N., Huang, K., Wong, T.P., Gerrow, K., Kang, R., Prange, O., Wang, Y.T., and El-Husseini, A. (2005). Neuroligins mediate excitatory and inhibitory synapse formation: involvement of PSD-95 and neurexin-1beta in neuroligin-induced synaptic specificity. The Journal of biological chemistry *280*, 17312-17319.

Levy, D., Ronemus, M., Yamrom, B., Lee, Y.H., Leotta, A., Kendall, J., Marks, S., Lakshmi, B., Pai, D., Ye, K., *et al.* (2011). Rare de novo and transmitted copy-number variation in autistic spectrum disorders. Neuron *70*, 886-897.

Linhoff, M.W., Lauren, J., Cassidy, R.M., Dobie, F.A., Takahashi, H., Nygaard, H.B., Airaksinen, M.S., Strittmatter, S.M., and Craig, A.M. (2009). An unbiased expression screen for synaptogenic proteins identifies the LRRTM protein family as synaptic organizers. Neuron *61*, 734-749.

Lisman, J., Schulman, H., and Cline, H. (2002). The molecular basis of CaMKII function in synaptic and behavioural memory. Nature reviews Neuroscience *3*, 175-190.

Marei, H.E., Ahmed, A.E., Michetti, F., Pescatori, M., Pallini, R., Casalbore, P., Cenciarelli, C., and Elhadidy, M. (2012). Gene expression profile of adult human olfactory bulb and embryonic neural stem cell suggests distinct signaling pathways and epigenetic control. PloS one *7*, e33542.

Marshall, C.R., Noor, A., Vincent, J.B., Lionel, A.C., Feuk, L., Skaug, J., Shago, M., Moessner, R., Pinto, D., Ren, Y., *et al.* (2008). Structural variation of chromosomes in autism spectrum disorder. American journal of human genetics *82*, 477-488.

Meyer, G., Varoqueaux, F., Neeb, A., Oschlies, M., and Brose, N. (2004). The complexity of PDZ domain-mediated interactions at glutamatergic synapses: a case study on neuroligin. Neuropharmacology *47*, 724-733.

Mosca, T.J., Hong, W., Dani, V.S., Favaloro, V., and Luo, L. (2012). Trans-synaptic Teneurin signalling in neuromuscular synapse organization and target choice. Nature *484*, 237-241.

Nam, C.I., and Chen, L. (2005). Postsynaptic assembly induced by neurexin-neuroligin interaction and neurotransmitter. Proceedings of the National Academy of Sciences of the United States of America *102*, 6137-6142.

Nguyen, T., and Sudhof, T.C. (1997). Binding properties of neuroligin 1 and neurexin 1beta reveal function as heterophilic cell adhesion molecules. The Journal of biological chemistry *272*, 26032-26039.

Papadopoulos, T., and Soykan, T. (2011). The role of collybistin in gephyrin clustering at inhibitory synapses: facts and open questions. Frontiers in cellular neuroscience *5*, 11.

Peixoto, R.T., Kunz, P.A., Kwon, H., Mabb, A.M., Sabatini, B.L., Philpot, B.D., and Ehlers, M.D. (2012). Transsynaptic signaling by activity-dependent cleavage of neuroligin-1. Neuron *76*, 396-409.

Pettem, K.L., Yokomaku, D., Takahashi, H., Ge, Y., and Craig, A.M. (2013). Interaction between autism-linked MDGAs and neuroligins suppresses inhibitory synapse development. The Journal of cell biology *200*, 321-336.

Philpot, B.D., Sekhar, A.K., Shouval, H.Z., and Bear, M.F. (2001). Visual experience and deprivation bidirectionally modify the composition and function of NMDA receptors in visual cortex. Neuron *29*, 157-169.

Poulopoulos, A., Aramuni, G., Meyer, G., Soykan, T., Hoon, M., Papadopoulos, T., Zhang, M., Paarmann, I., Fuchs, C., Harvey, K., *et al.* (2009). Neuroligin 2 drives postsynaptic assembly at perisomatic inhibitory synapses through gephyrin and collybistin. Neuron *63*, 628-642.

Poulopoulos, A., Soykan, T., Tuffy, L.P., Hammer, M., Varoqueaux, F., and Brose, N. (2012). Homodimerization and isoform-specific heterodimerization of neuroligins. The Biochemical journal *446*, 321-330.

Roche, K.W., O'Brien, R.J., Mammen, A.L., Bernhardt, J., and Huganir, R.L. (1996). Characterization of multiple phosphorylation sites on the AMPA receptor GluR1 subunit. Neuron *16*, 1179-1188.

Rosales, C.R., Osborne, K.D., Zuccarino, G.V., Scheiffele, P., and Silverman, M.A. (2005). A cytoplasmic motif targets neuroligin-1 exclusively to dendrites of cultured hippocampal neurons. The European journal of neuroscience *22*, 2381-2386.

Rothwell, P.E., Fuccillo, M.V., Maxeiner, S., Hayton, S.J., Gokce, O., Lim, B.K., Fowler, S.C., Malenka, R.C., and Sudhof, T.C. (2014). Autism-associated neuroligin-3 mutations commonly impair striatal circuits to boost repetitive behaviors. Cell *158*, 198-212.

Sanders, S.J., Ercan-Sencicek, A.G., Hus, V., Luo, R., Murtha, M.T., Moreno-De-Luca, D., Chu, S.H., Moreau, M.P., Gupta, A.R., Thomson, S.A., *et al.* (2011). Multiple recurrent de novo CNVs, including duplications of the 7q11.23 Williams syndrome region, are strongly associated with autism. Neuron *70*, 863-885.

Schapitz, I.U., Behrend, B., Pechmann, Y., Lappe-Siefke, C., Kneussel, S.J., Wallace, K.E., Stempel, A.V., Buck, F., Grant, S.G., Schweizer, M., *et al.* (2010). Neuroligin 1 is dynamically exchanged at postsynaptic sites. The Journal of neuroscience : the official journal of the Society for Neuroscience *30*, 12733-12744.

Schnell, E., Sizemore, M., Karimzadegan, S., Chen, L., Bredt, D.S., and Nicoll, R.A. (2002). Direct interactions between PSD-95 and stargazin control synaptic AMPA receptor number. Proceedings of the National Academy of Sciences of the United States of America *99*, 13902-13907.

Shen, C., Huo, L.R., Zhao, X.L., Wang, P.R., and Zhong, N. (2015). Novel interactive partners of neuroligin 3: new aspects for pathogenesis of autism. Journal of molecular neuroscience : MN *56*, 89-101.

Shipman, S.L., and Nicoll, R.A. (2012a). Dimerization of postsynaptic neuroligin drives synaptic assembly via transsynaptic clustering of neurexin. Proceedings of the National Academy of Sciences of the United States of America *109*, 19432-19437.

Shipman, S.L., and Nicoll, R.A. (2012b). A subtype-specific function for the extracellular domain of neuroligin 1 in hippocampal LTP. Neuron *76*, 309-316.

Shipman, S.L., Schnell, E., Hirai, T., Chen, B.S., Roche, K.W., and Nicoll, R.A. (2011). Functional dependence of neuroligin on a new non-PDZ intracellular domain. Nature neuroscience *14*, 718-726.

Song, J.Y., Ichtchenko, K., Sudhof, T.C., and Brose, N. (1999). Neuroligin 1 is a postsynaptic cell-adhesion molecule of excitatory synapses. Proceedings of the National Academy of Sciences of the United States of America *96*, 1100-1105.

Soykan, T., Schneeberger, D., Tria, G., Buechner, C., Bader, N., Svergun, D., Tessmer, I., Poulopoulos, A., Papadopoulos, T., Varoqueaux, F., *et al.* (2014). A conformational switch in collybistin determines the differentiation of inhibitory postsynapses. The EMBO journal *33*, 2113-2133.

Stoppini, L., Buchs, P.A., and Muller, D. (1991). A simple method for organotypic cultures of nervous tissue. Journal of neuroscience methods *37*, 173-182.

Suckow, A.T., Zhang, C., Egodage, S., Comoletti, D., Taylor, P., Miller, M.T., Sweet, I.R., and Chessler, S.D. (2012). Transcellular neuroligin-2 interactions enhance insulin secretion and are integral to pancreatic beta-cell function. J Biol Chem, (Epub ahead of print).

Sudhof, T.C. (2008). Neuroligins and neurexins link synaptic function to cognitive disease. Nature *455*, 903-911.

Sumita, K., Sato, Y., Iida, J., Kawata, A., Hamano, M., Hirabayashi, S., Ohno, K., Peles, E., and Hata, Y. (2007). Synaptic scaffolding molecule (S-SCAM) membrane-associated guanylate kinase with inverted organization (MAGI)-2 is associated with cell adhesion molecules at inhibitory synapses in rat hippocampal neurons. Journal of neurochemistry *100*, 154-166.

Suzuki, K., Hayashi, Y., Nakahara, S., Kumazaki, H., Prox, J., Horiuchi, K., Zeng, M., Tanimura, S., Nishiyama, Y., Osawa, S., *et al.* (2012). Activity-dependent proteolytic cleavage of neuroligin-1. Neuron *76*, 410-422.

Tabuchi, K., Blundell, J., Etherton, M.R., Hammer, R.E., Liu, X., Powell, C.M., and Sudhof, T.C. (2007). A neuroligin-3 mutation implicated in autism increases inhibitory synaptic transmission in mice. Science *318*, 71-76.

Tanaka, H., Miyazaki, N., Matoba, K., Nogi, T., Iwasaki, K., and Takagi, J. (2012). Higher-order architecture of cell adhesion mediated by polymorphic synaptic adhesion molecules neurexin and neuroligin. Cell Rep *2*, 101-110.

Thomas, N.S., Sharp, A.J., Browne, C.E., Skuse, D., Hardie, C., and Dennis, N.R. (1999). Xp deletions associated with autism in three females. Human genetics *104*, 43-48.

Treutlein, B., Gokce, O., Quake, S.R., and Sudhof, T.C. (2014). Cartography of neurexin alternative splicing mapped by single-molecule long-read mRNA sequencing. Proceedings of the National Academy of Sciences of the United States of America *111*, E1291-1299.

Tropea, D., Majewska, A.K., Garcia, R., and Sur, M. (2010). Structural dynamics of synapses in vivo correlate with functional changes during experience-dependent plasticity in visual cortex. The Journal of neuroscience : the official journal of the Society for Neuroscience *30*, 11086-11095.

Uemura, T., Lee, S.J., Yasumura, M., Takeuchi, T., Yoshida, T., Ra, M., Taguchi, R., Sakimura, K., and Mishina, M. (2010). Trans-synaptic interaction of GluRdelta2 and Neurexin through Cbln1 mediates synapse formation in the cerebellum. Cell *141*, 1068-1079.

Ullrich, B., Ushkaryov, Y.A., and Sudhof, T.C. (1995). Cartography of neurexins: more than 1000 isoforms generated by alternative splicing and expressed in distinct subsets of neurons. Neuron *14*, 497-507.

Varoqueaux, F., Jamain, S., and Brose, N. (2004). Neuroligin 2 is exclusively localized to inhibitory synapses. European journal of cell biology *83*, 449-456.

Venkatesh, H.S., Johung, T.B., Caretti, V., Noll, A., Tang, Y., Nagaraja, S., Gibson, E.M., Mount, C.W., Polepalli, J., Mitra, S.S., *et al.* (2015). Neuronal Activity Promotes Glioma Growth through Neuroligin-3 Secretion. Cell *161*, 803-816.

Wang, T., Allie, R., Conant, K., Haughey, N., Turchan-Chelowo, J., Hahn, K., Rosen, A., Steiner, J., Keswani, S., Jones, M., *et al.* (2006). Granzyme B mediates neurotoxicity through a G-protein-coupled receptor. FASEB journal : official publication of the Federation of American Societies for Experimental Biology *20*, 1209-1211.

Wittenmayer, N., Korber, C., Liu, H., Kremer, T., Varoqueaux, F., Chapman, E.R., Brose, N., Kuner, T., and Dresbach, T. (2009). Postsynaptic Neuroligin1 regulates presynaptic maturation. Proceedings of the National Academy of Sciences of the United States of America *106*, 13564-13569.

Woo, J., Kwon, S.K., Choi, S., Kim, S., Lee, J.R., Dunah, A.W., Sheng, M., and Kim, E. (2009). Trans-synaptic adhesion between NGL-3 and LAR regulates the formation of excitatory synapses. Nature neuroscience *12*, 428-437.

Yamagata, M., Sanes, J.R., and Weiner, J.A. (2003). Synaptic adhesion molecules. Current opinion in cell biology *15*, 621-632.

Yan, J., Feng, J., Schroer, R., Li, W., Skinner, C., Schwartz, C.E., Cook, E.H., Jr., and Sommer, S.S. (2008). Analysis of the neuroligin 4Y gene in patients with autism. Psychiatric genetics *18*, 204-207.

Yan, J., Oliveira, G., Coutinho, A., Yang, C., Feng, J., Katz, C., Sram, J., Bockholt, A., Jones, I.R., Craddock, N., *et al.* (2005). Analysis of the neuroligin 3 and 4 genes in autism and other neuropsychiatric patients. Molecular psychiatry *10*, 329-332.

Zhang, C., Milunsky, J.M., Newton, S., Ko, J., Zhao, G., Maher, T.A., Tager-Flusberg, H., Bolliger, M.F., Carter, A.S., Boucard, A.A., *et al.* (2009). A neuroligin-4 missense mutation associated with autism impairs neuroligin-4 folding and endoplasmic reticulum export. The Journal of neuroscience : the official journal of the Society for Neuroscience *29*, 10843-10854.

Zoghbi, H.Y., and Bear, M.F. (2012). Synaptic dysfunction in neurodevelopmental disorders associated with autism and intellectual disabilities. Cold Spring Harbor perspectives in biology *4*.

Michael A. Bemben

Present Address: 655 Elmcroft Boulevard Apt. 12208, Rockville, MD 20850, U.S.A.
Email: mbemben2@jhu.edu or bembenma@mail.NIH.gov

EDUCATION

Graduate Studies: Johns Hopkins University / National Institutes of Health
Major: Cell, Molecular, Developmental Biology & Biophysics (CMDB)
Department: Biology **Degree:** PhD **GPA**: 3.7 **Graduation Date:** 12/2015

Undergraduate Studies: University of Michigan-Ann Arbor
Dual Major: English & Cellular and Molecular Biology (CMB)
Graduation Date: May 2009 **English GPA:** 3.5 **CMB GPA:** 3.5

PUBLICATIONS (Graduate)

Bemben, M.A.*, Shipman, S.L.*, Nicoll, R.A., Roche, K.W. *The cellular and molecular landscape of neuroligins*. Trends in Neurosciences 2015, 38:496-505.

Li, Yan., Kane, L., **Bemben, M.A.**, and Roche, K.W. *Analysis of PINK1 and CaMKII Substrates Using Mass Spectrometry-Based Proteomics*. Neuromethods 2015, 85:1-16.

Bemben, M.A., Nguyen, Q.A., Wang, T., Li, Yan., Nicoll, R.A., Roche, K.W. *Autism-associated mutation inhibits protein kinase C mediated neuroligin-4X enhancement of excitatory synapses*. Proceedings of the National Academy of Sciences of the United States of America 2015, 112:2551-56.

Bemben, M.A., Shipman, S.L., Hirai, T., Herring, B.E., Li, Yan., Badger II, J.D., Nicoll, R.A., Diamond, J.S., Roche, K.W. *CaMKII phosphorylation of neuroligin-1 regulates excitatory synapses*. Nature Neuroscience 2014, 17:56-64.

PUBLICATIONS (Undergraduate)

Elsaeidi, F., **Bemben, M.A.***, Zhao, X.F.*, Goldman, D. *Jak/Stat signaling stimulates zebrafish optic nerve regeneration and overcomes the inhibitory actions of Socs3 and Sfpq*. Journal of Neuroscience 2014, 34:2632-44.

Veldman, M.B., **Bemben, M.A.**, Goldman, D. *Tuba1a gene expression is regulated by KLF6/7 and is necessary for CNS development and regeneration*. Molecular & Cellular Neuroscience 2010, 43:370-383.

Veldman, M.B., **Bemben, M.A.**, Goldman, D. *Gene expression analysis of zebrafish retinal ganglion cells during optic nerve regeneration identifies KLF6a and KLF7a as important regulators of axon regeneration*. Developmental Biology 2007, 312:596-612.

*Authors contributed equally to this work

PRESENTATIONS

Published Abstract: **Bemben, M.A.**, Nguyen, Q.A., Wang, T., Li, Yan., Nicoll, R.A., Roche, K.W. *Autism-associated mutation inhibits protein kinase C mediated neuroligin-4X enhancement of excitatory synapses*. Society for Neuroscience Conference 2015 Oct 18: A26, 204.04.

Published Abstract: **Bemben, M.A.**, Shipman, S.L., Hirai, T., Nicoll, R.A., Diamond, J.S., Roche, K.W. *CaMKII phosphorylation of neuroligin-1 regulates excitatory synapses*. Society for Neuroscience Conference 2013 Nov 12: C28, 513.18.

Published Abstract: **Bemben, M.A.,** Shipman, S.L., Hirai, T., Nicoll, R.A., Diamond, J.S., Roche, K.W. *CaMKII phosphorylation of neuroligin-1 regulates excitatory synapses*. "Excitatory Synapses & Brain Function" Gordon Research Conference 2013 June 10-11.

Published Abstract: **Bemben, M.A.**, Goldman, D. *Knockdown of tuba1a inhibits RGC axon regeneration and CNS development in zebrafish.* Society for Neuroscience Conference 2009 Oct 18: B91, 415.6.

RESEARCH EXPERIENCE

Graduate Research Experience:

Dr. Katherine Roche's Lab 08/11--Present
Senior Investigator, National Institutes of Neurological Disorders and Stroke, NIH
Contact: Dr. Katherine Roche (301) 496-3800
Address: NIH **E-mail**: rochek@ninds.nih.gov
Building 35, 2C-903
Bethesda, MD. 20892

Full-time graduate student at the National Institutes of Neurological Disorders and Stroke researching brain development and plasticity, which resulted in four publications. We discovered a novel cellular mechanism, which induces synapse development in the mammalian brain (*Nature Neuroscience* publication) and uncovered how a genetic mutation in autism shifts the balance between excitatory and inhibitory synapses in the developing brain, a potential cause of the disease (*PNAS* publication).

Post Undergraduate Employment:

Prof. Daniel Goldman's Lab 05/09--07/10
Research Professor, Department of Neuroscience, University of Michigan
Contact: Dr. Daniel Goldman (734) 936-2057
Address: 5045 BSRB **E-mail:** neuroman@umich.edu
109 Zina Pitcher Place
Ann Arbor, MI. 48109-2200

Full-time scientist for the Molecular & Behavioral Neuroscience Institute at the University of Michigan researching central nervous system regeneration. We discovered a transcription factor that induced axon regeneration (*Molecular & Cellular Neuroscience* publication). The work was supported by the Michigan Economic Development Corporation & National Glaucoma Research Foundation, Project Grant: F017160.

Undergraduate Research Experience:

Prof. Daniel Goldman's Lab 08/05--05/09
Research Professor, Department of Neuroscience, University of Michigan

Worked 20 hours a week during the fall and winter semesters and 40 hours a week during summer recesses as an undergraduate conducting neuroscience research. This time was spent learning basic molecular biology techniques and initiating a central nervous system regeneration project. Research focused on different tubulin isoforms required for the development and regeneration of neurons (*Molecular & Cellular Neuroscience* and *Developmental Biology* publications).

PRACTICUM EXPERIENCE

Graduate School Rotations:

Prof. Jeffrey S. Diamond 06/11--08/11
Senior Investigator, National Institutes of Neurological Disorders and Stroke
http://intra.ninds.nih.gov/Lab.asp?Org_ID=57
Contact: diamondj@ninds.nih.gov

Prof. Haiqing Zhao 11/10--02/11
Associate Professor, Department of Biology, Johns Hopkins University
http://www.bio.jhu.edu/Faculty/Zhao/
Contact: hzhao@jhu.edu

Prof. David Zappulla's Lab 09/10--11/10
Assistant Professor, Department of Biology, Johns Hopkins University
http://www.bio.jhu.edu/Faculty/Zappulla/
Contact: zappulla@jhu.edu

Prof. Katherine Roche's Lab 07/10--09/10
Senior Investigator, National Institutes of Neurological Disorders and Stroke
http://neuroscience.nih.gov/Lab.asp?Org_ID=407
Contact: rochek@ninds.nih.gov

Practical Laboratory Skills:

Experienced with the following equipment: cryostat, Zeiss Axiophot microscope, Leica dissecting and inverted fluorescent microscopes, Zeiss confocal microscopes, Virtual Optomotor System, surgical tools for various dissections and surgeries, centrifuges, NanoDrop spectrometer, PCR machines, BioWavePro, as well as tissue culture in bacteria free environment.

Mastered Techniques: breeding and raising zebrafish and mice, yeast husbandry, designing and implementing degron constructs in yeast, telomerase assays, nucleic acid/Morpholino injection into single embryos for gene knockdown and overexpression, growth factor extraction from embryos, optic nerve surgery, retina, brain, and lens isolation, retina explants for studying optic nerve regeneration in tissue culture, tissue section, immunohistochemistry, In situ hybridization on tissue sections, RNA isolation and production of cDNA RT-PCR, Real time PCR, Western blots, designing and purifying antibodies, immunoprecipitations, producing and isolating proteins in bacteria, in vitro phosphorylation assays, isolation of primary neuronal cultures, versed in using and accessing genome databases (Ensembl & BioGPS), Lasergene, MetaMorph, MFold, Microsoft Office, Prism, Adobe Software, and basic molecular biology lab techniques such as *in vitro* transcription, gene cloning, bacterial transformation, mutagenesis, and DNA sequencing.

TEACHING EXPERIENCE

Johns Hopkins University:

Teaching Assistant for Developmental Biology 373 01/11--5/11
Contact: Dr. Carolyn Norris (410) 516-7330 **E-mail:** crn@jhu.edu
Address: 308 Mudd Hall
3400 North Charles Street
Baltimore, MD 21218-2685

Taught and lectured junior and senior undergraduates in an upper level biology course
Teaching Assistant for Biochemistry 306 09/10--12/10
Contact: Dr. Robert Horner (410) 516-8067 **E-mail**: rdhorner@jhu.edu
Address: 313 Macaulay Hall
3400 North Charles Street
Baltimore, MD 21218-2685

Instructed 22 undergraduates in performing canonical biochemistry experiments

WRITING EXPERIENCE

Graduate School Newspaper 07/10--08/13
Writer and Co-editor

Began as a writer and advanced to a Co-editor for the *GSChronicles*, a monthly publication highlighting graduate student activities and science articles of interest at the National Institutes of Health. Provided an opportunity to further advance my writing skills and work on a team to produce an electronic newspaper.

Graduate Student Writer/Editor 04/11--07/11
Writer & Editor, Office of Pre-Professional Programs, Johns Hopkins University
Contact: Ana Droscoski (410) 516-4140
Address: Garland Hall Suite 300 **E-mail:** adrosco1@jhu.edu
3400 North Charles Street
Baltimore, MD 21219

Wrote and edited student cover letters that were submitted to graduate universities (medical school, law school, and various PhD programs) with the students' application on behalf of Johns Hopkins University. These cover letters were composed of summaries of the students' research experience, academic performance, volunteer activities, as well as other aspects that make the applicant unique.

ACTIVITIES

Society for Neuroscience 05/09--Present
Current member and presenter at the annual Society for Neuroscience Conference in 2009 (Chicago, IL), 2013 (San Diego, CA), and 2015 (Chicago, IL).

Football Referee/Coach (Montgomery County, MD**)** 08/13--12/13
Instructor, coach, and referee for youth football games in Kidball Organization.
Contact Information: Ronnie Jenkins (301) 983-0543

Big Brothers Big Sisters of America (Washtenaw County office, MI) 01/09--05/10
Big brother (mentor) for a 12- year old boy. Activities included community service, educational activities, and developmental programs.

Contact Information: Melanie Shaw (734) 975-4086 EXT. 110

Phi Kappa Psi Fraternity (Michigan Alpha Chapter) 01/06--05/09
Vice president of pledge class and participated in philanthropic events (Relay for Life and Secret Santa).